THE PROCEEDINGS OF
THE PHYSICAL SOCIETY

Section B

VOL. 65, PART 7 1 July 1952 No. 391 B

Electrical Counting Properties of Diamonds

BY F. C. CHAMPION
King's College, University of London

Communicated by J. T. Randall; *MS. received* 15*th June* 1951, *and in amended form* 4*th February* 1952

ABSTRACT. Examination was made of over 200 diamonds, most of which were of gem quality and many of which weighed only a few milligrams. About 25 of them showed good conduction properties when submitted to ionizing radiations. For depths of crystal penetration which exceeded a certain amount, all the counting specimens responded to both α-particles and β-particles with a response which was at least qualitatively dependent on the energies of the particles. In some cases, however, a marked drop in the counting properties was easily demonstrated with α-particles under conditions of feeble penetration. Even at maximum penetration 5-MEV α-particles produced oscillograph pulses in such crystals which were only about three times as large as those from 1-MEV β-particles. Strong correlation was established between the wavelength of the continuous ultra-violet transmission limit and the magnitude of the electrical counting response of the specimen.

§ 1. INTRODUCTION

EXPLORATORY experiments, notably on space-charge phenomena in diamond crystal counters (Chynoweth 1951) suggested that the counting properties of diamonds and other crystals might be used to throw light on some peculiarities in the structure of such crystals. Investigations have accordingly been made on greatly increased numbers of diamonds of small size and gem quality. While most attention has been paid to their response as counters of α-particles and β-particles, a certain number of parallel experiments have simultaneously been performed on some of the optical properties of the same specimens. Their X-ray diffraction properties have been examined elsewhere (Grenville-Wells 1951).

§ 2. EXPERIMENTAL

The apparatus does not differ essentially from that already described by other workers on crystal counters (Hofstadter 1950). In all cases, unless otherwise specifically stated, the path of the ionizing radiation was perpendicular to the direction of the electric field across the crystal. Most of the diamonds were in the form of small octahedra of volume less than 1 mm^3. Small brass electrodes were pressed in contact with one face of the diamonds, the distance between the electrodes being less than 1 mm. The field strength was varied somewhat according to the problem under consideration, but the average value was about 8 000 volts/cm. Checking experiments on the counting or non-counting properties of the specimens under β-particle bombardment were carried out with an alternative arrangement in which the electrodes were pressed in contact with opposite faces of the diamonds and in which the ionizing radiations were incident in a direction parallel to the electric field. In all these experiments the electrodes and the face of the crystal with which they were in contact were arranged horizontally and the ionizing radiation was incident vertically downwards. In still later experiments at grazing incidence the crystal was forced into a small aperture in the side of a vertical polythene block so that the effective face of the diamond was vertical and flush with the face of the polythene block. The direction of the ionizing radiation was still vertical, and therefore it was now parallel, instead of normal, to the crystal face. However, the imperfect collimation allowed a spread of a few degrees and hence many of the ionizing rays still impinged upon the crystal.

To prevent contamination of the apparatus by radioactive material, the α-ray source was completely enclosed except for a small aperture opposite to the collimating device, which was about 2 cm long. A steel shutter which moved between two stops was operated by a permanent magnet brought up outside the brass container, which was evacuated during the α-particle experiments. The source of β-particles was radium E, which emits β-particles of average energy about 0·3 MeV and of maximum energy about 1 MeV. It is difficult to define exactly what is meant by the range of particles from such a source, but the more energetic particles penetrated well over half way through the diamonds chosen, when the rays traversed the crystal normally. The behaviour of the β-particles is therefore indicative of the conditions prevailing in the interior of the crystal. The α-particles were from polonium, and they were homogeneous in energy at about 5 MeV. By the use of absorbing foils and by varying the gas pressure this energy could be reduced, but it still remained of good homogeneity. Even with α-particles of the maximum energy available incident normally, the penetration was less than 10^{-2} of that of the β-particles. This feeble penetration could be still further reduced by reducing the energy of the incident particles and by directing them at grazing incidence to the crystal surface. It was therefore conceivable that counting properties for α-particles under certain conditions might be indicative of the properties of the crystal near its surface as opposed to the interior.

§ 3. RESULTS

Over 200 diamonds of gem quality were examined, and the results are collected in the table. It is realized that from a crystallographic point of view a more useful table might have been constructed which included the general morphology and other properties of the individual specimens. However, the connection or otherwise between the various physical properties of diamond often appears obscure (Blackwell 1950), and the purpose of the present paper is to focus attention on what prove to be established correlated properties.

Number of diamonds	154	17	8	10	6	20
Maximum β-pulse height	<2	2–5	5–7	7–10	10–12	12–20
% with $\lambda < 2650$ Å	3	30	25	70	70	90

The average width of the noise level on the oscilloscope was 2–4 divisions. Hence the first entry in the second row of the table implies that no pulses were detected in these specimens. In any comparisons it is always the size of the largest pulses which are compared, electric field strength, amplification factors and other physical parameters being maintained as constant as possible throughout the entire range of measurements. A detailed investigation of the magnitudes of all the pulse heights recorded on the oscilloscope has not yet been made since so many factors are involved that such work will be very lengthy when applied to a large number of specimens. Apart from the dependence of the pulse heights on the strength and homogeneity of the electric field across the crystal, they also depend on the characteristics of the amplifier and the recorder, on the previous history and on the degree of polarization of the specimen at any given time and, of course, on the uniformity of energy and direction of the incident radiation. In order that the results might be regarded as truly representative in the presence of these possibly disturbing factors, all the specimens were treated in the same variety of ways as regards field strength, bombardment dosage and exposure to depolarizing agents such as light and ionizing radiation. For example, the same specimen was used at different times under different conditions, sometimes when the crystal had been bombarded by α- and β-particles for some time in the absence of a field and sometimes when it had been bombarded by ionic discharges arising from the ionization of air between the electrodes, the so-called air pulses which arise when α-particles are present and the apparatus has not been exhausted. On other occasions the container was removed for a short period for adjustments, and during that interval the crystal was often exposed to the illumination of the room. After such a variety of treatments, the height of the pulses and the counting rate varied between certain limits, but the average results for any specimen may be regarded as typical.

Comparison effects between α-particle and β-particle counting were carried out in quick succession and yet in a random manner for each diamond. With 5-Mev α-particles incident normally on the crystals, the general counting response ran parallel to that for β-particles, that is, good β-ray counters were also good α-ray counters and vice versa. With some crystals there was no quantitative correlation between the maximum pulse heights and the energy when the two types of radiation were compared; thus, when the pulse height for 1 Mev β-particles was 12–15 divisions, the corresponding pulse height for a 5-Mev α-particle rarely exceeded 35 divisions, whereas proportionately it should have been over 60 divisions.

The wide range of pulse heights observed when any crystal was bombarded by β-particles was consistent with the continuous energy distribution of the incident β-particles, but the fact that α-particles of homogeneous energy gave rise to pulse heights which varied at one and the same time from 35 down to a few divisions called for further examination. Gas straggling was eliminated by operation in a vacuum, while straggling at the source, together with scattering at the collimator, would give rise to inhomogeneity of only a very minor order. The degree of straggling in the crystal itself is not known exactly, but in photographic emulsions it is known to be of a similar order to gas straggling, namely, not more than about 15%. It is quite certain, therefore, that the wide variation in pulse heights observed cannot be attributed to straggling in this sense. In fact, provided that the proportion of energy lost by the ionizing particle in ionizing as opposed to non-ionizing processes inside the crystal does not fluctuate, a homogeneous incident beam would give rise to a constant pulse height independent of whatever straggling occurred in the range of the particles in the crystal. It does not appear possible that the proportion of ionizing to non-ionizing losses can fluctuate over a very wide range, otherwise it would not be possible to use scintillation counters for quantitative recording.

The homogeneity of the incident α-particles was confirmed from the behaviour of the air pulses between the electrodes when air was allowed to enter the apparatus. At higher pressures, if any α-particles of low range were present, these would not reach the electrodes since their distance from the source was about 3 cm and the range of the completely unimpeded α-particles from polonium is less than 4 cm at one atmosphere. If the gas pressure were reduced, however, these less energetic α-particles should, if present, now reach the electrodes and contribute additional pulses. No such variation of counting rate with pressure was observed, showing that the wide distribution in pulse height normally found when α-particles bombarded any one of the diamonds cannot be explained on the basis of inhomogeneity of the incident beam. In fact, for reasons connected with the lower specific ionization consequent upon reduced gas pressure, together with the fact that the counting apparatus was used with a definite set bias on the discriminator, the variation of counting rate with pressure went in the reverse direction to that expected if there were any appreciable inhomogeneity in the source.

The variation of the counting behaviour when the energy and direction of the incident particles were changed was examined, using some of the good counting diamonds. A silver foil of stopping power about 3 cm of air equivalent was placed across the collimator outlet, thus making the total effective distance between the source and crystal about 6 cm at normal pressure. Under these conditions the air pulses vanished, since the α-particles were of insufficient energy to penetrate this thickness of absorbing material. If the air pressure were now reduced to about 26 cm Hg, however, air pulses reappeared, indicating that the range of the α-particles now extended to the electrode system. The height of the air pulses was, of course, reduced, corresponding to the reduced air pressure. It may be remarked that throughout all these experiments the ease with which air pulses could be produced and interpreted formed a useful check on the alignment of the source, which was especially valuable in deciding when a given diamond was definitely a non-counter. Checks were similarly made on the genuine nature of the crystal pulses by observing the disappearance of the crystal pulses, but not the air pulses, when the crystal was replaced by a piece of polythene.

With the absorbing foil present and the container completely exhausted the air pulses naturally disappeared, and these should have been replaced by crystal pulses of a height corresponding to a residual range of about 1 cm of air—that is to say, to more than 1·5 MEV energy. Such a height should obviously be greater than that given by β-particles of 1 MEV energy. In practice, while such expected behaviour occurred with some crystals, in other specimens a few such pulses, which occurred at the beginning of the observations if the crystal was in a good state of depolarization, soon disappeared rapidly and the counting rate fell almost instantaneously to a level hardly appreciable above background.

Similar anomalous behaviour was observed in the experiments with these crystals when the ionizing radiation was at glancing incidence. With glancing angles of not more than 10°, and with the stopping foil present, no pulses at all were observed above background. When the foil was removed there were observed a few pulses somewhat greater in height than those found at normal incidence with foil present. The rate of polarization of the crystal was again extremely rapid, for it soon ceased to respond even to 5-MeV α-particles under these conditions of grazing incidence. On the other hand, when the β-particle source was used at grazing incidence, while the number of pulses was not so large as at normal incidence, there was not the same abrupt reduction which was so marked a feature when the direction of the α-particles was changed from normal to grazing incidence.

§ 4. DISCUSSION

From the detailed data, a summary of which is given in the table, a histogram has been constructed to show the correlation which exists between the ultra-violet absorption limit and the magnitude of the electrical response of the various specimens. In the figure the ordinates show the percentage of counting diamonds, while the abscissae give the corresponding ultra-violet data. The diagram shows that there is an 80% probability that any small transparent diamond of good optical quality whose ultra-violet absorption limit lies below about 2 650 Å will be at least a moderately good counter, whereas if the absorption limit lies above 2 850 Å the chance that it will count appreciably is less than 10%.

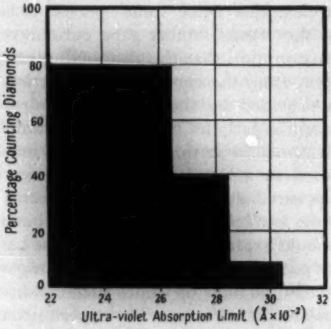

Correlation between ultra-violet limit and counting properties.

The suggestion (Friedman, Birks and Gauvin 1948), based on a few specimens, that there might be a correlation between the ultra-violet limit and the magnitude of the counting response may be regarded as established by the present results. While the details of the behaviour close to the absorption limit would be best revealed with a microphotometer (and this will eventually be used in a more detailed examination of the phenomena), visual observation proved adequate for the present general purpose of examining the suggested correlation with other properties of the crystals. Differences in the times of exposure, different orientations of the specimens, and variations in the photographic processes led to visual estimates of the absorption limits which did not differ for any given specimen by more than about 30 Å.

While in no case was a specimen found in which very good counting response accompanied a high absorption limit, some cases occurred in which excellent ultra-violet transmission was not accompanied by appreciable counting response. However, such anomalous specimens often possessed peculiarities in other ways also. For example, one such diamond was a crystal plate, many times larger than most of the other specimens; in addition, its ultra-violet spectrum showed an unusual isolated absorption band close to the upper limit. Further detailed work would be necessary to explain the precise significance of this, but from observations already made it has become clear that crystals of large size often exhibit different counting properties and different ultra-violet limits, according to the region of the crystal undergoing test, and, therefore, unless a detailed exploration has been made, the general response of large crystals is difficult to interpret. An accompanying paper (Stratton and Champion 1952) examines this point in some detail.

It seems of interest to report here that preliminary experiments conducted by Mr. Robinson on the infra-red absorption of about a dozen of the specimens also indicate the existence of a correlation between the magnitude of the infra-red transmission at $8\,\mu$ and the electrical counting properties. Three of the diamonds which were poor counters were also strongly absorbent, whereas five good counters were highly transparent to infra-red radiation of this wavelength. The remaining specimens occupied intermediate positions under either test.

Considering next the response of diamonds to α-particles of different energy and penetration, it is clear that while some specimens have essentially similar properties throughout the crystal, others gave curious results which can only be explained on the assumption that the conducting properties of the surface layers are quite different from the conducting properties of the interior. The strongest evidence is provided by the extremely poor response at the lower energy, when the incident α-particles were reduced from 5 MeV to about 1·5 MeV, the incidence being normal in both cases. Thus maximum pulse heights, instead of being reduced by a factor of about three, were reduced by a factor of ten, and often disappeared altogether after a few feeble pulses. The obvious interpretation is that the surface layers are much richer in electron traps than the interior, for this would explain the negligible pulse heights consequent upon a very short mean free path of the conduction electrons, while the rapidity with which a space charge could be built up under such conditions would explain the rapidity with which polarization sets in. The experiments at glancing incidence were made to check further this interpretation. At glancing angles of about 10° the vertical penetration of a 5-MeV α-particle is about equal to that of a 1·5-MeV α-particle at normal incidence. Since the path of every particle is not a single straight line but will deviate from this because of scattering in which small angle scattering will predominate, the 5-MeV particles at glancing incidence will be more frequently deflected into still shallower surface layers than the 1·5-MeV particles, since the undeflected direction of the latter is initially perpendicular to the surface. Further, the magnitude of the space charge developed by the 5-MeV α-particles will be much more intense, partly because of their greater total ionization and partly because of the increased density of electron traps which has been postulated to exist closer to the surface. The result should be that, while in specimens with uniform trap density there is fair proportionality between the pulse height and energy of the incident particle, in other specimens which have an increasing trap density nearer the surface the pulse height will fall off more rapidly than can be accounted for in terms simply of reduced energy of the incident particles. Further, because of the speed with which a strong polarization field will be established, a few initial pulses will be followed by an almost non-counting condition. This was, in fact, just what was found.

While there may be several causes contributing to the large spread in the pulse heights of even 5 MeV α-particles at normal incidence, such behaviour is consistent with the trap distribution suggested. Because of the finite angular spread of the particles emerging from the collimator, together with the existence of scattering and space-charge formation, those particles which are deflected appreciably towards the surface will give very inferior pulse heights compared with those particles which are incident vertically and which pursue a relatively undeflected path.

The experimental observation that for some crystals the pulse heights given by 5-MeV α-particles are only about three times those given by 1-MeV β-particles may also be explained on the same lines. The β-particles ionize largely in the interior of the crystal, where the trap density is lower, whereas the α-particle penetration is such that much of their ionization is close to the surface, where the trap density is much higher. There are, however, two possible objections to a direct comparison between pulse heights of α-particles and β-particles. The first of these is instrumental and arises from the fact that the amplifier may show saturation for very large pulses. Accordingly experiments were made to compare the pulse heights (*a*) with different known attenuations of the input pulse for α-particles and β-particles respectively, and (*b*) with diamonds of medium response where the α-ray pulse heights were well within the range of the amplifier for a fixed attenuation; the discrepancy in the ratio of the pulse heights still persisted. The second objection is that the existence of columnar ionization of far greater density along the α-particle tracks compared with the β-particle tracks might give rise to far greater recombination for the ions released by the α-particles. Further detailed experiments remain to be performed on the magnitude of the recombination coefficient when ionizing particles traverse crystals, but there are four reasons why it cannot contribute appreciably to an explanation of the present wide discrepancy between the α-particle and β-particle recording. First, we have already shown that the discrepancy is in evidence when intercomparison is confined to α-particles only, under different conditions. Second, since the path of the ionizing particles was directed perpendicular to the direction of a very powerful electric field across the crystal, the ions were immediately pulled apart laterally, and hence the chance of collision of ions of opposite sign was reduced to a minimum. Third, experiments were made using a wide variation in field strength, and the ratio of the pulse heights showed little change. Finally, other crystals used under the same conditions of geometry and field strength showed good proportionality of pulse height with energy for both α-particles and β-particles. We conclude that, while minor contributory factors may exist, the main cause of the lack of proportionality in the comparison of the α- and β-response lies in the differing density of the electron traps in the two regions where the two ionizing agents operate.

Subsidiary experiments were also consistent with this explanation. When β-particles were used at grazing incidence pulses were observed which, while not so numerous as those produced at normal incidence, did not show the abrupt reduction in magnitude and number which was observed when the direction of the α-particles was changed in the same way. Now β-particles cannot be collimated as well as α-particles and, together with the high degree of scattering always exhibited by electrons, there will always result a certain fraction of the β-particles which enter the crystal at quite high angles in spite of the direction being nominally that of grazing incidence. These scattered electrons give rise, of course, to pulse heights very similar to those produced by a β-ray beam incident normally. Further, even at grazing incidence the range of the β-particles is such that they will penetrate well into the region where we consider the conduction properties of the crystal to be superior.

§ 5. CONCLUSION

The experimental observations show that those diamonds which show good electrical counting properties for β-particles also record α-particles well and vice versa. A high degree of correlation exists between good counting diamonds of small size and gem quality and the wavelength of the ultra-violet transmission limit of the specimens. While the significance of this fact is not yet clear from physical theory, because of the relative simplicity of the ultra-violet apparatus and the independence of the ultra-violet limit on the state of polarization within the crystal, the optical method is quick and convenient as a means of selecting good counting diamonds. The existence of the correlation is also noteworthy when so many of the physical properties of diamond seem uncorrelated or the correlation is obscure.

With α-particles a marked drop in the counting properties occurs with some crystals if the penetration falls below a certain amount, and this is attributed to an increase in the electron trap density, part of which must presumably be due to gross surface irregularities. Such surface behaviour cannot easily be investigated from β-pulses since β-particles will produce too little ionization in such a shallow surface layer to give pulse heights above the noise level of the amplifier. With α-particles, however, some degree of exploration can be made and, if the dense space charge can be reduced or prevented, the counting properties of the surface layers may possibly be improved.

ACKNOWLEDGMENTS

The writer wishes to thank the Department of Scientific and Industrial Research for a grant for the electronic apparatus and also to thank Miss Grenville-Wells for the loan of the diamonds kindly supplied to her through the Industrial Diamond Information Bureau.

REFERENCES

Blackwell, D. E., 1950, *Ph.D. Thesis*, University of Cambridge.

Chynoweth, A. G., 1951, *Phys. Rev.*, **83**, 254.

Friedman, H., Birks, L. S., and Gauvin, H. P., 1948, *Phys. Rev.*, **73**, 186.

Grenville-Wells, H. J., 1951, *Ph.D. Thesis*, University of London.

Hofstadter, R., 1950, *Proc. Inst. Radio Engrs., N.Y.*, **38**, 726.

Stratton, K., and Champion, F. C., 1952, *Proc. Phys. Soc.* B, **65**, 473.

Electrical Counting Response of Two Large Diamonds under Beta-Irradiation

By K. STRATTON* and F. C. CHAMPION†

* Physics Department, Royal Free Hospital School of Medicine
† King's College, University of London

MS. received 4*th February* 1952

ABSTRACT. Two large diamonds S_1 and S_5, both of good optical quality, were subjected to β-irradiation and the electrical conduction responses were studied under a variety of conditions. With S_1 special attention was paid to the formation and removal of space charge. There is evidence that the mechanisms of space charge removal by β-irradiation and by illumination respectively are not quite the same. The efficiency of this diamond as a β-particle counter was not appreciably different from that of a standard Geiger counter.

Small volume elements of S_1 and S_5 were examined individually for β-counting efficiency. While S_1 did not show a variation greater than 20%, variations as large as ten to one were found in different parts of S_5. The results were not inconsistent with the existence of a correlation between the ultra-violet transmission and the counting efficiency of any selected volume element.

The β-response of S_1 was more than three times the best response from S_5 under comparable conditions, while the ultra-violet transmission limits were 2250 and 2850 Å respectively.

I. EXPERIMENTS WITH S_1

The experiments comprised a number of tests of the electrical conduction pulses in a diamond S_1 under various conditions, when subjected to β-ray bombardment. The principal points examined were (*a*) removal of space charge, (*b*) variation of counting rate with time, (*c*) variation of maximum pulse height with applied field, and (*d*) comparison of the counting efficiencies of S_1 and a Geiger counter.

§1. EXPERIMENTAL

The diamond S_1 was a flat plate-like crystal with approximate dimensions 4·5 mm × 2·5 mm × 1 mm. The two large faces were aluminized and one was placed in contact with an electrode leading to the grid of the input valve of the head amplifier. In order to apply a field across the crystal, the opposite aluminized face was connected to a high voltage supply. Almost the whole of this face of the crystal was exposed to β-radiation from a radium (D + E) source, the majority of the β-particles entering the crystal in a direction parallel to the applied field. A beam of white light from an ordinary projection lamp could be focused on to the crystal through a slit in the crystal holder. In the experiments using illumination small aluminized electrodes, covering only about one quarter of the large crystal faces, were used. The whole crystal could then be illuminated by light focused on to it obliquely. The crystal was supported by distrene and although some of the insulator was exposed to the β-radiation, a blank test showed that no disturbances or spurious pulses were caused by the irradiation.

An A.E.R.E. type 201 amplifier was used to amplify the pulses produced in the diamond by the β-particles. The pulses were then passed to a type 200A scaling unit and also to an oscilloscope. The discriminator bias of the amplifier was set so that the scaler would record only pulses greater than twice noise level. Positive or negative potentials of up to 1 080 volts could be applied across the crystal corresponding to a maximum electric field strength of 11 500 volts/cm. An E.H.M.2 Geiger counter with a mica window of about 2 mg/cm^2 was used for the efficiency comparison with the crystal counter. In this part of the experiment the diamond and the Geiger counter were placed in turn at the same distance below a collimated radium (D + E) source. To make the conditions as comparable as possible, the window of the Geiger counter was covered with a thick brass plate in which was cut a hole of area equal to the exposed area of S_1.

§ 2. RESULTS

The effect on the counting rate of illuminating the crystal with white light is shown in fig. 1. Initially the crystal was kept in the dark and on irradiation with β-particles the counting rate fell rapidly to a value less than 4% of its initial value. After a further period of two hours, the rate had risen slightly but it was still very low. Immediately the light was switched on the counting rate rose to about 70% of its initial value and when the light was sufficiently intense, this new counting rate remained constant indefinitely. On switching off the illumination, a small initial rise was followed by the usual rapid drop to the low counting rate originally recorded. This cycle could be repeated indefinitely. In fig. 2 are shown the results of applying various combinations of electric field, β-irradiation and light illumination. It will be noted that irradiation by the β-ray source, in the absence of illumination and of the electric field, was the most efficient way of restoring the initial high counting rate of the crystal.

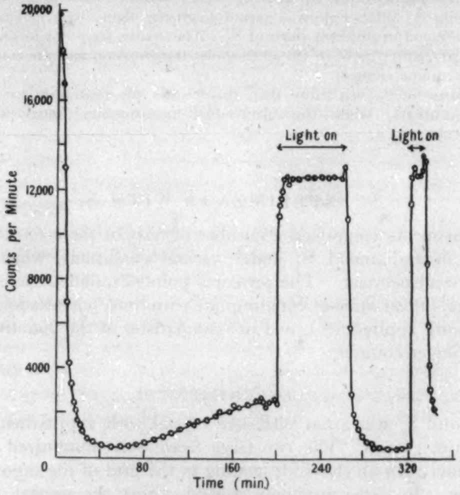

Fig. 1.

When a positive instead of a negative voltage was applied to the crystal, thus reversing the field, the initial counting rate was considerably higher. Moreover, no decay of the counting rate was observed when the positive field exceeded 8 000 volts/cm. For lower fields, some decay in the counting rate did occur but it was irregular and slower than the corresponding decay rate with negative voltages.

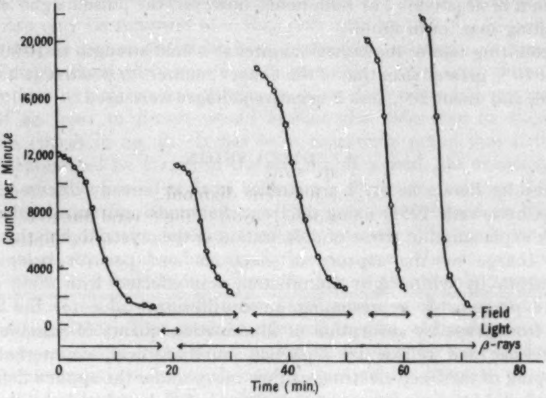

Fig. 2.

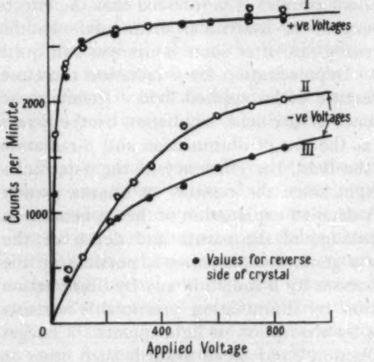

Fig. 3.

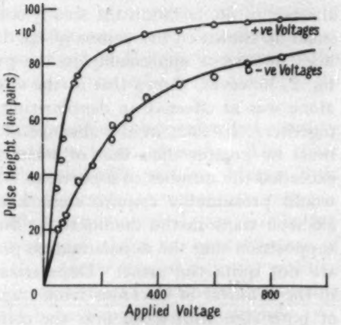

Fig. 4.

In fig. 3 are shown curves of the counting rate plotted against the applied field. Each value of the counting rate is that recorded for the crystal immediately after it had been restored by irradiation with β-particles in the absence of the field. Reversal of the face at which the β-particles entered made little difference to the counting rates for positive applied voltages (curve I). However, for negative applied voltages the curves are not identical when the crystal is reversed (curves II and III). The positive curve approaches saturation at fields greater than 2 000 volts/cm whereas the negative curves are still not saturated at fields greater than 8 000 volts/cm.

In fig. 4 are shown the curves for maximum pulse height against field strength for negative and positive applied voltages. Again the saturation pulse height is achieved at a much lower field strength when the applied voltage is positive than when it is negative. For both fields, however, the pulse height tends to the same limiting maximum value.

The counting rate of the crystal counter at a field strength of 10 000 volts/cm was about 10% greater than that of the Geiger counter for positive voltages across the crystal, and about 20% less if negative voltages were used.

§ 3. DISCUSSION

The results shown in fig. 1 are similar to those already discussed by other workers (Chynoweth 1951) using different diamonds and therefore receive the customary explanation in terms of polarization of the crystal due to the formation of space charge by the capture of electrons and positive holes in traps. Depolarization by white light illumination was effected with 70% efficiency, this figure presumably representing an equilibrium value for the release of electrons from traps by absorption of illumination quanta of suitable energies, thermal release and release by β-particle bombardment, counterbalanced by fresh trapping of the freed electrons as they move under the applied field. There was no evidence for any permanent 'activation' of S_1 by white light illumination, as reported by Willardson and Danielson (1950) for some good diamond counters, since fig. 1 shows that decay started soon after the illumination was cut off. However, since S_1 is an excellent counter it is inferred that the effects of illumination depend on factors peculiar to individual diamonds. In the absence of illumination the steady counting rate after some hours was still quite small as shown in the centre of fig. 1. Depolarization by β-radiation therefore does not occur appreciably in the presence of an applied field. Reference to fig. 2, however, shows that in the absence of the field, irradiation by the β-rays alone was as effective in depolarizing as the use of illumination and β-radiation together. In fact, in the absence of the field, the efficiency of the β-particles must be greater than that of white light since the number of quanta greatly exceeded the number of β-particles. A detailed explanation of these phenomena would presumably require some knowledge of the nature and depth of the electron traps in the diamond S_1, but a general explanation is possible on the supposition that the depolarization processes by β-radiation and by illumination are not quite the same. Depolarization by illumination presumably consists in the removal of electrons from traps by absorption of light quanta. Charges of both sign thus freed into the conduction band move towards each other in the absence of an external field and finally neutralize each other. In the presence of an external field the detrapped charges proceed to the electrodes and are eventually removed in that way. The effect of irradiation with β-rays, however, is essentially to throw many electrons (of which trapped electrons form only a small fraction) into the conduction band during the ionization process. If the external field is absent, these electrons and the corresponding positive holes move under the polarization field already present and hence distribute themselves in such a way as to neutralize the polarization field. If the external field is present it is opposed by the polarization field, the net field being small, and no appreciable movement (and hence no appreciable depolarization) is produced. Detrapping therefore plays a large part in depolarization by illumination but a small part in depolarization by β-irradiation.

The poor but steady counting rate shown in the centre of fig. 1 improves after some time if both source and illumination are absent but the field is left on continuously. The inference is that most of the charges are trapped so deeply that they can only be removed at a very slow rate by thermal release, but that each time release occurs the field gives secondary assistance in removing the released charges from the vicinity of a trap site. This supposition that the crystal contains its polarization charges in fairly deep traps after an exposure of about half an hour to β-rays would explain the difference in slopes of the polarization curves in fig. 2. It has been repeatedly noted that if the crystal has been depolarized by β-rays in the absence of a field, the subsequent decay rate during a further period of β-ray counting is always greater than if the crystal had been depolarized by illumination. This may be explained on the grounds already suggested, that the depolarization processes are different in the two cases. Illumination results in absolute depolarization, even the deeper traps being emptied, whereas β-irradiation essentially leaves the deeply trapped charge unaffected but allows fresh charge to be distributed in such a way as to neutralize the polarization field. This fresh charge will in general be largely confined to shallow traps especially if the β-irradiation takes place for only a few minutes. These shallow traps are relatively easily emptied by thermal processes and subsequent β-irradiation. Consequently the original polarization field arising from the deep traps which have never been emptied becomes effective in a much shorter time than that required for the production of a new polarization field if one started with a crystal which was initially completely detrapped. Polarization is produced more readily in crystals which have been 'depolarized' by β-irradiation because the polarization has never been destroyed although it has been rendered latent. On the other hand polarization is produced somewhat more slowly in crystals which have been depolarized by illumination because the original polarization has been largely destroyed and has to be created completely afresh.

With regard to the differences in the saturation fields for positive and negative voltages as shown in fig. 3, no simple explanation seems possible. The effect of reversing the crystal was to leave the behaviour with positive voltages little affected while making an appreciable change in the response to negative voltages. Such overall behaviour would require not only an asymmetrical trap distribution within the crystal but also the existence of regions where the concentration of electron traps was of greater density than the concentration of traps for positive holes. Rather than pursue an elaborate explanation of this kind it seems preferable to await further experimental evidence of the behaviour of other diamonds.

In contrast to the counting rate behaviour, the maximum pulse height was independent of the sign of the voltage at saturation field. Assuming that this maximum pulse height arose from the collection of all the ion pairs released by the most energetic β-particles present, namely those of energy about 1 Mev, the energy required to liberate an ion-pair in S_1 by β-particles was about 10 ev. Similar values have already been found by other workers using different specimens (Hofstadter 1950) although Ess and Rossel (1951) report a value of 89 ev for a specimen under α-particle bombardment.

II. EXPERIMENTS WITH S_5

It has been shown (Champion 1952) that there is a strong correlation between the ultra-violet wavelength transmission limit and the magnitude of the β-counting response of a large number of diamond specimens. A diamond S_5 was available which was sufficiently large for tests to be made of the ultra-violet transmission and β-counting response of different regions of the same crystal.

§ 1. EXPERIMENTAL

The diamond S_5 had two parallel, approximately rectangular faces 3·1 mm apart. The β-counting response was tested in the same way and with the same apparatus as for S_1. However, so that only a small area of S_5 should be irradiated at any one time, the incident beam of β-particles was collimated by means of a small hole of diameter 0·55 mm in each of a pair of parallel brass plates. These plates were each 1 mm thick and were spaced 1·2 cm apart, the lower plate being only 8 mm from the upper surface of the crystal. The collimating arrangement and the source were fixed to a carriage which could be moved in two mutually perpendicular horizontal directions and the movement measured on two vernier scales. In this way the source and collimating holes could be set vertically above any desired region of the crystal face. Figure 5 (*a*) shows the division of the crystal into areas for scanning; the diameter of the collimating holes was equal to the length of the side of one square. The field strength used throughout the experiments with this crystal was 2 400 volts/cm. Depolarization was effected by the method of β-particle irradiation with no applied field, as described above. In practice, each two minute counting period was followed by a recovery period of about four minutes duration, the whole crystal being irradiated by a non-collimated β-ray beam to ensure good overall recovery. Scanning was carried out on both sides of the crystal and two corresponding sets of results were obtained. The experiment was then repeated with the diamond S_1. In all these scanning experiments both faces were completely aluminized so that a uniform electric field could be obtained in the crystal.

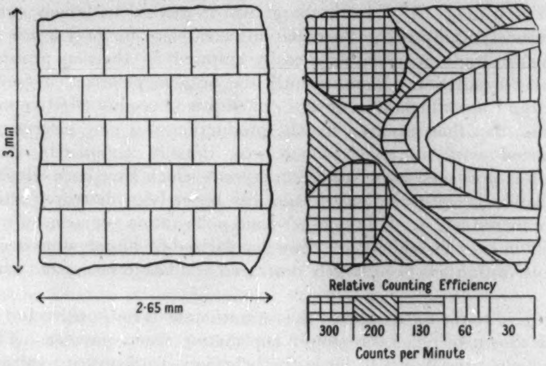

(*a*) (*b*)

Fig. 5.

§ 2. RESULTS

The variation of the counting rate over the area of the crystal S_5 is shown diagrammatically in fig. 5 (*b*). The ratio of maximum to minimum counting rate was greater than ten to one and, as expected, larger pulses were obtained in the areas of higher counting rate than in those of lower counting rate. Even under the best conditions the pulse height and counting rate were less than one-third of that shown by S_1 for the same field strength. The counting rate of the reverse side of the crystal S_5 was very inferior to that of the side first examined; in particular, the counting rate in all regions of the lower half was less than one-sixth of the counting rate of the upper half in the region where the latter was counting most efficiently. The transmission limit with ultra-violet light was determined in the same way as for all the diamonds described by Champion (1952). The areas subjected to ultra-violet transmission were considerably larger than in the β-counting experiments. Five observations were made, four of them relating to the corners and one to the centre of the crystal. The transmission limits were 2 850 Å in each corner and 2 865 Å in the centre as recorded photographically. Similar very slight differences were recorded in an approximate scanning with a microphotometer. In contrast to S_5, with S_1 no detectable change was found in the ultra-violet limit from the value 2 250 Å and the counting rate did not vary from place to place by more than about 20%.

§ 3. DISCUSSION

The poor counting rate of S_5 as a whole compared with S_1 provides further support for the correlation between β-ray response and the ultra-violet transmission limit since, while S_5 cut off at about 2 850 Å, S_1 transmitted to 2 250 Å.

The variation in ultra-violet transmission over different portions of S_5 is only just detectable, but the variation in its counting properties is as large as ten to one. It appears at first sight therefore that the β-response of a crystal is a far more sensitive test of structural peculiarities than the variation in the value of the ultra-violet transmission limit. However, a fuller consideration of the experimental conditions shows that while this may be true, it is necessary to accept this conclusion with reserve. Effects of β-particle scattering and the production of secondary electrons whose range extends outside the volume element under consideration would tend to smooth out differences in counting rate; hence the corrected differences must be at least as large as those observed experimentally. In fact the range of the most energetic β-particles barely extended half-way through the crystal and since the field strength was considerably below saturation, the charges released would travel a relatively short distance from their origins before being trapped. Hence we may conclude that fig. 5 (*b*) represents essentially the counting efficiency of different regions of the upper half of the crystal. The lower half of the crystal showed much poorer counting properties. Now while different volumes of the crystal could be isolated in this way when tested for counting properties, the ultra-violet transmission limit was determined under conditions where the illumination had to pass through both the relatively good counting upper half and the poor counting lower half of the crystal. With this arrangement, therefore, assuming that the correlation between ultra-violet transmission limit and counting properties holds good, the fact that the ultra-violet radiation had to traverse a poor counting region for at least the lower half of its path would imply that the limit would show a high value for all the observations made. This was found to be the case, the limit varying from 2 850 to 2 865 Å, the latter value corresponding to a position where the upper portion of the crystal was a poor counter as well as the lower half.

The conclusions to be drawn from these experiments are that large variations in β-counting efficiency can occur in different regions of a large crystal but that ultra-violet transmission experiments on the crystal as a whole may often lead to the assignment of a transmission limit which will be indicative only of the more highly absorbent portion of the total path traversed by the ultra-violet radiation in its passage through the specimen. These results are in agreement with recent conclusions of Freeman and van der Velden (1951) on the relation between the α-counting response of certain portions of a diamond and the corresponding ultra-violet transmission limits. However, Ahearn (1951) has suggested an alternative interpretation by supposing that good conducting channels frequently occur in diamonds and that the resulting inhomogeneities in the electric field may account at least partially for the variation of counting efficiency found in some specimens.

ACKNOWLEDGMENT

It is a pleasure to thank Dr. W. A. Leyshon for her interest in the problem.

REFERENCES

Ahearn, A. J., 1951, *Phys. Rev.*, **84,** 798.
Champion, F. C., 1952, *Proc. Phys. Soc.* B, **65,** 465.
Chynoweth, A. G., 1951, *Phys. Rev.*, **83,** 254.
Ess, H., and Rossel, J., 1951, *Helv. Phys. Acta*, **23,** 484.
Freeman, G. P., and van der Velden, H. A., 1951, *Physica*, **17,** 565.
Hofstadter, R., 1950, *Proc. Inst. Radio Engrs., N.Y.*, **38,** 726.
Willardson, R. K., and Danielson, G. C., 1950, *Phys. Rev.*, **77,** 300.

Rectification Phenomena Exhibited by Natural and Sulphurized Galena

By A. L. REIMANN and J. V. SULLIVAN
Physics Department, University of Queensland

Communicated by H. C. Webster; MS. received 12*th April* 1951, *and in amended form* 13*th February* 1952

ABSTRACT. Specimens of n-type galena were sulphurized, either by a wet chemical process or by exposure to sulphur vapour at various temperatures, and the resulting changes in rectification characteristics were observed, both with d.c. instruments and at 3 000 Mc/s, using various cats-whiskers. According to treatment given, either an improved n-type rectification was obtained or the polarity was changed to p-type. The results are briefly discussed in the light of present-day rectification theory.

§1. INTRODUCTION

According to present day theories of the rectifying properties of contacts between a semiconductor and a metal, important parameters determining these properties must be the nature and concentration of lattice defects in the semiconductor in the region of the contact. From the work of Eisenmann

(1940) and Hintenberger (1941, 1942) it appears that the relevant lattice defects in lead sulphide are normally in the nature of a stoichiometric disproportion between lead and sulphur, for by measurements of thermoelectric power and Hall effect these investigators found that heating in sulphur vapour converts n-type material to p-type, while heating in a vacuum converts p-type to n-type. In such response to treatment Eisenmann was unable to detect any difference between natural and artificially prepared lead sulphide. Eisenmann and Hintenberger were concerned only with the nature of the bulk conductivity, and accordingly subjected their specimens to sufficiently severe thermal treatments to affect the stoichiometric disproportion throughout their entire volume. Where we are concerned with rectification, however, interest attaches mainly to conditions in and near the barrier layer, and to effect changes in these conditions less drastic sulphurization and reduction treatments are indicated. The present paper deals mainly with effects due to sulphurization of material presumed (from rectification polarity) originally to have had an excess of lead, the sulphurization procedures being varied to produce modifications in composition down to different depths below the surface.

§ 2. EXPERIMENTAL

(i) *Material Used*

Only galena occurring in the form of large crystals was used in this work. Spectroscopic analyses* of samples of this material showed that it contained but little impurity, and such impurities as were found could not be correlated with observed rectification properties. It therefore seems reasonable to assume that these properties, like the conductivity of Eisenmann's and Hintenberger's specimens, were determined by stoichiometric disproportions between lead and sulphur.

The specimens used were in all cases cleavage fragments, and, for testing, these were set in Wood's metal, with a freshly cleaved marked face uppermost. In engaging a cats-whisker with this, a device was used which permitted both 'exploration' and good control of the pressure exerted. The same face was then tested again after treatment.

(ii) *Sulphurization*

The sulphurization treatments given were of two kinds, viz. immersion in a solution of ammonium sulphide at room temperature ('wet sulphurization'), and heating in sulphur vapour. Immersion for wet sulphurization was for about 1 hour, this producing the full effect obtainable. In thermal sulphurization the specimen was exposed to saturated sulphur vapour for 15 or 30 minutes at 200°, 300°, 400° or 500° c. Appropriate precautions were taken against incidental oxidation, such as might have resulted from exposure to water vapour evolved from the Pyrex container. Neither wet nor thermal sulphurization produced any change in the appearance of the galena.

(iii) *Tests at High Frequency*

The only high-frequency tests carried out were at 3 000 Mc/s. The part of the equipment containing the crystal is shown schematically in vertical section, and a pin-in-slot feature used for fine adjustment of tuning (see below) also in plan, in fig. 1. A klystron oscillator was coupled, via an attenuator, to one end of a waveguide and at the other end, near the plunger P used for tuning, provision was made for the measurement of the d.c. output of the rectifier unit, and for the adjustment of the contact through two windows W cut in the side of the waveguide. The cats-whisker was mounted on an elastically flexible system (not shown) made out of a short piece of rubber tubing and some annealed copper foil, and was in electrical contact with the top of the waveguide. The crystal was set in Wood's metal in a small brass pot, and this could be moved about on the flat top of a brass cylinder fitting easily into a hole in the bottom of the waveguide. The cylinder could be fixed in any position by tightening a rubber-tipped screw engaging with it laterally. The sides of the cylinder were lacquered to provide d.c. insulation, while at the same time allowing of full capacitive a.c. coupling with the bottom of the waveguide. The cylinder was connected to earth via a resistance box and a d.c. meter reading 1 mA full scale, the resistance of the two combined constituting the load. The equipment was adjusted by means of a calibrated silicon crystal unit to give an r.f. power input of 0·49 mw, and then, with the experimental crystal in position, the resistance and tuning were varied to find the maximum attainable d.c. power output. The load giving this was in most cases about 400 ohms.

---

* For these analyses we are indebted to Mr. A. C. Oertel, of the Waite Institute, C.S.I.R.O. Division of Soils, Adelaide.

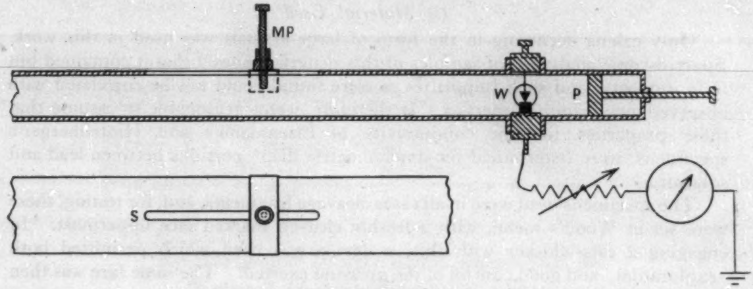

Fig. 1.

In maximizing the output for any given load the plunger P and a subsidiary matching pin MP working in the slot S were adjusted to give the maximum rectified current. By inserting a metal block into the slot the r.f. power fed to the crystal could be reduced to practically zero, enabling the static characteristic to be observed for the same contact.

By using the static testing equipment in conjunction with the waveguide system, an r.f. rectification test could be carried out with any desired voltage bias applied across the contact.

(iv) *Crystal Spottiness*

All surfaces tested exhibited the usual variation of rectification characteristics both with the region engaged by the cats-whisker and with contact area and pressure. Of these effects, those depending on area and pressure were found to be relatively minor, and accordingly no attempt was made to standardize either of these factors, beyond keeping the cats-whisker reasonably sharp and avoiding either too heavy or too light (and correspondingly unstable) an engagement with the crystal surface.

On most surfaces tested some spots exhibited marked rectification, varying in a consistent manner with treatment, while at others little or no rectification was observable. Since more interest obviously attaches to the former, these were the only ones whose characteristics were noted. Observations were made at some 20–30 spots on each surface, and the characteristics then recorded for a typical 'good' spot, or for a few such.

(v) *Cats-whiskers*

In general, the cats-whiskers used were confined to the three materials platinum, nickel and graphite. Other whiskers were occasionally employed, but these did not appear to produce any types of behaviour not observable with the materials named.

§3. RESULTS

(i) *Natural Galena*

Static characteristics. A selected good static characteristic obtained with untreated n-type galena and a graphite cats-whisker is shown by the curve N in fig. 2. For comparison the curve P shows a selected characteristic obtained by engaging a nickel whisker with untreated p-type galena. The signs of voltages and currents in the graphs have been adjusted so that the forward parts of the characteristics both appear on the right-hand side and above the voltage axis.

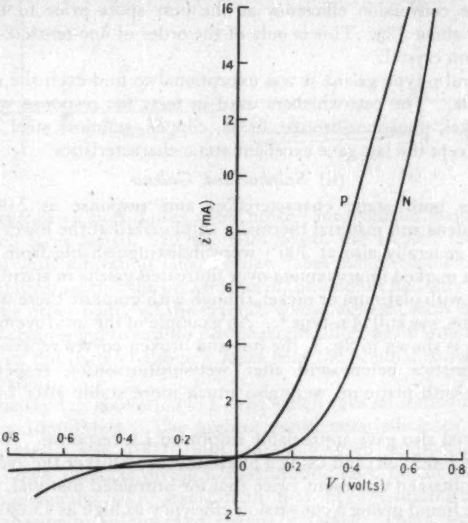

Fig. 2.

These curves are both typical of their kind. With the n-type material characteristics were obtained of which both forward and backward parts were everywhere convex towards the voltage axis. The p-type material, on the other hand, always gave a forward characteristic which became linear at higher voltages, and a saturating or semi-saturating tail. This feature of the tail persisted only up to a certain limiting voltage, however, of the order of 10–20 volts. Increase of the voltage beyond this limit gave rise to a sudden surge of current, accompanied by burn-out of the contact.

Qualitatively, characteristics of the same form were obtained when other whisker materials were used. Quantitatively, however, n-type galena was found to give the highest ratios of forward to backward currents when engaged with graphite, the next highest with platinum, and the lowest with nickel. With the p-type galena the order of merit of whisker materials was the reverse of this. Irrespective of the type of galena, forward currents were generally largest with nickel, smaller with platinum, and smallest of all with graphite.

The characteristics obtained with n-type galena were much less stable when platinum was used as the cats-whisker than with graphite or nickel; after the passage of a forward current of the order of 10 mA for a second or two the resistance in the reverse direction was generally found to have fallen to a much lower value.

The spottiness of the natural p-type galena was on a much larger scale than was that of n-type; it was not uncommon to find surface regions of p-type material giving substantially uniform rectification which had an area of 1 mm^2 or more.

Response at 3 000 *Mc/s.* The only untreated material found to give a significant response at 3 000 Mc/s was n-type galena when engaged with a plantium cats-whisker. The conversion efficiency at the best spots prior to burn-out was, however, only about 3%. This is only of the order of one-tenth of the efficiency of a good silicon crystal.

With natural p-type galena it was exceptional to find even the slightest trace of r.f. response. The cats-whiskers used in tests for response were tungsten, platinum, nickel, phosphor-bronze, brass, copper, stainless steel and graphite. All of these except the last gave excellent static characteristics.

(ii) *Sulphurized Galena*

As regards both static characteristics and response at 3 000 Mc/s wet-sulphurized galena and material thermally sulphurized at the lower temperatures (at 200°, and generally also at 300°) were indistinguishable from one another. Both showed a marked improvement over untreated galena in static characteristic when engaged with platinum or nickel, though with graphite there was no change. The rectification was still of n-type*. An example of the improvement produced with platinum is shown in fig. 3, the full and broken curves representing typical good characteristics before and after wet-sulphurization respectively. The characteristics with platinum were also much more stable after treatment than before.

This material also gave appreciably improved r.f. response. With optimum bias applied (0·3–0·5 volt) and using a platinum cats-whisker the average rectified power output obtained was about twice that for untreated material, but occasionally spots were found giving a conversion efficiency as high as 15–20%, i.e. better than the best obtainable with untreated crystals by a factor of about 6.

Some crystals sulphurized at 300°, and all those sulphurized at 400° and 500°, had their rectification polarity changed from n-type to p-type, owing, presumably, to a deeper penetration of the sulphur than at lower temperatures. Before considering these, however, we may note an interesting transition stage exhibited by one crystal sulphurized for 30 minutes at 300°. With platinum this gave good n-type rectification having static characteristics and r.f. response similar to that obtained with wet-sulphurized galena. With graphite, however, the rectification obtained at most contacts was definitely of p-type. Typical p-type ratios of forward to backward currents at 1 volt found with graphite were 4 : 1 to 6 : 1. The currents were abnormally small, e.g. in the forward direction 2 mA at 1 volt and 7 mA at 1·8 volts.

---

* By the expression 'n-type (or p-type) rectification' is meant 'rectification of polarity such as is normally given by n-type (or p-type) material'.

The crystals sulphurized at the higher temperatures were found to fall into two classes, the one giving saturating or semi-saturating tails such as were obtained with natural p-type crystals, and the other giving characteristics with non-saturating tails. Characteristics of the two types, both observed with a platinum cats-whisker, are shown in fig. 4, indicated respectively by a full and a broken line. No correlation could be found between the severity of the sulphurization treatment and the type of tail resulting.

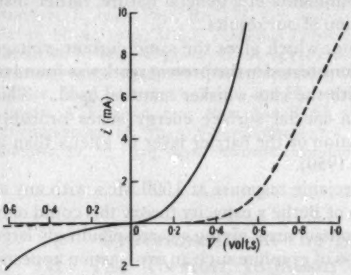

Fig. 3.

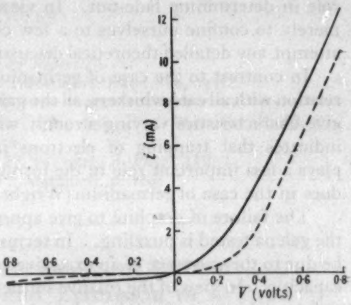

Fig. 4.

Several crystals of both kinds were broken into smaller fragments and the freshly cleaved faces tested. In all cases where the treated faces had given characteristics with saturating tails the new faces exhibited the original n-type rectification, indicating that the penetration of the sulphur had only been relatively slight. On the other hand, all the crystals whose exposed faces had given non-saturating tails continued to exhibit p-type rectification, again with non-saturating tails, on at least the parts of the new faces near the original surfaces, indicating deeper penetration.

None of the crystals converted to p-type which gave saturating tails responded appreciably at 3 000 Mc/s. The highest rectification efficiency ever observed with such crystals was 1·5%, and anything even approaching this was exceptional. With contacts giving non-saturating tails, on the other hand, the response was generally comparable with that of wet-sulphurized and low-temperature thermally sulphurized n-type crystals. There was, however, a considerable spread, and one contact made with a platinum cats-whisker was found to give a conversion efficiency as high as 29%.

None of the crystals tested in this work, whether before or after treatment, and irrespective of rectification polarity, was ever observed to give an appreciable r.f. response when a graphite cats-whisker was used.

§4. DISCUSSION

In recent years the theory of rectification at contacts between metals and semiconductors has undergone considerable elaboration. This has become necessary on account of new developments, such as the discovery of carrier injection and the recognition of the possibility of the existence of energy states of electrons at the surface of a semiconductor differing from those in the conduction band in the interior (Bardeen 1947). Both of these may concern us here. Thus Gebbie, Banbury and Hogarth (1950) have observed transistor action in some specimens of p-type lead sulphide. Again, apart from the general possibility of the existence of special surface electron energy states, Gibson (1950) has, more specifically, inferred from photoconductivity measurements that galena probably adsorbs oxygen atoms which capture electrons from the interior, forming O^- ions. Finally, contact capacity is no longer believed to be the only factor responsible for the fade-out of response at high-frequency as in Bethe's theory (1942); Douglas and James (1951) have suggested that the transit time of the electrons may play an important role in determining fade-out. In view of these complications we propose here merely to confine ourselves to a few comments of a general nature, rather than attempt any detailed theoretical discussion of our results.

In contrast to the case of germanium, which gives the same current–voltage relation with all cats-whiskers, all the galena tested in the present work was found to give characteristics varying strongly with the cats-whisker material used. This indicates that trapping of electrons in special surface energy states probably plays a less important role in the formation of the barrier layer in galena than it does in the case of germanium (Wright 1950).

The failure of graphite to give appreciable response at 3 000 Mc/s with any of the galena tested is puzzling. In terms of Bethe's capacity theory this could only be due to the existence of an excessive contact area, giving a correspondingly large capacity. In view of the relative softness of graphite such an explanation appears, at first sight, quite feasible. It is, however, difficult to understand the complete absence of some momentary response during the many carefully made trials, which must surely have included, even if only transitorily, some very light contacts. Also the high-frequency response with other whiskers was not found to be very sensitive to pressure. It is equally difficult to see why the electron transit time should be appreciably greater with graphite than with other cats-whiskers.

Presumably the barrier layers formed in both kinds of untreated natural galena, in wet-sulphurized or lightly thermally sulphurized n-type galena, and in n-type material converted to p-type by penetrating sulphurization were all essentially of the type known as 'natural'. On the other hand, the barrier layers in the somewhat more heavily thermally sulphurized material which remained of n-type were probably composite, an appreciable thickness of material beneath the surface having had the excess of lead strongly reduced or converted to a deficit. The extra thickness of the barrier layer should, according to Bethe's theory, have been particularly favourable to high-frequency response. The results do not, however, accord with this expectation; the best high-frequency response was obtained with specimens converted from n- to p-type by penetrating sulphurization and exhibiting non-saturating tails in their static characteristics.

The absence of response at 3 000 Mc/s shown by specimens with saturating tails is of special interest in the light of the recent work of Douglas and James (1951) on specimens of germanium. In this work the rectification efficiency at frequencies of 16, 50 and 100 Mc/s was found to fall with increasing turnover voltage in the reverse direction. Even at these frequencies the effect was quite marked for turnover voltages of 10–20 volts, corresponding to those observed by us with natural p-type galena. Unfortunately no systematic observations of turnover voltage were made in the present work.

ACKNOWLEDGMENTS

A portion of the work discussed in this paper was carried out in 1942–43 by one of us (A.L.R.) at the C.S.I.R.O. Radiophysics Laboratory in Sydney, and we are indebted to the Commonwealth Scientific and Industrial Research Organization for leave to publish this work, and for the loan since the end of the war of the 3 000 Mc/s testing equipment. The major part of the work has been carried out in the Physics Department of the University of Queensland on a grant from the Commonwealth Research Grants Committee.

REFERENCES

Bardeen, J., 1947, *Phys. Rev.*, **71**, 717.
Bethe, H. A., 1942, *M.I.T. Radiation Laboratory Report* 43/12.
Douglas, R. W., and James, E. G., 1951, *Proc. Instn. Elect. Engrs.*, **98**, 157.
Eisenmann, L., 1940, *Ann. Phys., Lpz.*, (5), **38**, 121.
Gebbie, H. A., Banbury, P. C., and Hogarth, C. A., 1950, *Proc. Phys. Soc.* B, **63**, 371.
Gibson, A. F., 1950, *Proc. Phys. Soc.* B, **63**, 756.
Hintenberger, H., 1941, *Naturwissenschaften*, **29**, 79; 1942, *Z. Phys.*, **119**, 1.
Wright, D. A., 1950, *Semiconductors* (London : Methuen), p. 104.

Experiments on the Mechanics of Rubber
II: The Torsion, Inflation and Extension of a Tube

By A. N. GENT and R. S. RIVLIN
British Rubber Producers' Research Association, Welwyn Garden City, Herts.

Communicated by W. P. Fletcher; MS. received 14th January 1952

ABSTRACT. The formulae derived by Rivlin (1949) for the forces necessary to produce simple extension, radial inflation and torsion in a tube of incompressible highly elastic material, which is isotropic in its undeformed state, are specialized to the case when the amount of torsion is small. The resulting formulae are compared with measurements on tubes of vulcanized natural rubber and conclusions as to the form of the stored-energy function are drawn, in general agreement with those reached from earlier experiments. The experiments indicate that hysteresis between the loading and unloading curves for the vulcanizate is associated with certain terms in the expression for its stored-energy function and, presumably, with the mechanism which accounts for the presence of these terms.

§1. INTRODUCTION

It has been shown (Rivlin 1949) that if a tube of incompressible highly elastic material which is isotropic in its undeformed state is acted on by a torsional couple it will elongate unless restrained from doing so. Even if this elongation is prevented, the tube will decrease in diameter unless an inflating pressure is applied on its inner surface to counteract this. Similar conclusions apply if the tube is held in an extended state during the process of twisting. The couple which must be applied in order to produce a given amount of torsion and the inflating pressure required to prevent the decrease in diameter have been calculated in terms of the stored-energy function for the material. It is predicted in § 2, from these results, that for sufficiently small values of the amount of torsion the torsional couple is proportional to the amount of torsion and the inflating pressure to the square of the amount of torsion.

In §§ 3 and 4 these results are verified experimentally for tubes of vulcanized natural rubber, and the implications of the measurements regarding the form of the stored-energy function W for the vulcanizates as a function of the two strain invariants I_1 and I_2 are discussed.

If the inflating pressure is not applied, and the tube is allowed to decrease in volume on twisting, it is predicted that for small amounts of torsion the fractional change in volume is proportional to the square of the amount of torsion. In § 5 this result is verified experimentally for various amounts of extension of the tube.

Then (§ 6) measurements are described of corresponding values of torsional couple, amount of torsion and inflating pressure required to maintain the volume of the tube unchanged for a series of tubes vulcanized to different extents. In the remainder of the paper the relation of the experimental results to the predictions of the kinetic theory are discussed.

§ 2. THEORETICAL CONSIDERATIONS

In a previous paper (Rivlin 1949) the forces required to maintain simultaneous extension, inflation and torsion in a uniform circular cylindrical tube of highly elastic material have been calculated. The material of the tube is considered to be incompressible and isotropic in its undeformed state, so that its elastic properties can be expressed in terms of a stored-energy function W which is a function of two quantities I_1 and I_2, defined in terms of the principal extension ratios λ_1, λ_2 and λ_3, by the formulae

$$I_1=\lambda_1^2+\lambda_2^2+\lambda_3^2 \quad \text{and} \quad I_2=\frac{1}{\lambda_1^2}+\frac{1}{\lambda_2^2}+\frac{1}{\lambda_3^2}. \qquad \ldots\ldots(2.1)$$

The deformation to which the tube is subjected is defined by the following three successive deformations: (i) a uniform simple extension of extension ratio λ, (ii) a uniform inflation of the tube in which its length remains constant and its external and internal radii change from their values of a_1 and a_2 respectively in the undeformed tube to $\mu_1 a_1$ and $\mu_2 a_2$ respectively, (iii) a uniform torsion in which planes perpendicular to the axis of the tube are rotated in their own plane through an angle proportional to the distance of the plane considered from one end, the constant of proportionality being ψ.

In this deformation a point of the tube which is initially at a radial distance r from its axis moves to a radial distance μr, where μ is given by

$$\lambda\mu^2 r^2=r^2+K \quad \text{and} \quad K=a_1^2(\lambda\mu_1^2-1)=a_2^2(\lambda\mu_2^2-1). \qquad \ldots\ldots(2.2)$$

It has been shown that this deformation can be maintained by the application of torsional couples M and tensile forces N to the ends of the tube together with a force R_v per unit area, measured in the deformed state, acting normally on the inner curved surface of the tube. M, N and R_v are given by

$$M=4\pi\psi\int_{a_2}^{a_1}\mu r^3\left(\lambda\mu\frac{\partial W}{\partial I_1}+\frac{1}{\lambda\mu}\frac{\partial W}{\partial I_2}\right)dr, \qquad \ldots\ldots(2.3)$$

$$\begin{aligned}N=\pi\int_{a_2}^{a_1}2r\Bigg[&\frac{2}{\lambda}\left(\lambda^2-\frac{1}{\lambda^2\mu^2}\right)\left(\frac{\partial W}{\partial I_1}+\mu^2\frac{\partial W}{\partial I_2}\right)\\&+\frac{1}{\lambda^2\mu^2}\left(\frac{1}{\lambda^2\mu^2}-\mu^2\right)\left(\frac{\partial W}{\partial I_1}+\lambda^2\frac{\partial W}{\partial I_2}\right)\left(1-\frac{a_2^2}{r^2}\right)\\&+\psi^2\frac{\partial W}{\partial I_1}(a_2^2-r^2)-2\frac{\psi^2}{\lambda}r^2\frac{\partial W}{\partial I_2}\Bigg]dr, \qquad \ldots\ldots(2.4)\end{aligned}$$

and
$$R_v=2\int_{a_2}^{a_1}\frac{1}{\lambda\mu^2 r}\left(\frac{1}{\lambda^2\mu^2}-\mu^2\right)\left(\frac{\partial W}{\partial I_1}+\lambda^2\frac{\partial W}{\partial I_2}\right)dr-2\psi^2\lambda\int_{a_2}^{a_1}r\frac{\partial W}{\partial I_1}dr. \qquad \ldots\ldots(2.5)$$

Equations (2.3) and (2.4) are given by eqns. (5.7) and (5.12) of the previous paper (Rivlin 1949), and eqn. (2.5) can be obtained by simple analysis from eqn. (5.13). In general, $\partial W/\partial I_1$ and $\partial W/\partial I_2$ are functions of I_1 and I_2, which are given by

$$I_1=\lambda^2+\mu^2+\frac{1}{\lambda^2\mu^2}+\psi^2\lambda^2\mu^2r^2 \quad\text{and}\quad I_2=\frac{1}{\lambda^2}+\frac{1}{\mu^2}+\lambda^2\mu^2+\psi^2r^2. \qquad \ldots\ldots(2.6)$$

If the tube is subjected to a simple extension only, then $\mu=\lambda^{-1/2}$. The forces which must be applied in order to maintain μ at this value, so that there is no change of radius when the tube is subjected to a torsion of amount ψ, are given by introducing into eqns. (2.3), (2.4) and (2.5) $\mu=\lambda^{-1/2}$. If, further, we consider the torsion to which the tube is subjected to be infinitesimally small, we obtain, writing $P=-R_v$, where P may be considered an inflating pressure applied to the inner surface of the tube,

$$\left[\frac{M}{\psi}\right]_{\psi=0}=\pi\left(\frac{\partial W}{\partial I_1}+\frac{1}{\lambda}\frac{\partial W}{\partial I_2}\right)(a_1^4-a_2^4), \qquad \ldots\ldots(2.7)$$

$$[N]_{\psi=0}=2\pi\left(\lambda-\frac{1}{\lambda^2}\right)\left(\frac{\partial W}{\partial I_1}+\frac{1}{\lambda}\frac{\partial W}{\partial I_2}\right)(a_1^2-a_2^2) \qquad \ldots\ldots(2.8)$$

and
$$\left[\frac{P}{\psi^2}\right]_{\psi=0}=\lambda\frac{\partial W}{\partial I_1}(a_1^2-a_2^2). \qquad \ldots\ldots(2.9)$$

In these equations I_1 and I_2 are given by

$$I_1=\lambda^2+2/\lambda \quad\text{and}\quad I_2=2\lambda+1/\lambda^2, \qquad \ldots\ldots(2.10)$$

obtained by introducing $\mu=\lambda^{-1/2}$ and $\psi=0$ into (2.6).

Again we may consider the case when the inner surface of the tube is maintained force-free, i.e. $R_v=0$. We then have, from (2.5),

$$\int_{a_2}^{a_1}\frac{1}{\lambda\mu^2 r}\left(\frac{1}{\lambda^2\mu^2}-\mu^2\right)\left(\frac{\partial W}{\partial I_1}+\lambda^2\frac{\partial W}{\partial I_2}\right)dr=\psi^2\lambda\int_{a_2}^{a_1}r\frac{\partial W}{\partial I_1}dr, \qquad \ldots\ldots(2.11)$$

in which I_1 and I_2 are given by (2.6). In the limit as $\psi\to 0$ we obtain

$$\left(\frac{\partial W}{\partial I_1}+\lambda^2\frac{\partial W}{\partial I_2}\right)\int_{a_2}^{a_1}\frac{1}{\lambda\mu^2 r}\left(\frac{1}{\lambda^2\mu^2}-\mu^2\right)dr=\tfrac{1}{2}\psi^2\lambda\frac{\partial W}{\partial I_1}(a_1^2-a_2^2), \qquad \ldots\ldots(2.12)$$

where I_1 and I_2 are now given by (2.10). Equation (2.12) yields (cf. Rivlin 1949, §8), writing $\lambda\mu_1{}^2=\epsilon_1$ and $\lambda\mu_2{}^2=\epsilon_2$,

$$\left[\log\frac{\epsilon_1}{\epsilon_2}-\left(\frac{1}{\epsilon_1}-\frac{1}{\epsilon_2}\right)\right]\left(\frac{\partial W}{\partial I_1}+\lambda^2\frac{\partial W}{\partial I_2}\right)=\psi^2\lambda^2\frac{\partial W}{\partial I_1}(a_1{}^2-a_2{}^2). \qquad \ldots\ldots(2.13)$$

Since the material of the tube is incompressible, we have also

$$\chi(\epsilon_1-1)=\epsilon_2-1, \qquad \ldots\ldots(2.14)$$

where $\chi=a_1{}^2/a_2{}^2$.

Writing $\epsilon_1{}'=\epsilon_1-1$ and $\epsilon_2{}'=\epsilon_2-1$ in (2.13), neglecting terms of higher degree than the first in $\epsilon_1{}'$ and $\epsilon_2{}'$ and employing the relation $\chi\epsilon_1{}'=\epsilon_2{}'$, obtained from (2.14), we have

$$\epsilon_2{}'=-\frac{\frac{1}{2}\psi^2\lambda^2a_1{}^2\,\partial W/\partial I_1}{(\partial W/\partial I_1)+\lambda^2(\partial W/\partial I_2)}. \qquad \ldots\ldots(2.15)$$

If V represents the volume contained by the inner curved surface of the tube in its undeformed state and ΔV represents the decrease in volume resulting from the deformation, then $\epsilon_2{}'=-\Delta V/V$. The formula (2.15) is, of course, strictly valid only in the limiting case of infinitesimal amounts of torsion ψ.

§3. EXPERIMENTAL ARRANGEMENT

From eqn. (2.7) it is seen that, for a given value of the extension ratio λ, the relation between the torsional couple M and amount of torsion ψ should be linear, for sufficiently small values of ψ, for a tube of incompressible highly elastic material such as vulcanized rubber, which may be regarded as isotropic in its undeformed state. Similarly, from eqn. (2.9), it is seen that the relation between the inflating pressure P, which must be applied in order to prevent any decrease in diameter of the tube on twisting, and ψ^2 should also be linear for sufficiently small values of ψ.

In order to investigate these relations experimentally for a vulcanizate of natural rubber three circular cylindrical tubes with steel end-plates bonded to them were prepared by a moulding process according to recipe A given in the Appendix. These three tubes had lengths of 6 in. and external diameters of 1 in., while their internal diameters were ½ in., ⅝ in. and ¾ in.; they will be referred to as tubes 1, 2 and 3 respectively.

The experimental arrangement used is shown schematically in fig. 1. The rubber tube T was mounted in a framework F of steel rods by means of its end-plates E_1 and E_2, one end-plate E_1 being fixed. The other end-plate E_2 was held through a tension ball-race B so that it was free to rotate about the axis of the tube. The ball-race B was in turn held in a slide S by means of which the tube could be extended and clamped in any desired state of extension. The torsion was produced by hanging equal weights to strings passing over the pulley H attached to the end-plate E_2. This also carried a scale marked in degrees, which rotated past a fixed pointer as the end-plate E_2 rotated. A glass tube G of internal diameter about 3 mm, bent in the form shown in the figure, was connected to the end-plate E_1, communicating with the interior of the rubber tube through a hole in E_1.

The rubber tube with the attached glass tube G was filled with water before mounting in the framework, care being taken to exclude entrapped air. After mounting, a water manometer and bicycle pump were connected to the free limb of the tube G. The water level in this limb of G was adjusted to a level approximately that of the axis of the rubber tube and a fixed fiducial mark was placed at this level.

In carrying out the experiments the rubber tube was extended to the desired extent and the extension ratio λ was determined by measuring the distances in the undeformed and deformed states between two circumferential lines on it sufficiently far from the ends for end-effects to be avoided. It was then subjected to various amounts of torsion by adjusting the torsional couple on the pulley, while the volume of the tube was maintained constant by adjustment of the air pressure above the free surface of liquid in the tube G by means of the bicycle pump. For each value of the torsional couple the corresponding pressure was measured by means of the water manometer and the relative rotation of the end-plates by means of the scale attached to E_2. From this value of pressure and the length of the tube the amount of torsion was calculated. Strictly, the amount of torsion should have been measured over the central region of the tube to avoid end-effects, but in a subsidiary experiment it was found that the differences between the values for the amount of torsion obtained by the two methods were negligible.

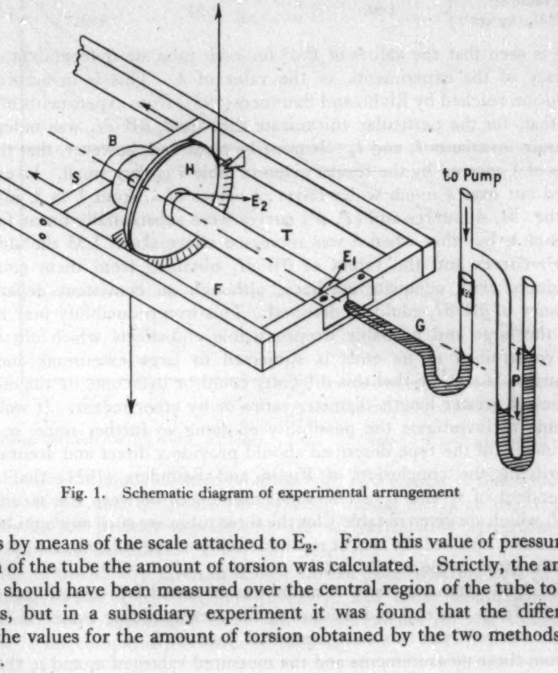

Fig. 1. Schematic diagram of experimental arrangement

§4. EXPERIMENTAL RESULTS

The corresponding values of M and ψ and of P and ψ^2, obtained experimentally in the manner described in the previous section for tubes 1, 2 and 3, yielded accurately linear relations for each value of λ employed over the range of values of ψ ($0-0{\cdot}15$ rad/cm approximately) covered by the experiments.

The slopes of the (M, ψ) and (P, ψ^2) curves are given in table 1 for various values of λ. From the values of P/ψ^2, together with the measured values of the external and internal radii (a_1 and a_2 respectively) of the tubes, we can calculate from eqn. (2.9), for each of the tubes, the value of $\partial W/\partial I_1$, corresponding to each value of λ employed. These are also given in table 1.

Table 1

Tube No.	1			2			3		
a_1 (cm)	1·27			1·27			1·27		
a_2 (cm)	0·635			0·794			0·953		
λ	1·00	1·17	1·27	1·00	1·16	1·315	1·00	1·205	1·30
M/ψ (kg cm^2/rad)	17·8	17·2	17·2	17·0	16·6	16·9	13·7	12·9	12·8
P/ψ^2 (kg/rad^2)	2·25	2·63	2·88	1·97	2·30	2·66	1·40	1·64	1·80
$\partial W/\partial I_1$ (kg/cm^2)	1·86	1·86	1·88	2·01	2·01	2·06	1·99	1·94	1·96
Mean value of $\partial W/\partial I_1$ (kg/cm^2)	1·86			2·03			1·96		

It is seen that the values of P/ψ^2 for each tube are independent, within the accuracy of the experiments, of the value of λ. This is in accord with the conclusion reached by Rivlin and Saunders (1951) from experiments of a different type that, for the particular vulcanizate they used, $\partial W/\partial I_1$ was independent of the strain invariants I_1 and I_2. It must be remarked, however, that the range of values of λ covered by the results given in table 1 is very small. In experiments carried out over a much wider range of values of λ, from 1 to 2, it was found that the (M, ψ) curves and (P, ψ^2) curves were substantially linear for all these values of λ, but that when λ was increased above about 1·35 the slopes of the (P, ψ^2) curves and the values of $\partial W/\partial I_1$ obtained from them could not be reproduced with adequate accuracy, although no consistent departure from constancy of $\partial W/\partial I_1$ could be detected. This irreproducibility may have arisen from the large and probably irreproducible end-effects which obtain when a tube constrained at its ends is subjected to large extensions and inflating pressures. It may be that this difficulty could be overcome by the employment of tubes of greater length–diameter ratios or by other means. It would appear desirable to investigate the possibility of doing so further since, in principle, experiments of the type described should provide a direct and accurate method of verifying the conclusion of Rivlin and Saunders (1951) that $\partial W/\partial I_1$ is independent of I_1 and I_2. The small differences between the mean values of $\partial W/\partial I_1$ which are given in table 1 for the three tubes are such as would be expected to occur as a result of the lack of reproducibility of the vulcanization process even when the same recipe is followed.

The load–extension ratio relation was obtained by suspending each tube vertically from one end and measuring the corresponding values of load N and distance between the two circumferential lines on it.

From these measurements and the measured values of a_1 and a_2 the values of $[\partial W/\partial I_1 + (1/\lambda)\partial W/\partial I_2]$ for various values of λ were calculated from eqn. (2.8) for each of the tubes. The relation between $[\partial W/\partial I_1 + (1/\lambda)\partial W/\partial I_2]$ and $1/\lambda$ was found to be linear in each case.

Assuming that $\partial W/\partial I_1$ is constant, as is indicated by the experiments of Rivlin and Saunders (1951) and (over a limited range of values of λ) by the results given in table 1, and taking as the value of $\partial W/\partial I_1$ appropriate to each tube the mean value given for it in table 1, we can obtain from these the relation between $\partial W/\partial I_2$ and λ for each of the tubes. With eqn. (2.10) this yields the relations between $\partial W/\partial I_2$ and I_2 for tubes 1, 2 and 3 which are plotted in fig. 2. The differences between these curves may, for the main part, result from experimental error since they can be accounted for by errors of about 2% in the values of $[\partial W/\partial I_1+(1/\lambda)\partial W/\partial I_2]$. It should be noted too that a small error in the value assigned to $\partial W/\partial I_1$ will give rise to much larger errors in the values of $\partial W/\partial I_2$ calculated in the manner described. For example, the broken line in fig. 2 is obtained from the $([\partial W/\partial I_1+(1/\lambda)\partial W/\partial I_2], 1/\lambda)$ relation for tube 1 by assuming a value for $\partial W/\partial I_1$ of 1·82 kg/cm² instead of 1·86 kg/cm². It is thus clear that no great accuracy must be attributed to the values of $\partial W/\partial I_2$ obtained.

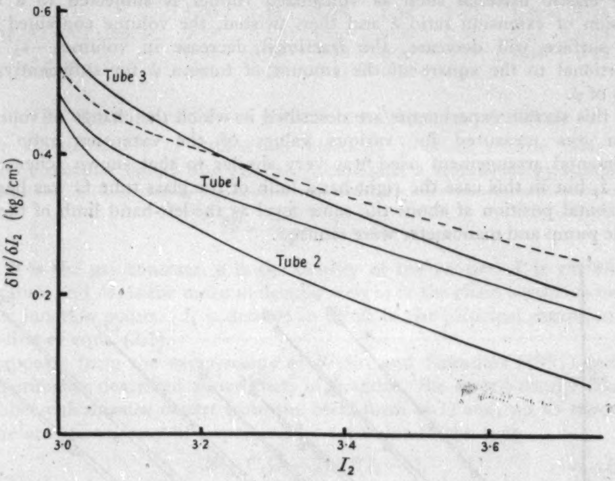

Fig. 2. Relations between $\partial W/\partial I_2$ and I_2 for tubes 1, 2 and 3. (Note : δ in ordinate should read ∂).

However, the general mode of their variation with I_2 is similar to that which was obtained by Rivlin and Saunders (1951) and, within the large experimental error involved, the present experiments are in quantitative agreement with those of Rivlin and Saunders.

From the values of M/ψ given in table 1 we can calculate from eqn. (2.7) the corresponding values of $[\partial W/\partial I_1+(1/\lambda)\partial W/\partial I_2]$, and these should agree with those obtained from the simple extension measurements for the values of λ considered. This comparison is made in table 2.

Table 2

Tube No.	1			2			3		
λ	1·00	1·17	1·27	1·00	1·16	1·315	1·00	1·205	1·30
$\partial W/\partial I_1+(1/\lambda)\partial W/\partial I_2$ from (M, ψ) curves (kg/cm²)	2·33	2·25	2·25	2·45	2·39	2·44	2·45	2·31	2·29
$\partial W/\partial I_1+(1/\lambda)\partial W/\partial I_2$ from simple extension measurements (kg/cm²)	2·35	2·21	2·15	2·50	2·35	2·24	2·55	2·35	2·28

The values of $[\partial W/\partial I_1 + (1/\lambda)\partial W/\partial I_2]$ for $\lambda = 1$ obtained from the simple extension measurements are those given by extrapolating the linear $([\partial W/\partial I_1 + (1/\lambda)\partial W/\partial I_2],\ 1/\lambda)$ relations to $\lambda = 1$. This procedure is not strictly correct, but the error involved is probably not greater than 1 or 2%.

A comparison similar to that in table 2 has already been made, by Rivlin and Saunders (1951) from more accurate measurements on a solid cylinder of vulcanized rubber.

§ 5. THE CHANGE OF VOLUME ON TORSION

From eqn. (2.15) it is predicted that if a circular tube of incompressible highly elastic material such as vulcanized rubber is subjected to a simple extension of extension ratio λ and then twisted, the volume contained by its inner surface will decrease, the fractional decrease in volume $-\epsilon_2'$ being proportional to the square of the amount of torsion ψ for sufficiently small values of ψ.

In this section experiments are described in which the change of volume on torsion was measured for various values of the extension ratio. The experimental arrangement used was very similar to that shown schematically in fig. 1, but in this case the right-hand limb of the glass tube G was bent into a horizontal position at about the same level as the left-hand limb of the tube, and the pump and manometer were omitted.

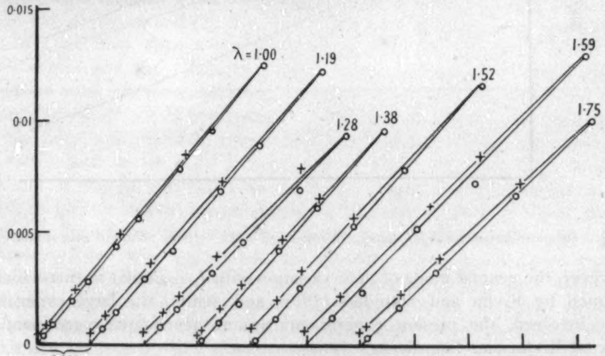

Fig. 3. Relation between fractional decrease of volume $-\epsilon_2'$ and $\lambda^2\psi^2$.

The change in volume resulting from torsion of the rubber tube was obtained by measuring the distance moved along the tube by the water meniscus. From a knowledge of the diameter of the tube, the volume change could then be calculated. The experiments were carried out for various values of the extension ratio λ in the range 1 to 1·75, using tube 3 employed in the experiments described in §§ 3 and 4.

The results obtained are shown in fig. 3, in which the fractional decrease in volume $-\epsilon_2'$ is plotted against $\lambda^2\psi^2$ for the various values of λ employed. The curves for successive values of λ are displaced parallel to the abscissa by

0·005 unit in order that they may be shown on a single graph. The circles denote the load increasing and the crosses the load decreasing directions. The apparent increase in hysteresis as λ increases may be noted. This will be discussed further in § 7. Here we shall restrict our remarks to the curves for the load increasing direction. It is seen that these are linear, in accordance with eqn. (2.15). From their slopes the values of $\frac{1}{2}a_1^2/(1+\lambda^2\Gamma)$ may be calculated for the various values of λ employed, where Γ is used to denote $(\partial W/\partial I_2)/(\partial W/\partial I_1)$. These values are given in table 3, together with the values of Γ calculated from them and those obtained from the values for $\partial W/\partial I_1$ and $\partial W/\partial I_2$ for tube 3 given in § 4.

Table 3

λ	1·00	1·19	1·28	1·38	1·52	1·59	1·75
$\frac{1}{2}a_1^2/(1+\lambda^2\Gamma)$ (cm²)	0·59	0·57	0·50	0·56	0·56	0·51	0·48
Γ	0·36	0·29	0·38	0·23	0·19	0·24	0·22
Γ (from § 4)	0·30	0·25	0·21	0·17	0·12		

§ 6. THE EFFECT OF STATE OF VULCANIZATION

The kinetic theory of rubber-like elasticity predicts, on the basis of an idealized molecular model of a rubber vulcanizate, a stored-energy function W given by

$$W=\frac{\frac{1}{2}\rho \boldsymbol{R}T}{M_c}(I_1-3), \qquad \ldots\ldots(6.1)$$

where $\boldsymbol{R}$ is the gas constant, ρ is the density of the rubber, T is the absolute temperature and M_c is the mean molecular weight of the chain segments between adjacent junction points. I_1 is defined in terms of the principal extension ratios by the first of eqns. (2.1).

It appears from the experiments of Rivlin and Saunders (1951) and from the experiments described above that, in practice, the stored-energy functions for rubber vulcanizates depart from the ideal form (6.1) and, up to moderately large deformations, may be expressed by formulae of the type

$$W=C_1(I_1-3)+f(I_2-3), \qquad \ldots\ldots(6.2)$$

where f is a decreasing function of (I_2-3).

The value of M_c, the mean chain segment molecular weight, for a rubber vulcanizate may be determined from measurements of the maximum volume to which the vulcanizate can be swollen by a suitable swelling agent. M_c is given by the Flory–Huggins formula (Flory 1942, Huggins 1942, Flory and Rehner 1943)

$$-\log(1-v_r)-v_r=\mu v_r^2+\frac{\rho V_0}{M_c}v_r^{1/3}, \qquad \ldots\ldots(6.3)$$

in which v_r is the volume fraction of dry rubber in the fully swollen vulcanizate, V_0 is the molar volume of the swelling agent and μ is an interaction constant characteristic of the particular rubber and solvent considered. The values of μ have been found experimentally by Gee (1946 a) for natural rubber swollen by a number of organic liquids.

It appears from the experiments of Rivlin and Saunders (1952) that the constant C_1 in eqn. (6.2) may be calculated roughly from the values of M_c for the vulcanizate so obtained by means of the formula

$$C_1=\tfrac{1}{2}\rho \boldsymbol{R}T/M_c. \qquad \ldots\ldots(6.4)$$

In this section we shall compare the values of C_1 so determined for a number of vulcanizates of different hardness with the values of $\partial W/\partial I_1$ (i.e. of C_1 in eqn. (6.2)) obtained by measurements of the type described in §§3 and 4.

Six tubes (4 to 9), each of length 15·0 cm and internal and external radii 0·794 cm and 1·28 cm respectively, were prepared by a moulding process according to recipes B given in the Appendix. It may be remarked that these vulcanizates are all sulphurless, and differ from each other only in the time for which they were vulcanized and the temperature at which the vulcanization was carried out. Steel end-plates were bonded to them as in the tubes used in the experiments described above. Simultaneous measurements of torsional couple M, amount of torsion ψ and inflating pressure P required to prevent any change in volume on twisting were made, with the tube in an unextended state ($\lambda=1$), in a manner similar to that described in §3. Particularly for the softer vulcanizates, it was not possible to attain a true equilibrium at each value of ψ, and in order to standardize the procedure the tubes were allowed to remain in each state of torsion for one minute before the reading was taken. The results of these measurements are shown in figs. 4 and 5, in which the circles represent measurements made for increasing load and the crosses those for decreasing load. In figs. 4 and 5 successive curves are displaced 0·05 unit and 0·005 unit respectively parallel to the abscissa for clarity of display.

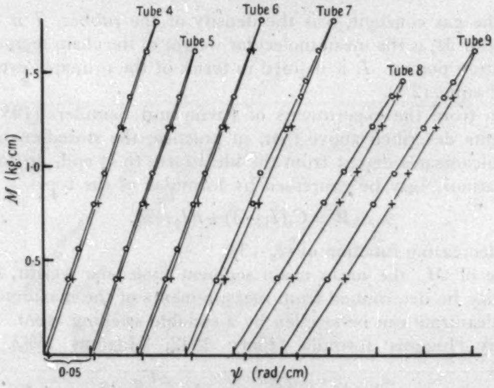

Fig. 4. Experimental relations between M and ψ for various degrees of vulcanization.

It will be noted that the amount of hysteresis exhibited by the (M, ψ) curves increases steadily as the rubbers become softer. On the other hand, the (P, ψ^2) curves show no appreciable hysteresis for any of the vulcanizates.

In order to determine the values of ρ/M_c for the vulcanizates, long strips were cut from each of the tubes and their lengths measured. These were then swollen in benzene for 24 hours at 21° c and their swollen volumes obtained from measurements of their swollen lengths. In each case the vulcanizate was immersed in benzene for a further 24 hours in order to verify that no appreciable further change in volume took place.

In each case the value of v_r in eqn. (6.3) is then given by the ratio of the volume of the dry rubber to that of the fully swollen rubber, and from this equation the values of ρ/M_c may be found for each of the vulcanizates, using the value 0·395 for μ obtained by Gee (1946 a) for the natural rubber–benzene system. From these values the values of C_1 (or $\partial W/\partial I_1$) given by eqn. (6.4) may be calculated.

In table 4 they are compared with the values of $\partial W/\partial I_1$ calculated from the (P, ψ^2) curves shown in fig. 5.

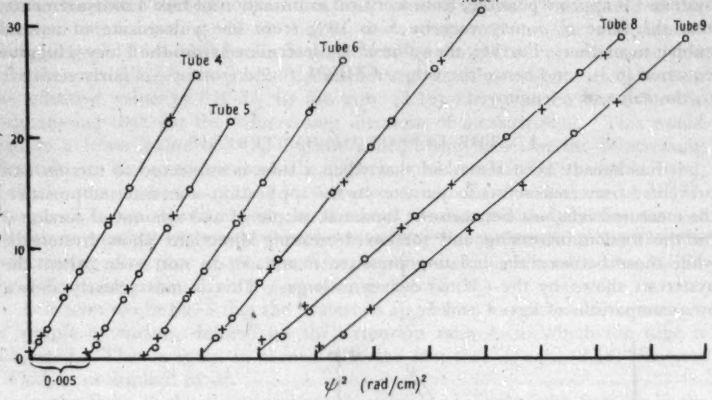

Fig. 5. Experimental relations between P and ψ^2 for various degrees of vulcanization.

Table 4

Tube No.	4	5	6	7	8	9
$\partial W/\partial I_1$ (kg/cm^2) (swelling)	1·69	1·63	1·48	1·20	0·75	0·58
$\partial W/\partial I_1$ (kg/cm^2) (from (P, ψ^2) curves)	1·68	1·63	1·49	1·24	0·87	0·86

It is seen that the agreement between the values of $\partial W/\partial I_1$ determined by the two methods is good, except in the last two cases, in which the vulcanizates were under-cured.

Similar determinations of $\partial W/\partial I_1$ from swelling measurements were made on strips cut from the three tubes used in the experiments described in §§ 3 and 4. The values so obtained for tubes 1, 2 and 3 were 1·82, 1·89 and 1·82 kg/cm^2 respectively, and that obtained from the (P, ψ^2) curves were, from table 1, 1·86, 2·03 and 1·96 kg/cm^2 respectively.

It appears possible from these experiments, and from those of Rivlin and Saunders (1952), that for adequately vulcanized rubbers the value of $\partial W/\partial I_1$ obtained from measurements of the load-deformation relations for a vulcanizate can be identified with that given by the kinetic theory from measurements of the mean chain segment molecular weight M_c by a swelling technique. If this is indeed the case, then from the value of $\partial W/\partial I_1 (= C_1)$ for a vulcanizate obtained by suitable load-deformation measurements—in particular the (P, ψ^2) relations obtained for the small torsion of a tube—it should be possible to calculate the value of M_c for the vulcanizate from eqn. (6.4). Further, in conjunction with maximum swelling volume measurements, this value of M_c could be used to determine the interaction constant μ in eqn. (6.3) for the rubber–liquid system concerned. However, it may be that the agreement between the values of $\partial W/\partial I_1$ found from load-deformation measurements and those calculated on the basis of the kinetic theory from the values of M_c determined from maximum swelling volume measurements is to some extent fortuitous. In calculating the values of M_c from the measurements of maximum swelling volume, the value of μ used was that determined by Gee (1946a) for the natural rubber–benzene system. It appears possible, from a critical examination of Gee's measurements, that the value of μ may vary by 5 to 10% from one vulcanizate of natural rubber to another. Further, the value of M_c determined from the Flory–Huggins equation (6.3)—and hence the value of $\partial W/\partial I_1$ found from it—is fairly sensitive to the value of μ employed.

§7. THE EFFECT OF HYSTERESIS

It has already been remarked that when a tube is subjected to torsion and prevented from contracting in diameter by the application of an internal pressure, the measured relations between the torsional couple M and amount of torsion ψ for the torsion increasing and torsion decreasing directions show hysteresis, while those between the inflating pressure P and ψ^2 do not, even when the hysteresis shown by the (M, ψ) curves is large. This is most clearly shown by a comparison of figs. 4 and 5.

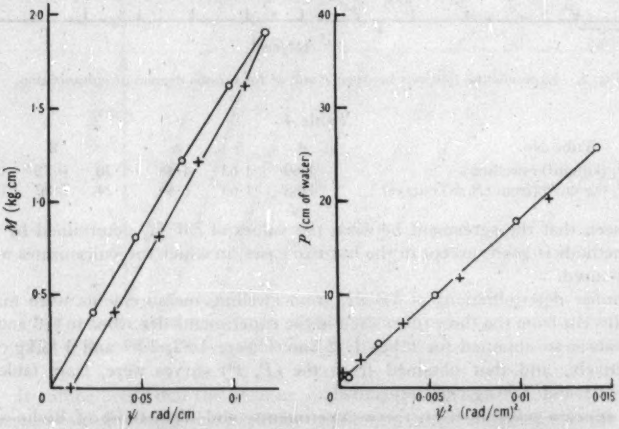

Fig. 6. Experimental relations between M and ψ and P and ψ^2 for Thiokol tube.

That this effect is not peculiar to natural rubber vulcanizates is shown by the curves of fig. 6, in which are plotted (M, ψ) and (P, ψ^2) relations for a tube of Thiokol rubber. These were obtained in a manner similar to that employed in §6, and using a tube of similar dimensions. The tube was prepared by a moulding process according to recipe C given in the Appendix.

Since the value of P for a given value of ψ is determined by $\partial W/\partial I_1$, while that of M is determined by $\partial W/\partial I_1 + \partial W/\partial I_2$, it is natural to assume that the hysteresis is associated with the terms in the stored-energy function W for the material which give rise to the term $\partial W/\partial I_2$, i.e. with the term $f(I_2-3)$ in the expression (6.2) for W.

The same conclusion is reached by a comparison of figs. 3 and 4. In fig. 4 it is seen that the (torsional couple M, amount of torsion ψ) relations measured in the direction of increasing torsion lie above those measured in the direction of decreasing torsion. On the other hand, from fig. 3 it is seen that the curves for the fractional decrease of volume $-\epsilon_2'$ plotted against ψ^2 measured in the direction of increasing ψ^2 lie below those measured in the direction of decreasing ψ^2. If the hysteresis demonstrated by the (M, ψ) curves is associated with the term $\partial W/\partial I_1$ in eqn. (2.7), then, for a given value of ψ, we should expect the effective value of $\partial W/\partial I_1$ in the eqn. (2.15) for ϵ_2' to be lower for the ψ-decreasing than for the ψ-increasing direction of measurement. This would lead to a lower value of $-\epsilon_2'$ for the ψ-decreasing than for the ψ-increasing direction, in disagreement with the experimental result. On the other hand, if the hysteresis shown by the (M, ψ) curves is associated with the term $\partial W/\partial I_2$ in eqn. (2.7), we should expect the observed result, since the effective value of $\partial W/\partial I_2$ in eqn. (2.15) would then be lower for the ψ-decreasing than for the ψ-increasing direction of measurement, leading to a higher value of $-\epsilon_2'$ for the ψ-decreasing than for the ψ-increasing direction.

It is seen too in fig. 3 that the hysteresis appears to increase with the amount of simple extension, defined by the extension ratio λ, to which the tube is subjected. This is again in accord with the fact that in eqn. (2.15) the term $\partial W/\partial I_2$ is multiplied by λ^2.

In the light of the above remarks it appears likely that the features in the structure of the vulcanizate which are responsible for the existence of hysteresis are those—or closely connected with those—which give rise to the term $f(I_2-3)$ in the stored-energy function for the material, i.e. to the terms $\partial W/\partial I_2$ in the load-deformation relations. The experiments described in § 6 and those of Rivlin and Saunders (1952) indicate that this term may also represent the departure, under static deformation conditions, of the stored-energy function for the material from the predictions of the kinetic theory.

It will, of course, be appreciated that the existence of any large amount of hysteresis in the vulcanizate strictly invalidates the use of a stored-energy function for the material in discussing its load-deformation relations, since such discussion depends on the assumption that the stored-energy function is related to the state of deformation. However, since our remarks regarding the relation of hysteresis and certain terms in the stored-energy function have been of a qualitative character only, the conclusions reached should not be invalidated.

§ 8. GENERAL CONCLUSIONS

It is seen from the foregoing experiments that the predictions of the theory of large elastic deformations regarding the forces necessary to maintain a state of torsion in a tube of incompressible highly elastic material are borne out by experiments with tubes of natural rubber vulcanizates. Moreover these experiments are in accord with the stored-energy functions W for the vulcanizates used, depending on the strain invariants I_1 and I_2 in a manner similar to that obtained by Rivlin and Saunders (1951). It appears that $\partial W/\partial I_1$ is a constant and $\partial W/\partial I_2$ decreases as I_2 increases, both of the quantities $\partial W/\partial I_1$ and $\partial W/\partial I_2$ being positive. It appears also that $\partial W/\partial I_2$, and hence the terms in the stored-energy function in I_2, are due to a mechanism in the highly elastic material which involves the hysteresis. Gee (1946 a) has conducted a series of experiments on the load-deformation relations for the simple extension of rubber vulcanizates swollen to different extents. His measurements for a natural rubber vulcanizate swollen in toluene are re-plotted in the form of a relationship between $v_r^{-1/3}[\partial W/\partial I_1+(1/\lambda)\partial W/\partial I_2]$ for the swollen vulcanizate and $1/\lambda$ for various values of v_r, the volume ratio of the dry rubber in the swollen vulcanizate, in fig. 7. It is seen that the relation for $v_r=0{\cdot}331$ has substantially the form

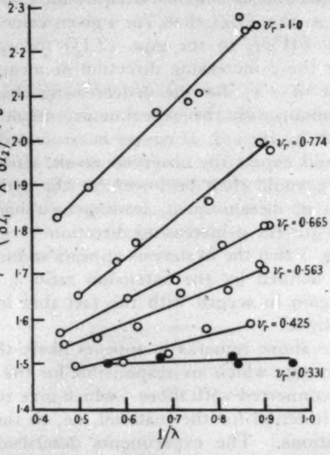

Fig. 7. Relations between $\partial W/\partial I_1+(1/\lambda)\partial W/\partial I_2$ and $1/\lambda$ for vulcanizates swollen in toluene to various extents (re-plotted from Gee's data). (Note : δ in ordinate should read ∂).

predicted by the kinetic theory of rubber-like elasticity, according to which, for a swollen vulcanizate, $\partial W/\partial I_2=0$ and $\partial W/\partial I_1$ is a constant proportional to $v_r^{1/3}$. Thus the relation plotted in fig. 7 for $v_r=0{\cdot}331$ represents the values for $[\partial W/\partial I_1+(1/\lambda)\partial W/\partial I_2]$ predicted on this basis for the dry rubber, while that plotted for $v_r=1$ represents the actual values for the dry rubber. It is seen that as the extension proceeds the difference between these two values decreases.

The experiments of Rivlin and Saunders (1952) suggest that the value of $\partial W/\partial I_1$ predicted by the kinetic theory for a dry vulcanizate, from the value of the mean chain segment molecular weight determined by measurement of the maximum swelling volume, can be identified roughly with that obtained from measurements of the load-deformation relations for a dry rubber. A similar conclusion is reached from the experiments described in § 6 of the present paper. However, in both cases the accuracy of this identification is open to question in view of our inaccurate knowledge of the correct value for the Huggins interaction constant used in determining $\partial W/\partial I_1$ from the measurement of the maximum swelling volume and the possibility of other complicating features in our interpretation of the swelling measurements. Gee (1946 b) has suggested that the departures of the load-deformation relation for the simple extension of a dry rubber vulcanizate are due to some form of secondary cross-linkages between the chain segments. This suggestion receives further support from the experiments described in the present paper and from those of Rivlin and Saunders (1952), and we can now summarize some of the properties which such cross-linkages would have to possess, as follows: (i) they can be broken by deformation of the rubber and, presumably, can reform in the deformed state in such positions as to relax part of the free energy of deformation of the macro-molecular network; (ii) they can be broken by swelling the rubber; (iii) hysteresis is associated with their breaking or re-formation; the property (iii) suggests that such linkages, if they exist, involve a relatively large number of molecules, as was envisaged by Gee.

If it transpires from future work that the values of $\partial W/\partial I_1$ for the dry vulcanizate calculated from measurements of its maximum swelling volume can, in fact, be identified with that obtained from load-deformation measurements on the dry vulcanizate, then it would further appear likely that all of the secondary linkages which can be destroyed by swelling of the rubber are also broken by deformation.

ACKNOWLEDGMENT

This work forms part of a programme of fundamental research undertaken by the Board of the British Rubber Producers' Research Association. Our thanks are due to Dr. G. Gee for allowing us to use his experimental data from which fig. 7 is plotted and for much helpful discussion.

REFERENCES

Flory, P. J., 1942, *J. Chem. Phys.*, **10**, 51.
Flory, P. J., and Rehner, J., Jr., 1943, *J. Chem. Phys.*, **11**, 521.
Gee, G., 1946 a, *Trans. Faraday Soc.*, **42**, 33; 1946 b, *Ibid.*, **42**, 585.
Huggins, M., 1942, *Ann. N.Y. Acad. Sci.*, **43**, 1.
Rivlin, R. S., 1949, *Phil. Trans. Roy. Soc.* A, **242**, 173.
Rivlin, R. S., and Saunders, D. W., 1951, *Phil. Trans. Roy. Soc.* A, **243**, 251; 1952, *Trans. Faraday Soc.* (in the press).

APPENDIX

PREPARATION OF THE VULCANIZATES

Recipe A. The mix employed had the following composition in parts by weight: natural rubber (smoked sheet) 100, sulphur 3, 2-mercaptobenzothiazole 0·5, stearic acid 1·0, zinc oxide 5, aldolnaphthylamines 1·0. Vulcanization was effected by heating for 45 min at 140° c.

Recipes B. The mix employed had the following composition in parts by weight: natural rubber (smoked sheet) 100, *tert*-butyl perbenzoate 2·5. The vulcanization conditions employed for the various tubes were:

Tube No.	4	5	6	7	8	9
Time of vulcanization (min)	60	30	25	40	25	15
Temperature of valcanization (°c)	140	140	140	130	130	130

Recipe C. The mix employed had the following composition in parts by weight: Thiokol RD 100, zinc oxide 5, N-cyclohexyl-2-benzthiozylsulphenamide 0·75, sulphur 1·5, tricresylphosphate 20, stearic acid 1. Vulcanization was effected by heating for 30 min at 153° c.

Thermal and Electrical Conductivity of Porous Metals made by Powder Metallurgy Methods

By P. GROOTENHUIS,* R. W. POWELL† and R. P. TYE†

* Mechanical Engineering Department, Imperial College of Science, London
† National Physical Laboratory, Teddington, Middlesex

MS. received 23rd January 1952

ABSTRACT. Measurements are reported of the thermal conductivity and electrical resistivity over the range of 20° c to 200° c on several specimens of a sintered porous bronze material (89% Cu, 11% Sn). The constituent powder particles were substantially spherical in shape and the specimens studied covered particle diameters ranging from 0·00133 to 0·040 cm and had densities from 5·27 to 7·01 g/cm³. The modified Lorenz relationship between the thermal conductivity K the electrical resistivity ρ and the absolute temperature T was found to apply, the experimental results satisfying the straight line $K=0{\cdot}58\times10^{-8}T/\rho+0{\cdot}005$. Existing data for solid bronzes of similar composition also conformed to this line. It is shown that, to a first approximation, the conductivities are independent of the particle size of the powder from which the specimen has been made, but can be correlated to a density basis, the values falling along a straight line drawn from the point for the solid material to cut the abscissa at a density corresponding to the maximum porosity which can be attained on packing equal sized spheres. This method of correlation is also confirmed by data from the literature for the electrical conductivity of copper, nickel and iron. Suggestions are made for estimating the thermal conductivities of similar porous materials.

§ 1. INTRODUCTION

Porous metallic materials are made from metal powder compacted under pressure and sintered in a reducing atmosphere at a temperature below the melting temperature of the metal. Very few thermal conductivity measurements have been reported for such materials, although some electrical resistivity data are available. A knowledge of the conductivity is required when the materials are exposed to a heat source (Grootenhuis, Mackworth and Saunders 1951). These porous materials differ from beds of particles in that there are two continuous phases in the former, the sintered material and the fluid filling the pores, whereas the latter has one continuous phase in the fluid filling the pores and one discontinuous phase in the particles. With the sintered materials most of the heat is conducted through the continuous solid structure, but in beds of particles the contact resistance between the particles is very large and most of the heat transference is due to the fluid filling the pores. Extensive correlation of thermal conductivity measurements for beds of particles such as those of Wilhelm, Johnson, Wynkoop and Collier (1948) cannot be applied to these sintered materials.

Measurements of the thermal and electrical conductivity of a porous bronze material with air filling the pores are given in this paper. In this instance the air in the pores has a negligible influence on the overall conductivity as the metal phase has a conductivity many times greater than that of air.

§2. DETAILS OF SPECIMENS

The material was a porous bronze alloy made from 89% Cu, 11% Sn powder by powder metallurgy methods,* and graded according to the particle size of the powder, grade A being made from the finest powder and grade E from the coarsest. The powder was made by the atomization process, which produces particles substantially spherical in shape. The size distribution and mean particle diameter of each grade was determined with a microscope. For grades A to E the diameters were 0·00133, 0·00493, 0·01275, 0·02113, 0·0400 cm respectively.

The specimens were in the form of discs, 26 in number. All but one of these were divided in five batches, containing one disc of each grade, and made up of three batches (suffix 1, 2, 3) of nominal thickness of 0·95 cm and two batches (suffix 4, 5) of nominal thicknesses 0·65 cm and 0·3 cm respectively. The density of each disc was determined from its weight and measured volume. The powder itself has a specific gravity of 8·7. The details of the specimens are given in table 2.

The remaining disc was an additional specimen of grade B, denoted as B_1', and was used to investigate the uniformity of the material. A bar 7·6 cm long and of 0·85 cm square section was cut from this disc in a diametrical position, and the room temperature electrical resistivity of the bar was measured over 1 cm lengths located at mean distances of 2, 3, 4, 5 and 6 cm from one end. The values obtained were 57·5, 56·6, 57·4, 54·5 and 54·4 microhm-cm. For two other small bars cut from the disc so that their lengths were perpendicular to the surface of the disc and equal to its thickness, resistivities of 53·8 and 56·5 microhm-cm were obtained. These measurements indicated the material to be fairly homogeneous.

Further tests indicated that any variation in density which might occur near the cut edges of the square sectioned bar would have a negligible effect on the conductivity of this bar, and it was concluded that such specimens would be suitable for the thermal conductivity determinations.

§3. EXPERIMENTAL METHOD

(i) *Thermal Conductivity and Electrical Resistivity Measurements—Batch* 1

A square sectioned bar machined from each specimen was joined to a standard bar of known thermal conductivity and a heating coil wound on the free end of the test bar. The composite bar was mounted centrally within a vertical guard tube, the test bar being uppermost and the lower end of the standard bar water cooled. The interspace between the bars and the guard tube was packed with heat insulating powder. A steady temperature was maintained in the specimens and lateral heat leakage prevented by suitable adjustment of the temperature of the guard tube. The temperature gradients in the test and standard bars were obtained from readings of thermocouples attached at points along their lengths and the heat flow in the test specimen was derived from the gradient set up in the standard bar. Electrical resistivity determinations were made in the course of the same experiment, using the thermocouples as the electrical contacts. The apparatus used has been described in an earlier paper (Powell and Hickman 1939). The temperature range was limited to 200° c because of severe oxidation of the material at higher temperatures.

---

* Supplied by Messrs. Sintered Products, Ltd., under the trade name of 'Porosint'.

.B
55
52

(ii) *Electrical Resistivity Measurements—Batches* 2–5.

The discs of batches 2–5 were required for other experiments and could not be cut into square bars as with batch 1. The resistivity at room temperature was determined by soldering two wires to the disc at diametrically opposite points and measuring the voltage drop along that diameter with two probes when a steady known current was passing through the disc. As all the discs were of substantially the same diameter the measured voltage drop multiplied by the effective thickness of the disc is proportional to the resistivity. The conversion factor between these readings and the absolute value of the resistivity was determined by a further test on a solid brass disc of dimensions similar to the specimens. A square bar was subsequently machined from this disc and its measured resistivity provided the required data to calculate the conversion factor.

The voltage drop across the discs was measured with two needle-like probes, rigidly mounted in a non-conducting support and held in contact with the disc under the weight of the support. Different pressures of contact gave no measurable difference in the reading. The probes were connected to potentiometer capable of being read to the nearest 0·001 millivolt. The use of a potentiometer ensured that no current actually passed through the probes. The probes were mounted 3·8 cm apart and placed an equal distance from each terminal point on the disc. Deliberate misplacings of the probes by as much as 0·25 cm did not give any appreciable variation in the reading. Various sizes of soldered joints for the current carrying wires were also tried but no measurable difference in the readings was observed. Several readings were taken on one specimen—in grade D—having four terminals situated at diametrically opposite points to check the uniformity of the material. This particular specimen was taken as it had the largest variation in thickness—±15 mm—from the mean thickness. The readings given in table 1 show that the material is uniform.

Table 1

Current (amp)	5	6	7	8	9	10
Direction I	0·098	0·122	0·146	0·164	0·183	0·205
Repeat I	0·098	0·122	0·145	0·163	0·184	0·206
Perpendicular to direction I	0·098	0·121	0·144	0·163	0·184	0·207

Values are in millivolts.

The coarser grades have a markedly rougher surface on one side than the other. Some measurements were taken for each side of these discs, but no measurable difference could be observed. All readings were subsequently taken on the smooth side. For the thinner specimens the effective thickness was taken to be the mean thickness as measured with a micrometer less one particle diameter. The specimens to which this correction was applied are indicated by an asterisk in table 2.

§ 4. RESULTS OF EXPERIMENTS

The experimental results for the six specimens of batch 1 are given in figs. 1 and 2. The measured resistivity values at 20° c and the thermal conductivity values derived for 50° c from fig. 1 are given in table 2.

The values of the thermal conductivity K and the electrical resistivity ρ were read for temperatures of 50, 100, 150 and 200° c from the curves drawn in the figures. In fig. 3 these values of K are plotted against T/ρ where T is the

Table 2. Details of Porous Bronze Specimens and Experimental Values

Specimen	Length of bar (cm)	Mean thickness (cm)	Density (g/cm³)	ρ at 20° c (microhm-cm)	K at 50° c (cal/cm sec °c)
A_1	8·87	0·882	6·45	33·0	$0{\cdot}061_5$
B_1	8·89	0·889	6·30	38·5	0·053
B_1'	7·60	—	5·85	57·1	$0{\cdot}035_5$
C_1	8·88	0·948	5·55	81·5	$0{\cdot}028_5$
D_1	8·89	0·932	5·75	52·0	$0{\cdot}039_5$
E_1	8·89	0·945	5·50	60·1	0·036
	Diam. of discs (cm)				
A_2	8·79	0·858	7·01	30·1	
B_2	8·80	0·871	6·31	38·9	
C_2	8·87	0·930	6·09	43·5	
D_2	8·87	0·884	6·76	32·1	
E_2	8·85	0·920	5·57	62·0	
A_3	8·87	0·884	7·00	27·5	
B_3	8·88	0·884	6·25	38·6	
C_3	8·87	0·967	5·60	79·4	
D_3	8·89	0·976	5·50	74·2	
E_3	8·85	0·940	5·50	63·2	
A_4	8·86	0·632	6·85	30·5	
B_4	8·86	0·642	6·13	41·0	
C_4	8·87	0·716	5·53	65·8	
D_4	8·85	0·703*	5·27	93·6	
E_4	8·86	0·604*	5·53	64·5	
A_5	8·75	0·297	6·90	30·4	
B_5	8·82	0·302	6·03	42·7	
C_5	8·80	0·293	5·28	92·0	
D_5	8·78	0·286*	5·58	63·3	
E_5	8·80	0·363*	5·70	60·6	

* Thickness as measured with a micrometer, less one particle diameter.

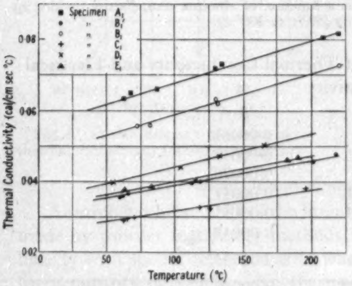

Fig. 1. Porous bronze: variation of thermal conductivity with temperature.

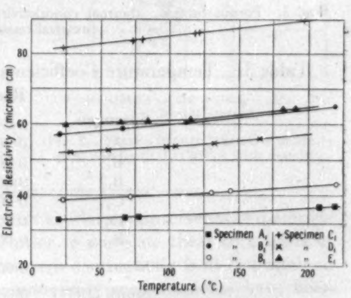

Fig. 2. Porous bronze: variation of resistivity with temperature.

corresponding absolute temperature. All the experimental points are seen to lie close to the straight line represented by the equation $K = 0{\cdot}58 \times 10^{-8} T/\rho + 0{\cdot}005$ where K is in cal/cm sec °c and ρ in ohm-cm.

Values for solid cast bronzes by Griffiths and Schofield (1928) for a bronze of 91·7% Cu, 8·0% Sn and 0·3% P at temperatures of 75° c to 250° c, and of

Smith (1931) for a bronze of 89·52% Cu, 10·4% Sn, 0·03% P, 0·005% Fe and 0·01% Pb at temperatures of 20° c to 200° c are included in fig. 3 and are seen to lie close to the extrapolated line through the present experimental points.

The effect of temperature on both the thermal conductivity and the electrical resistivity is represented in the form of temperature coefficients in table 3, which includes values derived from Smith's results. The temperature coefficient of thermal conductivity over the range 50–200° c is given by $\alpha = (K_{200} - K_{50})/150\,K_{50}$ and the temperature coefficient of electrical resistivity over the range 20–200° c is given by $\beta = (\rho_{200} - \rho_{20})/180\rho_{20}$. The mean values for the porous materials are in close agreement with the values for the cast material.

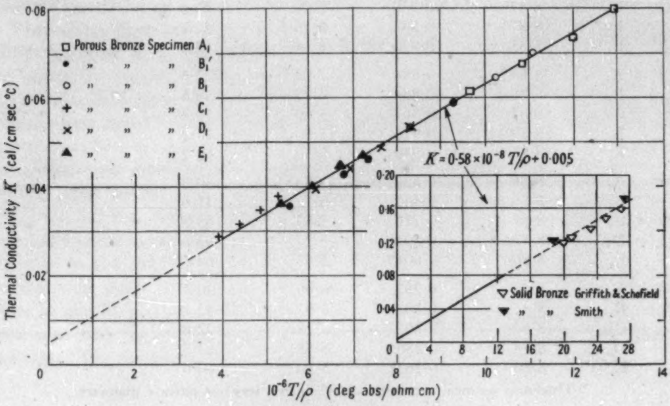

Fig. 3. Porous bronze: thermal conductivity as a function of absolute temperature divided by electrical resistivity (50° c to 200° c).

Table 3. Temperature Coefficients of Thermal Conductivity and Electrical Resistivity

Specimen	α	β
A_1	0·002	0·00061
B_1	0·0021	0·00059
B_1'	0·002	0·00070
C_1	0·0021	0·00057
D_1	0·0023	0·00053
E_1	0·002	0·00047
Mean	0·0021	0·00058
Smith (1931)	0·0021$_5$	0·00059

§ 5. DISCUSSION OF RESULTS

(i) *Experimental Data for Porous Bronze*

The results in figs. 1 and 2 show that the conductivities are independent of the particle size of the powder from which the specimens of the different grades were made. For example, the specimen of grade C_1 has the lowest conductivity, whilst B_1' differs appreciably from B_1 and has a conductivity of the same order as that of E_1, although the particle size of the latter grade is about eight times that of the former.

A correlation to a base of the density of the specimens is shown in fig. 4 for the thermal conductivity values at 50° c and in fig. 5 for the electrical conductivity values at 20° c. A point for solid bronze has been included in each figure and the experimental data are found to conform to the straight line drawn from this point to cut the zero abscissa at a density of 4·55 g/cm³. This density for zero conductivity corresponds to the maximum porosity which can be attained on packing equal sized spheres. The type of packing is then 1 on 1, and the porosity $100\ (1-\pi/6)$, which is 47·64%, and is independent of the size of the spheres. The corresponding density depends on the specific gravity of the material of the spheres and is equal to sp. gr. of sphere − sp. gr. of sphere × 47·64/100 which in the present instance reduces to 4·55 g/cm³.

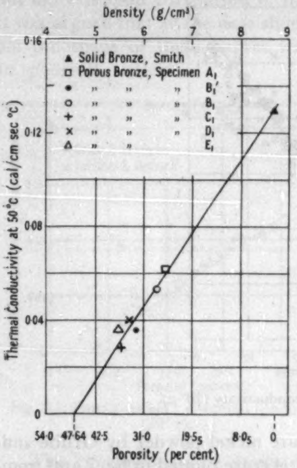

Fig. 4. Porous bronze: variation of thermal conductivity (50° c) with density.

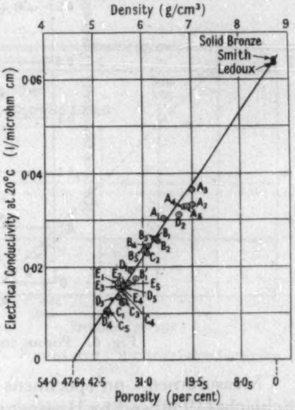

Fig. 5. Porous bronze: variation of electrical conductivity (20° c) with density.

(ii) *Other Materials—Analysis of the Literature*

A search has been made of the literature for similar measurements of materials made by powder metallurgy methods in order to correlate these to a basis of density with special reference as to whether zero conductivity is in fact attained for a porosity of 47·6%. No thermal conductivity measurements have been found other than those by Schwarzkopf (1946) for tantalum and WC–Co mixtures and Sandford and Trent (1947) for WC–TiC–Co alloys and in each case only one measurement was reported per alloy precluding any correlation to a specific gravity basis.

The electrical resistivity measurements are more numerous, particularly for pure copper. Only those measurements for which density data were also given have been correlated as shown in fig. 6, which gives the electrical conductivity at 20° c to a basis of density. A straight line drawn from the point for pure cast copper ($1/\rho = 0{\cdot}588$ (microhm-cm)$^{-1}$ for a density of 8·89) to zero conductivity for a density of 4·65, corresponding to 47·64% porosity, is a fair mean for most of the points by Adlassnig and Foglar (1950), Goetzel (1940), Hausner (1948), Hensel, Larsen and Swazy (1945), Kieffer and Hotop (1943) and Sauerwald and Kubik (1932). The data of Trzebiatowski (1934) seem to diverge considerably, but some doubt must be expressed as to the nature of the material experimented with, as the hardness figures reported seem extremely high. A Brinell number of up to 190 was given for several specimens. The copper powder was obtained by chemical decomposition of a copper oxalate.

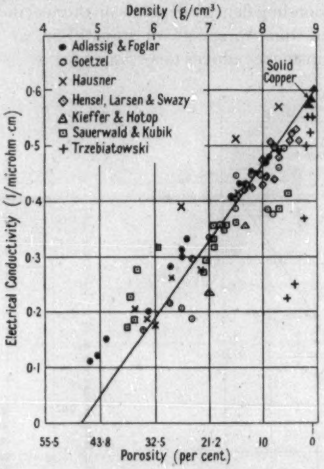

Fig. 6. Porous copper: electrical conductivity (20° c).

Measurements on specimens made from pure nickel powder by Grube and Schlecht (1938) and by Hausner and Dedrick (1949) are plotted in fig. 7 and from pure iron powder by Oliver (1947) and Sauerwald and Kubik (1932) in fig. 8. In both figures a straight line has been drawn from the point for the cast material to zero conductivity for a density corresponding to 47·64% porosity. Despite some considerable departures at low densities, a fair correlation along such a line is obtained for both metals.

Most of the data in figs. 6, 7 and 8 were obtained by reading the required quantities from various graphs in the publications. This leads to a certain degree of inaccuracy, particularly in the case of Sauerwald and Kubik (1932) who give curves of density plotted against sintering temperature which show a marked increase in density for a small increase in temperature. Kieffer and Hotop (1943) give a range of conductivity values for each density; a mean value has been plotted in fig. 6. The powders from which the specimens were made for all these experiments differed widely in size and shape. The points which are furthest from the straight line in fig. 6 are for those specimens which were made under conditions far removed from the accepted standards. For instance the lowest points by Trzebiatowski (1934) are for hot pressed specimens at 100 tons/in² but sintered at a temperature of only 20° c for the lowest point and 100° c for the next point. On the other side of the line the three highest points are by Hausner (1948) for specimens pressed at 10 tons/in² and sintered at 1 000° c which is very close to the melting point of copper.

These correlations also suggest that the particle size or shape has little direct effect on the electrical conductivity of porous metallic materials. This has also been observed by Rhines and Colton (1941) for Cu–Ni alloys, but no correlation between their observed values and density was given. The Cu–Sn powder used in the present experiments was of spherical shape and the copper powder used by Goetzel (1940) and by Hausner (1948) was non-spherical, being produced electrolytically. The iron powder used by Oliver (1947) was also non-spherical. Huttig (1950) and Huttig and Torkar (1949) have given a somewhat similar but more limited correlation of the electrical conductivity to a basis of density. It was argued that all the data should fall within a region bounded by two curves, but the shape of these curves was not derived. The correlation was limited to spherical particles.

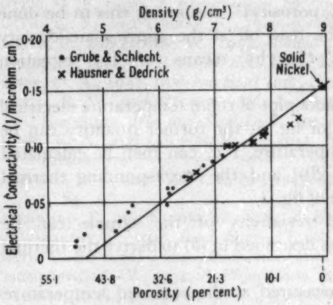

Fig. 7. Porous nickel : electrical conductivity (20° c).

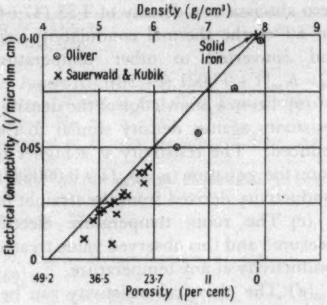

Fig. 8. Porous iron : electrical conductivity (20° c).

The conclusion to be drawn from these correlations is that the resistance to the flow of heat and electricity is mainly confined to the particles and not to the inter-particle bonds. If the latter were of importance then the particle dimensions would have a marked effect on the resistivity values as the nature of the bond depends on the particle size and shape and also on the manufacturing process used. The density, however, gives a measure of the volume of material present and if the resistance to the flow of electricity or heat is within the material, it is then dependent on the density alone. This applies to fully sintered, but not completely fused materials. Figure 6 shows that for specimens compacted under a high pressure but only partially sintered at a low temperature a high density is obtained but a low electrical conductivity. In this case the inter-particle bond contributes an appreciable amount to the resistance to the flow of electricity. On the other hand, for a sintering temperature close to the melting point of the material a general fusing of the particles occurs giving a high conductivity but not necessarily a correspondingly high density.

That zero conductivity is indicated for a density corresponding to that for the most porous type of packing with spheres is understandable for the specimens made from spherical powders as greater porosities could only be obtained in uniformly packed systems by a loss of contact between the particles, but it is not so apparent why this correlation should hold for specimens made from non-spherical powders. An insight into the mechanism of sintering is, however, afforded by this correlation for specimens made from originally irregular shaped particles, in that on sintering the grain growth between the particles at the points of contact produces a system having a density distribution similar to a system formed from particles originally spherical in shape.

(iii) *Methods for Estimating the Thermal Conductivity of Porous Metallic Materials*

On the basis of the above correlations several methods appear available for the estimation of the thermal conductivity of porous metallic materials. The porous bronze of the present experiments will be used as an example.

(*a*) Once the thermal conductivity of the solid cast bronze has been determined for any temperature within the required range a figure similar to fig. 4 can be constructed by joining the point for this maximum density to the zero abscissa at a density of 4·55 (47·64% porosity). Assuming this to be done for 50° c, the thermal conductivity can be read off at the appropriate density and converted to other temperatures $t°$ c by means of the equation $K_t = K_{50}[1 + 0{\cdot}0021\,(t-50)]$.

(*b*) From a knowledge of the density and a plot of room temperature electrical resistivity against density similar to that of fig. 5, the former quantity can be deduced. The resistivity at a higher temperature, $t°$ c, can then be calculated from the equation $\rho_t = \rho_{20}[1 + 0{\cdot}00058\,(t-20)]$ and the corresponding thermal conductivity derived from the straight line of fig. 3.

(*c*) The room temperature electrical resistivity of the sample can be measured and this observed value treated as described in (*b*) to derive the thermal conductivity at any temperature.

(*d*) The electrical resistivity can be measured at the required temperature and used directly with fig. 3 for the estimation of the corresponding thermal conductivity.

By way of illustration table 4 contains the observed values obtained for the thermal conductivity of each sample at 200° c, and estimated values as derived by each of the foregoing methods, (*a*)–(*d*).

Table 4. Comparison between the Observed and Estimated Values for the Thermal Conductivity at 200° c

Grade	Density	Observed	Estimated			
			(*a*)	(*b*)	(*c*)	(*d*)
A_1	$6{\cdot}4_5$	0·080	0·077	0·076	0·080	0·080
B_1	6·3	0·070	0·070	0·070	$0{\cdot}069_5$	$0{\cdot}069_5$
B_1'	$5{\cdot}8_5$	0·046	0·052	0·053	$0{\cdot}048_5$	$0{\cdot}047_5$
C_1	$5{\cdot}5_5$	$0{\cdot}037_5$	0·040	0·041	$0{\cdot}035_5$	$0{\cdot}035_5$
D_1	$5{\cdot}7_5$	0·053	0·048	0·049	0·053	0·053
E_1	5·5	0·047	0·038	0·039	0·046	0·047

As would have been anticipated, the methods involving an actual measurement of the electrical resistivity are to be preferred.

ACKNOWLEDGMENTS

The thermal conductivity and electrical resistivity determinations to 200° c on the samples from batch 1 were carried out in the Physics Division of the National Physical Laboratory and the room temperature resistivity measurements on the other samples were made in the City and Guilds College.

The paper is published with the approval of the Chief Scientist of the Ministry of Supply and of the Director of the National Physical Laboratory.

REFERENCES

Adlassnig, K., and Foglar, O., 1950, *Radex-Rundschau*, Pt. 2, 79.

Goetzel, C. G., 1940, *J. Inst. Met.*, **66**, 319.

Griffiths, E., and Schofield, F. H., 1928, *J. Inst. Met.*, **39**, 337.

Grootenhuis, P., Mackworth, R. C. A., and Saunders, O. A., 1951, *Proc. Instn. Mech. Engrs., Discussion on Heat Transfer*, London.

Grube, G., and Schlecht, H., 1938, *Z. Elektrochem.*, **44**, 367.

Hausner, H. H., 1948, *Powder Met. Bull.*, **3**, 4.

Hausner, H. H., and Dedrick, J. H., 1949, *The Physics of Powder Metallurgy Symposium, Sylvania Electrical Products Inc.* (London : McGraw-Hill, 1951), p. 321.

Hensel, F. R., Larsen, E. I., and Swazy, E. F., 1945, *Metals Technology*, **12**, No. 5, Paper T.P. 1810.

Huttig, G. F., 1950, *Z. Elektrochem.*, **54**, 89.

Huttig, G. F., and Torkar, K., 1949, *Kolloidzschr.*, **115**, 24.

Kieffer, R., and Hotop, W., 1943, *Kolloidzschr.*, **104**, 208.

Ledoux, R., 1912, *C. R. Acad. Sci., Paris*, **155**, 35.

Oliver, D. A., 1947, *Iron and Steel Inst., Special Report* No. 38 (9), p. 63.

Powell, R. W., and Hickman, M. J., 1939, *Second Report of the Alloy Steels Research Committee, Iron and Steel Inst., Special Report* No. 24, p. 242.

Rhines, F. N., and Colton, R. A., 1941, *Symposium on Powder Metallurgy, Amer. Soc. Metals*, 67.

Sandford, E. J., and Trent, E. M., 1947, *Iron and Steel Inst., Special Report* No. 38 (13), p. 84.

Sauerwald, F., and Kubik, St., 1932, *Z. Elektrochem.*, **38**, 33.

Schwarzkopf, P., 1946, *Prod. Engr.*, **17**, 268.

Smith, C. S., 1931, *Trans. Amer. Inst. Min. Met. Engrs., Metals Division*, **93**, 176.

Trzebiatowski, W., 1934, *Z. Phys. Chem.* A, **169**, 91.

Wilhelm, R. H., Johnson, W. C., Wynkoop, R., and Collier, D. W., 1948, *Chem. Eng. Progr.*, **44**, 105.

Effects associated with the Flow of Vacancies in Intermetallic Diffusion

By R. S. BARNES

Atomic Energy Research Establishment, Harwell, Berks.

MS. received 7th January 1952

ABSTRACT. Experiments on the interdiffusion of copper–alpha-brass and copper–nickel couples and sandwiches have shown that there is an increase of volume in the diffusion zone as a result of diffusion. This increase in volume is associated with the formation, in the diffusion zone, of voids with crystallographic faces. These voids appear near to the original interface and on that side from which there is a net loss of atoms, or a net gain of vacancies, as shown by the movement of inert markers. Grain boundaries influence the movement of the markers in regions where there has been preferential grain-boundary diffusion. A close micrographical examination of the diffusion zone shows it to have an unusual structure, various observations pointing to the presence of strain, and x-ray back reflection photographs of a copper–nickel couple show that the diffusion zone is polygonized. Subsidiary experiments suggest how strain in the diffusion zone arises.

A vacancy diffusion mechanism where there is a preferential flow of vacancies in the one direction, is used to explain the above phenomena. This flow will produce strain in the diffusion zone if vacancies are generated on one side of the original interface and collapse on the other. Mechanisms are discussed for the generation and condensation, within the diffusion zone, of the large numbers of vacancies necessary for the process. To explain the volume increase and formation of voids it is postulated that not all the vacancies on the one side of the interface are eliminated by the lattice collapsing, but that some vacancies coalesce to form microscopic voids which enlarge by assimilating further vacancies.

§1. INTRODUCTION

A STUDY of the diffusion mechanism is necessary because of the technological importance of diffusion itself, but as diffusion is an atomic process these studies can be used as an additional means of gaining information on the atomic configuration in metals. This should prove invaluable in the study of lattice imperfections which play so large a part in the behaviour of metals.

The calculations of Huntingdon and Seitz (1942) were until recently the only indication to the atomic mechanism of diffusion. They showed that a vacancy mechanism is more probable than either a direct atomic interchange or an interstitial mechanism by comparing the calculated activation energies for these three mechanisms using a theoretical model for the copper atom. This comparison has recently been extended by Zener (1950) to include a cyclic mechanism involving more than two atoms, but even this process is less probable than a vacancy mechanism (Seitz 1950).

Smigelskas and Kirkendall (1947) in their experiments with copper–alpha-brass couples demonstrated that inert markers placed at the original interface move towards the zinc-rich side as diffusion proceeds (the 'Kirkendall effect') suggesting that there is an unequal flow of atoms over the original interface. This has now been confirmed by Correa da Silva and Mehl (1951) using various types of marker at the interface of various couples. The existence of this unequal flow rules out the possibility that the sole diffusion mechanism is one of direct interchange as was pointed out by Seitz (1950). Darken (1948) and Seitz (1948) have discussed the Kirkendall effect from a theoretical point of view.

It is the purpose of these experiments to look more closely into the Kirkendall effect and particularly to study the effects of the large number of vacancies upon the nature of the diffusion zone.

§ 2. MARKER MOVEMENTS IN A COPPER–ALPHA-BRASS COUPLE

In view of the importance of the experiment of Smigelskas and Kirkendall (1947) their experiment was repeated in a slightly modified form. A block of commercial purity 72/28 alpha brass was machined and ground so that the two largest faces were flat and parallel. A wolfram wire was wrapped round this block, then electrolytically cleaned, and embedded in the two largest faces by pressing between two flat steel blocks. The two faces were once again ground flat and parallel, so that the included wolfram wires were flush with the surface, having lost their circular cross section. The whole block was then chemically cleaned and plated with copper in a copper sulphate bath to a thickness of about half a centimetre. Two new surfaces, one on each side of the block, were then machined in this plated copper, parallel to the two wire-marked surfaces. A wolfram wire was embedded in these as before, and a further layer of copper deposited. Figure 1 is a diagram of the cross section of the final arrangement.

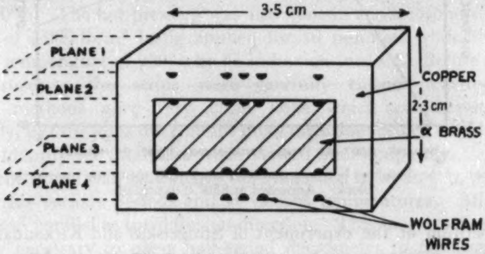

Fig. 1. Copper–α-brass block.

After measuring the distances between planes 2 and 3, and 1 and 4 (fig. 1) with a travelling microscope, the block was annealed *in vacuo* at 400° c to remove any gases entrapped in the electrodeposit, and then given diffusion anneals for various periods at 850° c in an argon atmosphere. Brass filings were placed near the exposed brass surface of the block to reduce the evaporation of zinc from the block. After removing about 2 mm from the cross sectional surface by machining and polishing, the distances between the planes were measured after each anneal.

The mean distances between the two sets of planes 2 and 3 and 1 and 4 are plotted against the square root of the annealing time in fig. 2. These results confirm that the interface markers move towards the zinc-rich region, a distance which is roughly proportional to the square root of the annealing time. The movement in this case (0·001 cm/h$^{1/2}$/interface) is more rapid than that obtained by Smigelskas and Kirkendall, consistent with the fact that these workers used a lower temperature of 785° c.

The two extra planes 1 and 4, however, showed rather surprising movement, for they moved apart, the distance also obeying a (time)$^{1/2}$ law (fig. 2). An increase in the annealing temperature produced more rapid changes in both distances.

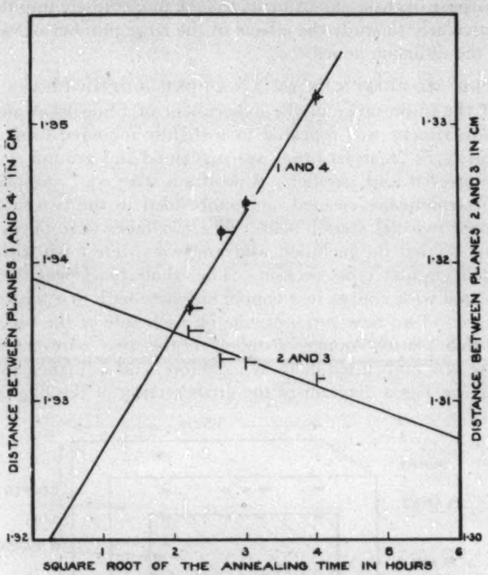

Fig. 2. Variation of the distances between marked planes with annealing time in the copper–α-brass block. Annealed at 850° c in argon.

This repetition of the experiment of Smigelskas and Kirkendall confirmed that the interface markers move towards the zinc-rich region as diffusion proceeds. The results can be explained if the zinc diffuses more rapidly than the copper, causing a net loss of atoms from the zinc-rich region, as was first suggested by Smigelskas and Kirkendall (1947).

Further to this result, however, the movement of the outer sets of wires suggests that the volume of the couple is increasing, and as the increase is proportional to the square root of the annealing time, it suggests that this too is a result of diffusion, and that it occurs in the diffusion zone. However, as the movement is only about 1% of the distance between the planes, any slight change in the volume of the material between the outer markers might produce such a movement. Several causes for the relative movement of the planes 1 and 4 can be envisaged; the electrodeposited copper may swell on annealing, or zinc vapour may diffuse in, to give a volume increase.

§ 3. VOLUME INCREASE IN COPPER–NICKEL SANDWICHES

The above experiments served to confirm the Kirkendall effect in copper–alpha-brass couples, but it remained to be established whether the volume change was a result of the diffusion process and not a special property of this system, or dependent upon the presence of electrodeposits, etc.

Multiple sandwiches of thin interleaved sheets of two metals were used so that any increase of volume in the diffusion zone would produce a very large easily measured increase in the volume of the sandwich as a whole; the effect of volume changes in the undiffused metals would be relatively small. The copper–nickel system was chosen as it is one that has complete solid-solubility and evaporates less than any system containing zinc. The large block used in the previous experiment had been turned down in a lathe to remove the surface layer after each anneal, before the measurements were taken, and this might have introduced severe distortion into the block. This was now avoided by reducing the size of the specimen so that it could be conveniently ground down by hand.

Six different types of sandwich (see table) were prepared either by hot-rolling or hot-pressing stacks of copper and nickel strips. These strips were of either commercial purity copper and nickel or Johnson Matthey spectroscopically standardized copper and nickel which had been rolled into strip. The spectroscopically standardized copper had been prepared by melting and casting the metal *in vacuo*. The copper and nickel strips used were of approximately the same thickness. The hot-rolled sandwiches were produced by rolling a stack of alternate copper and nickel strips to about 50% of their original thickness, while in an atmosphere of hydrogen to deoxidize the surfaces, and at a temperature of about 700° c. The hot-pressing was also done in an atmosphere of hydrogen, a pressure of 3 000 lb/in^2 being applied for 10 minutes, while the metal was heated to a temperature of 900° c by an induction furnace. Before both of these welding processes the strips were carefully cleaned chemically. Both fabricating methods gave very clean joins which could not be broken mechanically, but the joins did contain small inclusions which could conveniently be used to identify the interfaces when viewed microscopically.

Pieces cut from these sandwiches were annealed in hydrogen, purified argon, or vacuum for various periods and at various temperatures. All increased in the dimension parallel to the diffusion direction. This increase was so large that it was only necessary to use a ball-ended micrometer to measure the change. Figure 3 is a graph showing the increase of thickness plotted against the square root of the annealing time for two similar hot-rolled sandwiches made from commercial material, which were annealed separately at 1 000° c.

The increase in the thickness in these sandwiches might have been a result of a change in shape rather than an increase of volume, but measurements taken in the two directions perpendicular to the direction of diffusion also increased, so the increase in thickness really did represent an increase in volume of the sandwiches. The percentage change in these two dimensions perpendicular to the diffusion direction are also plotted in fig. 3. The lengths measured parallel to the rolling direction and perpendicular to it gave identical percentage increases, the increases being very small until after 36 hours of annealing when the rate of increase became similar to the rate of increase of the thickness.

As a further demonstration that the *volume* of the sandwiches was increasing, the densities of the sandwiches were measured using a simple displacement method, and these results are also plotted in fig. 3. The density decrease which was also proportional to the square root of the annealing time, confirmed that the volume does increase since the weights of the sandwiches remained constant. The increase in the volume as calculated from the density measurement correlates well with the increase calculated from the increases in linear dimensions, for annealing times up to 36 hours, but thereafter the density measurements indicate a volume increase less than that given by direct measurements. At about 200 hours the density began to increase although the direct dimensional measurements suggested the volume was still increasing. This discrepancy may be explained by the porosity which was observed in sandwiches annealed for over 100 hours. Such porosity would cause the density measurements to become unreliable for anneals of this length of time.

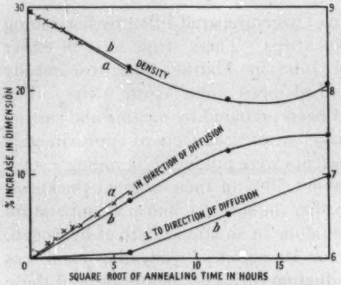

Fig. 3. Variation of the dimensions and density of two sandwiches prepared by hot-rolling commercial copper and nickel strips and annealed at 1000° c in argon.

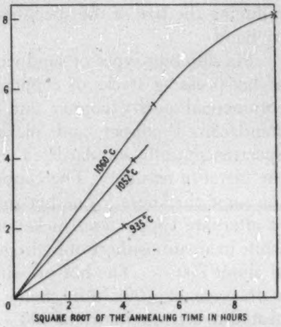

Fig. 4. Increase in thickness of three similar sandwiches prepared by hot-pressing spectroscopically standardized copper and commercial nickel and annealed in hydrogen at different temperatures.

The more rapid increase of volume at higher temperatures is illustrated by the graph in fig. 4 which is for similar sandwiches prepared by hot-pressing.

The increase in volume was found to deviate from its dependence upon the square root of time for long annealing times as can be seen in figs. 3 and 4. This reduction occurs at about the time when neighbouring diffusion zones meet.

As it was conceivable that the volume increase occurred during the heating to and cooling from the annealing temperature, a piece of a sandwich was thermally cycled from room temperature to 1 000° c, for five complete cycles, the heating period being approximately equal to the cooling period and of about five minutes duration. However, no increase in volume occurred, although these sandwiches when maintained at the high temperature increased in thickness as did the others.

The table gives values of the increase in thickness per copper–nickel interface for six various types of sandwich when all were annealed together in hydrogen for 25 hours at 1 065° c. It can be seen that for this short annealing time, where the saturation effect would not be expected to be important, the increase in thickness per interface is roughly the same for different sandwiches, although sample 6 showed a decrease in thickness, presumably because of evaporation from the exposed copper surface, this being the only sample not having nickel surfaces both at the top and bottom. Sample 6, although it had only one copper–nickel interface had eleven welded interfaces, as it was made from strips similar to those used in sample 3, but the strips were stacked with all the nickel strips and all the copper strips together. The table thus shows conclusively that the increase in thickness is dependent upon the number of diffusion interfaces, and not merely upon the number of welded interfaces in the sample.

Increase in thickness for six types of sandwich annealed in hydrogen for 25 hours at 1 065° c

Type of Sandwich	Materials		Number of Cu–Ni interfaces	Thickness (cm)	Increase in thickness (10^{-3} cm)	Incr/Cu–Ni interface (10^{-3} cm)
1 Rolled	Commercial	Cu	46	0·8075	74·0	1·61
	,,	Ni				
2 Rolled	Commercial	Cu	40	0·7160	59·5	1·49
	,,	Ni				
3 Pressed	Spec. pure	Cu	26	0·4920	22·5	0·865
	Commercial	Ni				
4 Rolled	Spec. pure	Cu	18	0·4290	19·5	1·08
	,, ,,	Ni				
5 Rolled	Spec. pure	Cu	4	0·3450	8·0	2·0
	,, ,,	Ni				
6 Pressed	Spec. pure	Cu	1	0·2065	−2·0	−2·0
	Commercial	Ni				

The following conclusions can be deduced from these experiments: (i) The increase in thickness of the sandwiches is proportional initially to the square root of the annealing time, but becomes less than this after prolonged annealing. (ii) The dimensions in the directions perpendicular to the diffusion direction increase appreciably only after about 36 hours of diffusion at 1 000° c. (iii) The higher the annealing temperature the more rapid is the volume increase. (iv) The volume increase is not caused by thermal cycling. (v) The volume increase occurs in all types of sandwich used and whether the annealing is performed in argon, hydrogen or vacuum. (vi) The volume increase occurs in the diffusion zone and is proportional to the number of copper–nickel interfaces. (vii) The increase in volume is much greater than could be expected from a lattice parameter effect alone.

§4. VOIDS IN THE DIFFUSION ZONE

The large decrease in the density of the diffusion zone suggested the presence of voids large enough to be seen under the microscope, and electropolished couples and sandwiches do show a series of roughly spherical pits, on the copper-rich side of the copper–nickel couples and on the zinc-rich side of the copper–alpha-brass couples. Figure 5 (Plate I) illustrates these pits in a copper–nickel couple. However, it was not certain that the pits did not result from the polishing process, and even if they were a result of voids in the material, the void shape would have been destroyed by the electrolytic process. Two copper–nickel couples were therefore mechanically polished very slowly for several hours using fine alumina. After polishing in this way a series of definite voids was revealed in the same position as the pits noticed on electrolytic polishing. It was found that any slight working of the surface layer tended to smear metal into the voids so that they were liable to be missed. Photomicrographs of these voids (fig. 6 Plate I) show their cross section to possess straight sides, indicating that the voids themselves are polyhydral in shape. A microradiograph* (Betteridge and

---

* The microradiograph was taken by Mr. R. S. Sharpe of the Bristol Aeroplane Co. Ltd.

Sharpe 1948) of a 0·002 in. section of a diffused sandwich confirms this (fig. 7, Plate I) and as this x-ray method reveals the shape of all the voids present, including those entirely within the metal, the polyhedral nature of the voids cannot be merely a result of the polishing process.

Although it is very difficult to obtain a true shape of the voids from the cross sections seen on polishing, many of the straight sides are found to be parallel to slip lines in the same grain, suggesting that the void faces are parallel to {111} planes. Furthermore, many of the cross sectional shapes can be correlated with cross sections of a regular octahedron. Voids lying in one grain can be correlated with one orientation of an octahedron, and in other grains with other orientations. These observations are not conclusive because of the rather irregular nature of micrographs such as fig. 6, but do suggest that each void is a regular {111} octahedron.

An examination of the voids in the two photomicrographs in fig. 6 reveals that although the number of voids in a given length is approximately the same, that couple which has been annealed at 1 010° c contains voids on the whole smaller than those in the couple annealed for the same time at 1 080° c. Figure 8 (Plate II) illustrates the effect of annealing time upon the voids. Although the sandwich has been electropolished, the pit size does indicate that the voids progressively increase in size as diffusion proceeds, although the number of voids seems to remain constant.

An estimation of the total volume occupied by the voids shown in fig. 6 (*b*) gives a value of 0·001 cm^3 per cm^2, and this is of the same order as the increase in volume per unit area per interface of similar sandwiches annealed under similar conditions.

The voids are seen to lie roughly in a plane parallel to the original interface, but some little distance from it (fig. 5), the regularity of this plane being particularly marked in those samples annealed at high temperatures.

Thus, micro-examination of the samples has demonstrated that voids exist in the diffusion zones of all couples and sandwiches investigated, regardless of their preparation or treatment. That these voids are probably the main cause of the observed volume increase on diffusion is suggested by the fact that the total volume is of approximately the value necessary to explain the volume increases observed in sandwiches, and also as the size of the voids is seen to increase when either the annealing time or the temperature is increased.

§ 5. MICROSTRUCTURE OF THE DIFFUSION ZONE

By making the couples from a stack of strips instead of from two solid blocks the inclusions at each weld could be used to mark planes in the copper and nickel (e.g. DE and FG, fig. 9, Plate II) and the relative movement of the markers at the original interface, HI, could be easily observed. The movement was towards the copper-rich region, as reported by Correa da Silva and Mehl (1951).

In those couples which show marked preferential diffusion along the grain boundaries of the nickel, the row of small inclusions demarking the original interface shows a bulge towards the copper-rich side in those regions where preferential diffusion has occurred. Figures 10 and 11 (Plate III) illustrate the nature of some of these bulges. The couples have been electropolished and etched as previously described (Barnes 1950) to locate the position of a particular concentration contour. This reveals the extent of the diffusion of the copper into the nickel and clearly demonstrates the greater penetration into the grain boundaries. The radius of curvature of the bulge is larger in those cases where the diffusion zone is larger as can be seen by examining the two figures. In those couples annealed at high temperatures, where the preferential grain-boundary diffusion is negligible, bulges do not occur (see fig. 5). These bulges demonstrate the fact that the Kirkendall shift is larger in the neighbourhood of a grain boundary than it is where only normal lattice diffusion is taking place.

These photomicrographs are perhaps the most clear proof of the existence of a Kirkendall shift and, further, demonstrate that the preferential grain-boundary diffusion is a result of copper atoms diffusing into the boundary rather than nickel atoms diffusing out of the boundary; this latter would produce a bulge into the nickel-rich region.

The configuration of the grain boundaries in the diffusion zone and particularly on the nickel-rich side of the original interface, bears very little resemblance to that outside the zone. Twin boundaries in this region are very often curved (see fig. 11), an indication that the region has suffered violent distortion. Also several weak 'ghost' boundaries can be seen in micrographs such as fig. 5.

The presence of these features in the micro-structure suggest the existence of strain in the diffusion zone. An x-ray investigation was undertaken in an attempt to verify this.

§6. X-RAY INVESTIGATION OF THE DIFFUSION ZONE

A series of x-ray back-reflection Laue photographs using gold radiation was taken using a microbeam camera, to be described by Cahn, with a 50μ collimator, and with facilities for locating precisely the area to be photographed on the sample. Figure 9 is a photomicrograph of the region which was investigated, the small circles representing the individual areas of which x-ray photographs were taken.

Areas outside the diffusion zone gave quite sharp spots in the Laue pattern, but all areas within the diffusion zone gave a pattern with a series of spots near each position where a single spot normally appeared, revealing that the diffusion zone was polygonized. Figure 12 (Plate IV) is a typical back-reflection photograph taken of the region marked O in fig. 9. Each photograph could be interpreted as showing the presence of from two to four 'polygons' in the small area irradiated, the angle between each polygon being about 2°. The boundaries of these polygons were perhaps those faint ghost boundaries referred to above.

§7. EXPERIMENTS TO ILLUSTRATE THE CAUSE OF STRAIN IN THE DIFFUSION ZONE

Two subsidiary experiments were performed to indicate how the strain in the diffusion zone could arise.

A thin nickel foil about 0·005 cm thick was welded between thick copper sheets to form a sandwich, using the hot-pressing technique outlined above. This was then annealed *in vacuo*, and since copper evaporates more readily than nickel, the nickel at the edges was left raised above the level of the surrounding copper after the anneal. However, this raised nickel-rich portion was no longer straight but extremely distorted. Presumably an increase in the volume of the nickel had caused the free portion of the nickel to take up this distorted form, whereas that portion which was restricted by the copper was unable to relieve its stresses in this manner, and had, presumably, expanded only in the direction of diffusion.

The other experiment demonstrated that nickel free from external restraint could also distort in shape as a result of copper atoms diffusing into it. Two thin polycrystalline nickel foils, one 0·012 cm and the other 0·024 cm thick were annealed and then exposed while hot, on one side only, to copper atoms, by placing them in an alumina boat with a copper foil over the top and heating the arrangement in a vacuum furnace for 18 hours at 1 080° c. The copper evaporated on to the exposed surfaces of the nickel foils and diffused in, the foils increasing in weight and thickness as a result. At the completion of this treatment, the foils were both curved so that their centres of curvature lay on the side away from the copper foil. The radius of curvature of the thicker of the two foils was approximately 1 cm and that of the thinner 0·5 cm. Similar foils which were shielded from the copper atoms remained flat.

An x-ray back-reflection Laue photograph of the thinner strip, as it was when introduced to the furnace, gave a normal pattern, but after evaporated copper had been diffused in the bent strip was found to be polygonized (fig. 13, Plate IV). A comparison of fig. 13 with the Laue photograph taken of the diffusion zone of a couple (fig. 12) suggests that the polygonization arises from the same cause in the two cases.

§ 8. DISCUSSION OF RESULTS

Measurements on the copper–alpha-brass block confirmed that the marked original interface moves towards the zinc-rich side during diffusion and also suggested that the volume of a diffusion couple increases on diffusion, but the experimental arrangement was such that no definite conclusion could be drawn on this latter point. However, the results using copper–nickel sandwiches, besides confirming that the original interface moves, in this case towards the copper-rich region, definitely reveal a volume increase in the diffusion zone as a result of diffusion. It is apparent that the microscopic voids which appear as a result of diffusion are the main cause of this volume increase.

Figure 14 represents (*a*) a couple consisting of metals A and B, and (*b*) this couple after diffusion has occurred. The movement of the original interface, the volume increase, the extent of the diffusion zone, and the voids are all represented in this figure. If in the case of the copper–alpha-brass couple the metal A represents the copper and B the brass, and for the copper–nickel couple A represents the nickel and B the copper, then the figure represents the results for both couples.

To account for the movement of the original interface y in the negative direction, as shown in fig. 14, it is necessary to postulate a net flow of atoms in the positive direction and this is equivalent to a net flow of vacancies in the negative direction. If the interface moves 0·01 cm during the course of diffusion, and this is the order of the movement obtained, then this represents a net transport of the order of 10^{21} vacancies across unit area of the interface. To maintain this large flow of vacancies, it is necessary that vacancies should be generated on the A-rich side of the interface. The generation and diffusion away of such a large number of vacancies, which is equivalent to the gain of an equal number of atoms, will cause the A-rich region to expand and produce an increase in the distance xy (fig. 14) as is observed. Also, the large number of vacancies arriving on the B-rich side of the original interface will quickly cause the equilibrium number of vacancies in the region to be exceeded. As the distance yz (fig. 14) is observed to decrease on diffusing the couples, some of the vacancies, which have roughly the same volume as an atom, must disappear, otherwise yz would remain very nearly constant.

If, however, it is postulated that not all of the vacancies disappear, but that some coalesce to form voids, then the volume increase of the couple, and the voids found in the region with the net gain of vacancies, can be accounted for.

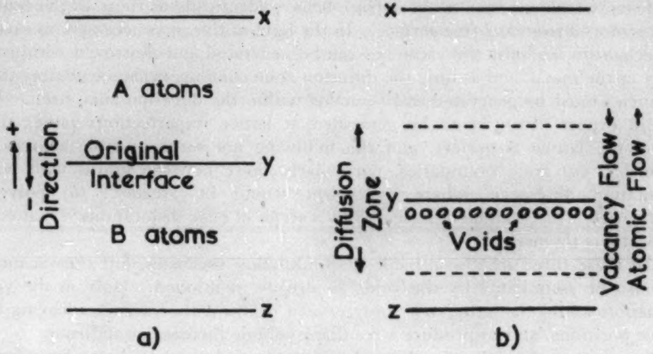

Fig. 14. Representation of the cross section of a diffusion couple (*a*) before diffusion and (*b*) after diffusion.

The volume increase, which results from the growth of the voids, is a function of the diffusion process. This is apparent as the volume increase is concentrated in the diffusion zone, and is dependent upon the square root of the annealing time and upon the temperature. The voids form and grow in samples prepared from both rolled commercial copper and spectroscopically standardized copper, which has been melted and cast *in vacuo*. Degassing the nickel before welding does not modify the voids. Further, the voids form when any of the samples were annealed in purified argon, nitrogen, hydrogen, or *in vacuo*. At the high temperatures used for diffusion anneals, any hydrogen dissolved during the welding process would be quickly removed during the vacuum anneals. However, the voids formed in this case are identical in size and number with those found when the annealing is performed in hydrogen, when the metal will be saturated with this gas. These results suggest that the void formation is not connected in any way with gases in the metals.

The *growth* of the void can certainly be explained by the diffusion and adsorption of some of the excess numbers of vacancies on the void surfaces. However, it is possible that where a supersaturation of vacancies occurs, they can coalesce to *form* small voids in a manner analogous to the formation of water drops in a supersaturated water vapour. Once a sufficient number of vacancies come together to form a void larger than a critical size, then, provided that at no stage did it collapse, it would persist and be able to grow by assimilating further vacancies.

That the voids appear to have crystallographic faces is not surprising; such shapes evidently possess a lower surface energy than spherical voids, and a process of surface diffusion would be quite capable of allowing the surfaces to adopt the lower energy, as is shown by the experiment performed by Lukirsky (1945) in which a single crystal sphere of rock salt assumed crystallographic shapes on annealing.

It remains now to discuss the generation and removal from the lattice of the large number of vacancies which do not form voids. These vacancies cannot be generated or lost primarily at the metal surfaces as those sections of a multiple sandwich which are near to the surface behave identically as those in the centre, well removed from any free surface. In the light of this, it is necessary to invoke a mechanism whereby the vacancies can be generated and destroyed within the body of the metal, and as only the diffusion zone contains evidence of strain, the vacancies must be generated and removed within the diffusion zone itself. We should expect vacancies to be generated at lattice imperfections rather than where the lattice is perfect, and the following are some possible sources of vacancies: (*a*) grain boundaries, particularly those between grains with large orientation difference, where the misfit would be greatest; (*b*) polygon boundaries, which can be represented by a series of edge dislocations; (*c*) at edge dislocations themselves.

All these three are also capable of annihilating vacancies, but the vacancies can also be assimilated by the voids as already mentioned. Only in the void formation would the lattice not contract as a result of the vacancies leaving the lattice positions, and so produce a resultant volume increase on diffusion.

Vacancies generated or annihilated on grain boundaries or polygon boundaries would not be expected to eliminate the boundary, since the orientation difference of the lattices on each side would prevent this, and these sources and sinks of vacancies could be permanently used. However, a simple edge dislocation would be eliminated once the excess plane of atoms was removed by the absorption of vacancies, or grew to extend right through the lattice by the creation of vacancies.

The edge component LM of a dislocation line LMN illustrated in fig. 15 will, however, not be destroyed by the above process. The annihilation of vacancies on the ledge LM of the edge region will cause this portion of the dislocation line to rotate about the screw component MN so that successive layers of atoms are removed which will cause the upper part of the crystals, which does not contain a screw dislocation, to descend. Similarly, the generation of vacancies on the ledge would cause the ledge to rotate in the opposite direction, *inserting* successive atomic layers. In fact, such an arrangement would behave in a manner completely analogous to the similar configuration postulated by Frank (1949) to explain the growth of crystals from the vapour. As in the treatment by Frank the edge component would be expected to spiral. Also, as in crystal growth, an edge dislocation located on two screw dislocations, one at each of its ends, can act in a similar manner if the screw dislocations are greater than a critical distance apart. The extra layers will then grow as double spirals and this is perhaps the more likely in practice, as the dislocation lines must, in a severely distorted metal, be very complex.

No matter which of the three types of imperfection act, the generation and annihilation of vacancies will cause the lattice to be in a state of compressive or tensile stress respectively if it is prevented from deforming, in which case an equilibrium would be reached where no further vacancies were generated or annihilated. If, however, the metals can plastically deform, there would be an expansion where vacancies are generated and a contraction where they disappear. The dimensional changes would occur in those directions where there was least restraint.

The presence of a substructure in the diffusion zone, as was indicated by the presence of ghost boundaries and confirmed by the X-ray study, does suggest that the whole diffusion zone has been in a stressed state. The presence of polygonization of the same nature in the nickel strip after evaporated copper atoms had diffused into one side of it suggests that the cause is the same in both cases, and as this latter experiment is rather simpler than the normal one, it is worth considering it in greater detail.

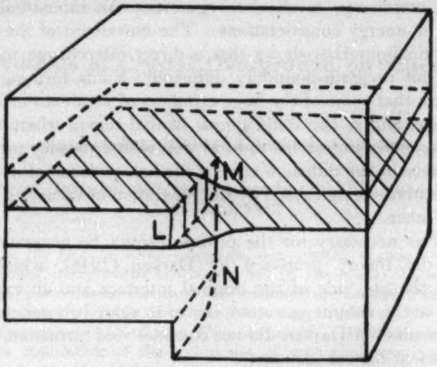

Fig. 15. Edge dislocation LM ending on a screw dislocation MN.

It might be thought that the differing coefficients of linear thermal expansions of copper $(16{\cdot}7 \times 10^{-6}/^{\circ}\mathrm{c})$ and nickel $(12{\cdot}8 \times 10^{-6}/^{\circ}\mathrm{c})$ were the cause of the curvature, but if this was so, then the nickel strip would be expected to bend with the copper-rich side innermost. For in this simple arrangement, the couple only forms while the strip is hot, and no stresses would be expected to arise from this cause until the strip was cooled at the end of the anneal, when the copper-rich side would contract more than the other. The curvature observed is in the opposite sense to this, further the magnitude of the effect would be much smaller than that observed. Thus the thermal expansion cannot be the controlling factor.

The lattice parameter of copper is approximately 2% greater than that of nickel and as the curvature produced by this factor would be in the same sense as that observed, i.e. with the copper-rich face outermost, it is more likely to be the cause than was the thermal expansion. However, this effect alone would not be sufficient to produce the curvature observed for, even if there was pure copper on the one face and pure nickel on the other face with a linear change in composition through the strip, the expected radius of curvature would be about three times that obtained with the thinner strip.

The only satisfactory way in which the curvature of the strip can be explained is by using a vacancy mechanism which will cause a severe bending of the foil in the correct sense, and would operate in conjunction with any lattice parameter effect. As the thicker of the two strips curves less than the thinner although the same amount of copper has diffused into each, it can only be concluded that the pure nickel on the undiffused side prevents the strip from bending to the full. If the same amount of copper was evaporated on to one surface of a thick large nickel block, the block would be expected to remain flat, and merely to expand a little in the direction of diffusion where the undiffused nickel does not cause a restraint.

§ 9. CONCLUSIONS

The main reason for believing that diffusion in metal solid solutions takes place by means of a vacancy mechanism is that as a result of diffusion, the inert markers at the interface move a distance greater than would be expected merely from lattice parameter considerations. This rules out the possibility that a direct atomic interchange mechanism operates. An interstitial mechanism is most unlikely on energy considerations. The movement of the markers in the region of a grain boundary shows that a direct interchange mechanism must also be ruled out in grain-boundary diffusion. Voids forming as a result of diffusion suggest that some of the large numbers of vacancies involved condense out of the lattice, and as the voids appear in that region where there would be a net gain of vacancies this seems to fit in well with a vacancy mechanism. The existence of strain in the diffusion zone is further evidence of a vacancy flow in this region, the strain being caused by the generation of vacancies in one part and the loss in the other.

The vacancies necessary for the process cannot be generated at the metal surfaces and the theory proposed by Darken (1948), which postulates a contraction on the one side of the original interface and an expansion on the other to preserve the volume per atom, seems to agree in a general way with the experimental results but Darken did not consider void formation, or the detailed atomic processes in his calculations.

The vacancies may be generated on grain boundaries, polygon boundaries, and on the edge components of dislocations, and they may condense on all three, causing the lattice to collapse, but they may also coalesce to form voids and so produce a volume increase.

The stresses in the lattice resulting from the diffusion process will create further lattice defects upon which further vacancies may be generated or annihilated, and such a process could perhaps account for the large numbers of vacancies involved. However, these stresses, besides producing further sources and sinks for vacancies, also produce extra easy paths of diffusion, for as grain boundaries allow preferential diffusion, so the degeneration of the lattice resulting from diffusion should also provide easy paths for further diffusion. The introduction of these easy paths which do not occur in self-diffusion, where no stresses are produced, may well explain why chemical diffusion coefficients rarely agree with theoretical values, while those for self-diffusion are in reasonable agreement (Nowick 1951), and perhaps helps to explain why the activation energy for chemical diffusion is generally found to be less than that for self-diffusion.

ACKNOWLEDGMENTS

The author wishes to thank Mr. A. D. Le Claire and Dr. H. M. Finniston for their interest in this work, and the Director of the Atomic Energy Research Establishment for his permission to publish this paper.

REFERENCES

Barnes, R. S., 1950, *Nature, Lond.*, **166**, 1032.
Betteridge, W., and Sharpe, R. S., 1948, *J. Iron Steel Inst.*, **158**, 185.
Correa da Silva, L. C., and Mehl, R. F., 1951, *Trans. Amer. Inst. Min. Met. Engrs.*, **191**, 155.
Darken, L. S., 1948, *Trans. Amer. Inst. Min. Met. Engrs.*, **175**, 184.
Frank, F. C., 1949, *Discussions of the Faraday Society, Crystal Growth*, 5.
Huntingdon, H. B., and Seitz, F., 1942, *Phys. Rev.*, **61**, 315.
Lukirsky, P. I., 1945, *C. R. Acad. Sci. U.R.S.S.*, **46**, 274.
Nowick, A. S., 1951, *J. Appl. Phys.*, **22**, 1182.
Seitz, F., 1948, *Phys. Rev.*, **74**, 1513; 1950, *Acta Crystallogr.*, **3**, 355.
Smigelskas, A. D., and Kirkendall, E. O., 1947, *Trans. Amer. Inst. Min. Met. Engrs.*, **171**, 130.
Zener, C., 1950, *Acta Crystallogr.*, **3**, 346.

New Observations of Crystal Overgrowth on Silicon Carbide

By A. R. VERMA
Royal Holloway College, University of London

Communicated by S. Tolansky; MS. received 24th January 1952, *and in amended form 12th March* 1952

ABSTRACT. On the faces of some silicon carbide crystals showing 'growth spirals' superimposed oriented overgrowths can sometimes be observed. These oriented overgrowths which took place during the process of manufacture consist of stepped triangular pyramids with craters at their peaks, the pyramids having heights up to a few wavelengths of light, and built sometimes on platforms of similar heights. These conclusions have been arrived at by the application of the techniques of multiple-beam interferometry and light-profile microscopy. In addition to the pyramids some trigonal, hexagonal and their compound figures have also been observed, which by the application of multiple-beam interference fringes are shown to be molecular oriented layers. These oriented molecular layers, the existence of which is revealed from the observation of the above overgrowths on silicon carbide crystals, may be silica deposit or possibly the growth of silicon carbide on itself.

§ 1. INTRODUCTION

Recently several workers have studied oriented overgrowth of crystals on different substrates. A substrate flat to molecular dimensions is required for this study and usually a cleavage face of a crystal is chosen for this purpose. Thus Schultz (1951) has studied the overgrowths of alkali halides on a cleavage face of mica, Lucas (1951) has studied the thin layers of ZnO, grown on a cleavage face of Zn, and Pashley (1952 a, b) has used cleavage faces of crystals and electrolytically polished silver surfaces as substrates.

In these experiments the thickness of the overgrowth layers deposited on the substrate is only a few Ångström units thick. Therefore it becomes increasingly important to know the flatness of the substrate for drawing reliable conclusions.

As has recently been shown by the author (Verma 1951), growth spirals are sometimes observed on the basal planes of silicon carbide crystals. The step height between the successive arms of the spiral has been shown to be equal to the height of the x-ray unit cell, and for type II crystals this step height is only 15 Å.

The area between successive steps is molecularly plane. Thus silicon carbide crystal surfaces, which are flat and plane to this extent provide a good substrate on which to study overgrowths.

§ 2. OVERGROWTHS ON SILICON CARBIDE CRYSTALS

Triangular Pyramids

We have not yet studied the overgrowth of crystals deposited artificially on silicon carbide crystals as substrate. However by using techniques previously described (Verma 1951), the examination of some of these silicon carbide crystals themselves reveals oriented overgrowths which took place during the process of manufacture. Figure 1 (Plate I) shows six trigonal pyramids observed on the basal plane of a silicon carbide crystal. On the rest of the crystal face faint step lines of an interlaced spiral of the type described previously (Verma 1951) can be seen as background. The step height between the successive edges of such a spiral would be 15 Å. Thus the scale of flatness of the substrate is superimposed on the picture.

The two pyramids at the top left corner in fig. 1 are oriented at 60° with respect to the remainder. It can also be seen that the three edges of the pyramids are rounded and are more or less similarly oriented to the edges of the interlaced spiral. Sometimes these overgrowths overlap and are 'twinned'. In fig. 2 are shown two such cases of overlapping. On the right-hand side the overlapping pyramids are similarly oriented, whereas in the middle of the figure showing the overlapping of three pyramids, the pyramids are alternately Δ and ∇ in orientation. The pyramids are seen to have a stepped structure. The steps are nearly triangular in their contour but at the three corners a characteristic dimple can be seen for all of them. At the peak of every pyramid there appears to be a crater. Similar craters can be observed at the edges of some of the pyramids and elsewhere on the crystal surface.

Interferometric and Light Profile Microscopic Examination

To study the triangular overgrowths the techniques of multiple-beam interferometry (see Tolansky 1948) and light-profile microscopy (Tolansky 1952) have been applied. In multiple-beam interferometry both the Fizeau fringes and fringes of equal chromatic order have been utilized. Figure 3 shows the multiple-beam Fizeau fringes passing over these features. To obtain fringes of equal chromatic order shown in fig. 4, the image of a Fizeau fringe passing over the peak of a pyramid was projected on the slit of a spectrograph. The fringes so obtained are seen to be convex towards the violet end of the spectrum showing clearly that these triangular features are hills, i.e. pyramids. The heights of these pyramids range from a few hundred Ångström units to a few wavelengths of light; the particular pyramid studied in fig. 4 is approximately 1 000 Å high. The discontinuity of the fringes in figs. 3 and 4 at the edges of the pyramids shows that the pyramids are built on platforms whose heights vary and may be as much as a few light wavelengths.

The light-profile microscope (recently developed by Tolansky (1952)) demonstrates these facts vividly. In this technique the field of view of the microscope is crossed by a dark profile line which is the image of the opaque fine line placed at the field iris and projected on the surface of the specimen by an off-centre illumination. The profile gives the line contour of the surface of the specimen where the changes in level are registered as lateral shifts of the profile. It is seen in fig. 5 that the profile line shifts towards the left after crossing the edge of the pyramid showing it to be an elevation above the general level of the crystal. By the interferometric calibration given by Tolansky, this shift corresponds to a change in height of about 1 μ, which is the height of the platform on which the pyramid is built in this particular case. At the peak of the pyramid the shift of the profile towards the right shows it to be a crater. Over a small area the bottom of the crater is nearly flat and its depth is nearly equal to the total height of the pyramid.

Behaviour of the Growth Fronts

The step lines of the successive growth fronts are seen in figs. 1 and 2 to be slightly deformed after they have travelled past these overgrowths, which act as obstacles. This deformation of the step lines indicates that the surface of the crystal had continued to grow after the formation of the overgrowths. In fig. 2 the growth fronts, which are advancing from the top to the bottom, break up into two halves on arriving at the overgrowths. After crossing these obstacles they rejoin and fill up the shadow region. The step lines in doing so fork out leading to interlacing of step lines of the type described previously (Verma 1951, fig. 14).

.B
5
2

§ 3. ORIENTED MOLECULAR LAYERS ON SILICON-CARBIDE CRYSTALS

A different type of overgrowth observed on silicon carbide crystals is shown in figs. 6, 7 and 9. Triangular, hexagonal and compound figures formed by the overlapping of the former with the edges slightly rounded are seen in these figures. In fig. 9 a plainly visible dot can be observed at the centre of some of the figures. Figure 8 shows the multiple-beam Fizeau fringes passing over the areas of figs. 6 and 7. Under this high dispersion there appears to be a very small kink when the fringes cross the boundary of these figures (the third fringe from the top passes over the hexagonal figure and the fourth and the fifth fringes over the triangular figure shown in fig. 6. The eighth and the ninth fringes pass over the lower and the upper figures of fig. 7 respectively). The kink has been measured to correspond to a change in height of 35 ± 5 Å. Thus one can assume that the triangular and hexagonal figures are molecular layers since for silicon carbide type II the height of the unit cell is 15 Å.

The edges of these molecular layers have a dotted appearance which may be due to the deposition of some impurity. This will then explain the rather high visibility of the edges.

§ 4. CONCLUSIONS

The observations of figs. 6, 7 and 9 show that a molecular layer is initially deposited on the crystal face. These monolayers which take definite orientations and shapes are fairly large in extent and form the nucleus for further oriented overgrowth. The dots observed in the centres of the figures in fig. 9 may be some foreign matter which acts as the nucleus for the laying down of the first molecular layer on the crystal face. These dots may develop into the craters observed at the peaks of the pyramids of figs. 1 and 2. The further observations of figs. 1 and 2 that some of the pyramids are built on a platform may mean that this oriented monolayer could grow up to the height of the platform by a repetition of the process of the formation of the first monolayer. This will happen if the atomic pattern of the 'embryo' and hence that of the substrate resembles the atomic pattern of a plane, in the normal lattice of the deposit (van der Merwe 1949).

In the manufacture of silicon carbide the different elements present inside the furnace are silicon, carbon and oxygen, so that these overgrowths may consist of any of these elements in combination. As is well known silica deposits are often observed on silicon carbide crystals and from the symmetry of the figures it is thought that these may be the overgrowth of silicon carbide on itself. If this is so, it demonstrates an interesting mode of crystal growth, of a crystalline substance growing on itself. Even in such a case, the configuration of a surface layer of the crystal is different from that of an interior layer by reason of Verwey displacements (Frank 1951). It will, however, be interesting to apply electron diffraction techniques to study these overgrowths.

ACKNOWLEDGMENTS

I wish to express my thanks to Professor S. Tolansky for his interest. This work has been carried out during the tenure of a scholarship by the British Council while on study leave from the University of Delhi.

REFERENCES

FRANK, F. C., 1951, *Proc. Phys. Soc.* A, **64**, 941.
LUCAS, L. N. D., 1951, *Proc. Phys. Soc.* A, **64**, 944.
VAN DER MERWE, J., 1949, *Discussions of the Faraday Society*, **5**, 201.
PASHLEY, D. W., 1952 a, *Proc. Roy. Soc.* A, **210**, 354; 1952 b, *Proc. Phys. Soc.* A, **65**, 33.
SCHULTZ, L. G., 1951, *Acta Crystallogr.*, **4**, 483.
TOLANSKY, S., 1948, *Multiple-beam Interferometry of Surfaces and Films* (Oxford: University Press).
VERMA, A. R., 1951, *Phil. Mag.*, **42**, 1005.

Influence of the Apparatus Function on Crystallite Size Determinations with Geiger Counter Spectrometers

BY F. R. L. SCHOENING*, J. N. VAN NIEKERK* AND R. A. W. HAUL†
* National Physical Laboratory, Council for Scientific and Industrial Research, Pretoria, South Africa
† National Chemical Research Laboratory, Council for Scientific and Industrial Research, Pretoria, South Africa

Communicated by S. M. Naudé; MS. received 30*th October* 1951, *and in final form* 12*th February* 1952

ABSTRACT. A brief survey of the various methods used for determining crystallite sizes from x-ray diffraction line broadening is given. It is shown that the diffraction profiles determined experimentally with a Geiger counter x-ray spectrometer can be represented by functions of the type $y=c/(1+k^2x^2)^2$. Using these functions a correction curve for instrumental influence on line breadth measurements is derived by solving the integral equation $B(x)=\int_{-\infty}^{+\infty} b(v)\beta(x-v)dv$ by means of the Fourier transform method. The apparatus function $b(x)$ is determined by using a standard substance. Experiments are described which illustrate the effect of sample preparation, absorption, etc. on measurements of line breadth.

§1. INTRODUCTION

Since the profiles of x-ray diffraction lines are invariably influenced by instrumental conditions, it is necessary to eliminate these before the shape and breadth of the profiles can be used to determine other factors such as crystalline size, lattice distortion, etc. which affect the profiles. The instrumental influence can be expressed mathematically (Jones 1938) as

$$B(x)=\int_{-\infty}^{+\infty} b(v)\,\beta(x-v)\,dv \qquad \ldots\ldots(1)$$

where $\beta(x)$ represents the profile of a diffraction line not affected by instrumental conditions and β is the integral line breadth of $\beta(x)$. The apparatus function $b(x)$ includes all the broadening effects due to instrumental conditions and b is the integral line breadth of $b(x)$, $B(x)$ is the resultant profile which is measured and B is the integral line breadth of $B(x)$. The functions $B(x)$ and $b(x)$ can be determined experimentally.

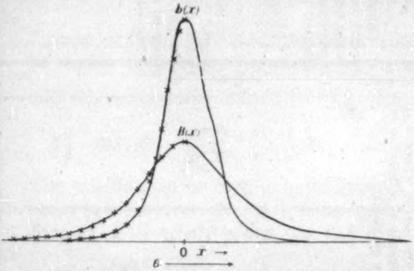

Fig. 1. Full lines represent the experimental profiles $B(x)$ and $b(x)$ obtained from two MgO samples. Crosses indicate values calculated from the function $y=c/(1+k^2x^2)^2$.

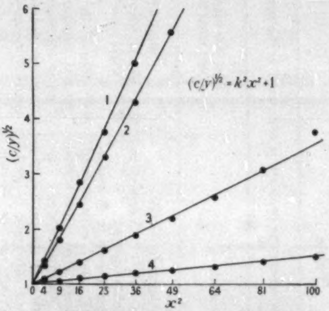

Fig. 2. Full lines represent the function $c/(1+k^2x^2)^2$. Circles are the values of the experimentally obtained profiles.

1 : MgO profile not broadened by crystallite size.
2 : W profile not broadened by crystallite size.
3, 4 : MgO profiles broadened by crystallite size.

A brief survey of the underlying principles of the various methods of eliminating the instrumental influence is given in table 1. Of these, the methods due to Stokes, Berry and Patterson are the most general. The numerical work involved is, however, time consuming, so that the methods of Shull* and Wood and Rachinger appear to be more suitable for practical application. The functions suggested by these authors for representing the diffraction profiles were tried during the present investigation. They did not, however, fit the profiles obtained with a Geiger counter spectrometer. These profiles can be represented remarkably well by functions of the type $y=c/(1+k^2x^2)^2$, where x is the abscissa measured from the profile maximum and c and k are constants. This is illustrated in fig. 1.

---

* For the representation of the broadened profile Shull uses the function

$$k(x)=\exp(-p^2x^2)+\tau\exp(-g^2x^2).$$

It may be noted that the applicability of this function cannot be tested by a semi-logarithmic plot as erroneously indicated by Shull.

Table 1

Early Crystal Size Determination	Recent Crystal Size Determinations where the problem is expressed in the integral equation $B(x)=\int_{-\infty}^{+\infty} b(v)\beta(x-v)\,dv$			
	An assumption for $\beta(x)$ is made		The two experimentally obtainable profiles $B(x)$ and $b(x)$ are used to solve the integral equation for $\beta(x)$	
Scherrer (1920) First application of the correction formula $\beta=B-b$ Laue (1926) General theoretical treatment of the problem. Brill and Pelzer (1928, 1930) Allowance for b under special experimental conditions is made.	Warren and Biscoe (1938) $\beta(x)$: $\exp(-k^2x^2)$ $b(x)$: $\exp(-l^2x^2)$ $B(x)$: need not be known, B is measured. Correction formula $\beta=(B^2-b^2)^{1/2}$ is obtained. Taylor (1941) An arbitrary mean of the Scherrer and Warren correction formulae is taken $\beta=\{(B^2-b^2)^{1/2}(B-b)\}^{1/2}$. Jones (1938) $\beta(x)$: $(1+k^2x^2)^{-1}$, $\exp(-k^2x^2)$, $\sin^2 k(x)/(kx)^2$. $b(x)$: measured profile of a standard substance. $B(x)$: need not be known, B is measured. Correction curves where β/B is expressed as a function of b/B are obtained. Kochendörfer (1944) $\beta(x)$: $(1+k^2x^2)^{-1}$, $\exp(-k^2x^2)$, $\sin^2 k(x)/(kx)^2$. $b(x)$: determined from instrumental and experimental conditions. $B(x)$: need not be known, B is measured. Correction formulae and curves are obtained.	Alexander (1950) $\beta(x)$: $(1+k^2x^2)^{-1}$ (Verified by the Stokes method). $b(x)$: determined from instrumental and experimental conditions. (In actual crystal size determinations the breadth b of the profile of a standard substance is used.) $B(x)$: Need not be known. B is measured. Correction curves where β/B is expressed as a function of b/B are obtained.	Shull (1946) $b(x)$: $\exp(-n^2x^2)$ $B(x)$: $\exp(-p^2x^2)+\tau\exp(-g^2x^2)$. $\beta(x)$: found by solving the integral equation by the Fourier transform method. Correction formula for β in terms of n, p and g is obtained. Wood and Rachinger (1949) $b(x)$: $(1+a^2x^2)^{-1}$ $B(x)$: $(1+c^2x^2)^{-1}$. $\beta(x)$: found by solving the integral equation by the Fourier transform method. Correction formula $\beta=B-b$ is obtained. Present Authors $b(x)$: $c_1/(1+k_1{}^2x^2)^2$. $B(x)$: $c_2/(1+k_2{}^2x^2)^2$. $\beta(x)$: found by solving the integral equation by the Fourier transform method. Correction curve where β/B is expressed as a function of b/B is obtained.	Berry (1947) $b(x)$: represented by a Hermitian polynomial series. $B(x)$: represented by a Hermitian polynomial series. $\beta(x)$: found by solving the integral equation by the Fourier transform method. Stokes (1948) $b(x)$: represented by a Fourier series. $B(x)$: represented by a Fourier series. $\beta(x)$: found by solving the integral equation by the Fourier transform method. Patterson (1950) $b(x)$: experimental profile is used directly. $B(x)$: experimental profile is used directly. $\beta(x)$: found by solving the integral equation by approximating it by a set of linear equations.

An evaluation of the correction for instrumental influence for this type of profile is given in § 2. Such profiles were obtained from the experiments described in § 3.

§ 2. EVALUATION OF THE CORRECTION FOR INSTRUMENTAL CONDITIONS

The solution of eqn. (1) by the Fourier transform method as given below implies that the experimental profiles can be represented by functions of the type $y=c/(1+k^2x^2)^2$. Suppose $B(x)$, $b(x)$ and $\beta(x)$ are all even functions and their Fourier transforms are defined by

$$\left\{\begin{matrix} L(t) \\ M(t) \\ N(t) \end{matrix}\right\} = \left(\frac{2}{\pi}\right)^{1/2} \int_0^\infty \left\{\begin{matrix} B(x) \\ b(x) \\ \beta(x) \end{matrix}\right\} \cos(tx)\, dx. \qquad \ldots\ldots(2)$$

It can be shown that $N(t)=L(t)/(2\pi)^{1/2}M(t)$. $\beta(x)$ can then be obtained from the inverse Fourier transformation

$$\beta(x)=\left(\frac{2}{\pi}\right)^{1/2}\int_0^\infty N(t)\cos(xt)\,dt. \qquad \ldots\ldots(3)$$

Except for favourable cases the integral on the right-hand side of eqn. (3) cannot be readily evaluated. An explicit evaluation is, however, not necessary because only the integral line breadth $\beta=2\int_0^\infty \beta(x)\,dx/\beta(0)$ is required where

$$2\int_0^\infty \beta(x)\,dx=\frac{L(0)}{M(0)} \quad \ldots\ldots(4) \qquad \text{and} \qquad \beta(0)=\frac{1}{\pi}\int_0^\infty \frac{L(t)}{M(t)}\,dt. \qquad \ldots\ldots(5)$$

The solution up to here is quite general. Equations (4) and (5) are, however, easier to solve than eqn. (3). Substituting the functions $b(x)=C_1/(1+k_1^2x^2)^2$ and $B(x)=C_2/(1+k_2^2x^2)^2$ in eqn. (2), $L(t)$ and $M(t)$ become

$$L(t)=\left(\frac{\pi}{2}\right)^{1/2}\frac{C_2}{k_2}\left(1+\frac{t}{k_2}\right)\exp-\left(\frac{t}{k_2}\right); \quad M(t)=\left(\frac{\pi}{2}\right)^{1/2}\frac{C_1}{k_1}\left(1+\frac{t}{k_1}\right)\exp-\left(\frac{t}{k_1}\right).$$

For the $\beta(x)$ profile the integral intensity and the maximum intensity $\beta(0)$ are obtained by substituting $L(t)$ and $M(t)$ in (4) and (5). $\beta(0)$ can then be written in the form

$$\beta(0)=\frac{1}{\pi}\frac{C_2k_1^2}{C_1k_2^2}\left[\int_0^\infty \exp\left(-t\left\{\frac{1}{k_2}-\frac{1}{k_1}\right\}\right)dt \right.$$
$$\left. +(k_2-k_1)\int_0^\infty \frac{1}{k_1+t}\exp\left(-t\left\{\frac{1}{k_2}-\frac{1}{k_1}\right\}\right)dt\right]$$

which on integrating and substituting limits becomes

$$\beta(0)=\frac{1}{\pi}\frac{C_2k_1^2}{C_1k_2^2}\left[\frac{k_1k_2}{k_1-k_2}-(k_2-k_1)\exp\left(k_1\left\{\frac{1}{k_2}-\frac{1}{k_1}\right\}\right)\mathrm{Ei}\left\{-k_1\left(\frac{1}{k_1}-\frac{1}{k_2}\right)\right\}\right]^*$$

The true broadening β is then finally given by

$$\frac{1}{\beta}=\frac{1}{\pi}\frac{k_1}{k_2}\frac{1}{(k_1-k_2)}\left[k_1k_2+(k_1-k_2)^2\exp\left(\frac{k_1-k_2}{k_2}\right)\mathrm{Ei}\left\{-\frac{k_1-k_2}{k_2}\right\}\right]. \qquad \ldots\ldots(6)$$

Jones (1938) has shown that it is convenient to express the correction for instrumental conditions graphically by plotting b/B against β/B. By using the values $B=\pi/2k_2$ and $b=\pi/2k_1$, obtained by evaluating the integral line breadths,

---

* For definition and tabulation of Ei see *Funktionentafeln* by E. Jahnke and F. Emde.

Jones' procedure can now be followed. Substituting $b/B=k_2/k_1=s$ (say) in eqn. (6) it becomes

$$\frac{B}{\beta}=\frac{1}{2}\frac{1}{s^2(1-s)}\left[s+(1-s)^2\exp\left(\frac{1-s}{s}\right)\mathrm{Ei}\left(-\frac{1-s}{s}\right)\right]. \qquad \ldots\ldots(7)$$

Assuming values for s between 0 and 1, corresponding values of B/β were calculated from eqn. (7). These are shown by curve c, fig. 3. By using a different method Alexander and Klug (1950) found a correction curve which is very similar to curve c. The figure also shows the correction curves given by Jones (1938), Scherrer (1920) and Warren and Biscoe (1938).

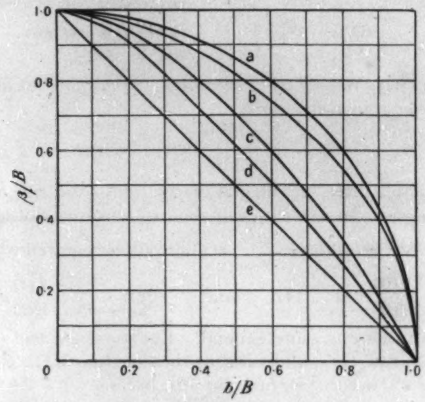

Fig. 3.
a : correction curve given by Warren.
b, d : correction curves given by Jones.
e : correction curve given by Scherrer.
c : correction curve given by Authors.

§ 3. EXPERIMENTAL PROCEDURE

During this investigation the Philips High Angle Goniometer with filtered CuKα radiation and the following slit system was used, tube slit 1°, Geiger counter slits 0·003″ and 1°. The automatic recording unit was found to be linear with the input counts over the full range of recording. The maximum intensity I_0 and, using a scanning speed of $\frac{1}{8}°$ 2θ per minute, the integral intensity I of the relevant diffraction lines were measured by taking counts, paying due regard to background corrections and to statistical fluctuations. The integral line breadth given by I/I_0 must then be corrected for (*a*) lost counts, (*b*) overlapping of the K$\alpha_1\alpha_2$ doublet, and (*c*) broadening due to experimental arrangement.

(i) *Lost Counts*

The resolving time τ of the Geiger counter as determined by the two-source method (Alexander, Kummer and Klug 1949) was found to be 165×10^{-6} sec. The corrected counting rate N at the peak maximum is given by $N=N_0/(1-N_0\tau)$ (Cochrane 1950), where N_0 is the measured counting rate. The corrected integral intensity of a diffraction line is given by the equation

$$I_{\text{corrected}}=\int_{-\infty}^{+\infty}\frac{N_0/(1+k^2x^2)^2}{1-N_0\tau/(1+k^2x^2)^2}\,dx,$$

where the measured profile is approximated by the function $N_0/(1+k^2x^2)^2$. Evaluation of this integral gives

$$\frac{I_{\text{corrected}}}{I_{\text{measured}}}=\frac{1}{[N_0\tau\{1-(N_0\tau)^{1/2}\}]^{1/2}}-\frac{1}{[N_0\tau\{1+(N_0\tau)^{1/2}\}]^{1/2}}.$$

In practice it was found that if $N_0=100$ counts/sec, then $I_{\text{corrected}}/I_{\text{measured}}=1{\cdot}012$. Hence if N_0 is kept below 100 counts/sec, the error introduced by neglecting correction for lost counts is approximately 1% or less.

(ii) $K\alpha_1\alpha_2$ *Correction*

For line profiles of the type $y=c/(1+k^2x^2)^2$ the $K\alpha_1\alpha_2$ correction curve was calculated and found to be the same as that given by Jones (1938).

(iii) *Broadening due to Experimental Arrangement*

In general there are two ways of obtaining the apparatus function $b(x)$. The first is to calculate it from the geometry of the apparatus as was done by Fricke and Heinle (1951) and by Alexander (1950) and Wilson (1950) for Geiger counter spectrometers. The second and more direct way is to measure the profile of a standard substance consisting of undistorted crystallites large enough not to give line broadening. This method was first introduced by Jones (1938) and was used during this investigation. For convenience the two main features of a profile, its shape and breadth, will be treated separately.

Determination of the profile shapes. With the substances MgO, CaO, SiO_2, NaCl and W taken as standards, profiles of their diffraction lines at 2θ 42·9°, 32·3°, 36·5°, 45·4° and 40·3° respectively were recorded. In all cases the low angle side of the profiles (i.e. that part least influenced by $K\alpha_2$), could be represented by functions of the type $y=c/(1+k^2x^2)^2$ (figs. 1 and 2). In fig. 2 lines 1 and 2 give the two extreme cases found for MgO and W respectively. The values obtained for CaO, SiO_2 and NaCl also gave straight lines falling between lines 1 and 2.

A series of MgO and CaO samples, with crystallite sizes ranging from about 60 Å to more than 1 000 Å, were examined. The broadened diffraction lines obtained could all be represented by functions of the same type (fig. 1 and fig. 2 lines 3 and 4). When plotting these functions it was found that for high values of x even considerable deviations from a straight line showed negligibly small discrepancies at the foot of the corresponding experimental profile.

It is interesting to note that the experimental profiles obtained with the older type of Philips x-ray spectrometer could also be approximated very closely by the same functions.

Measurements of instrumental line-breadth. Table 2 illustrates the consistency of the results obtained for the integral line breadths before and after correction for the $K\alpha_1\alpha_2$ doublet, when several readings were taken with the same MgO specimen. In table 3 the line breadths obtained over a period of several days for different MgO specimens, all prepared in the same manner from the same sample, are shown. These results illustrate the stability of the instrument and show that specimen preparation is not very critical. This point was further tested by carrying out experiments on tight-, normal- and loose-packed MgO specimens. The results of these experiments, shown in table 5, seem to confirm the above statement.

In table 4 the results of an investigation of the dependence of line breadth on reflection angle are given. These show that, for the focusing conditions of this particular instrument, a systematic angular dependence can hardly be detected.

The possible variation of the measured instrumental line breadth when using as standard a number of substances, all cubic except SiO_2, and having a wide range of linear absorption coefficients was also investigated. From these results, shown in table 6, it would appear that in the absence of preferred orientation and provided the linear absorption coefficient of the standard substance is not very low, (as in in the case of LiF) the choice of standard substance is not very critical.

Table	Substance	Degrees 2θ	I_{integral} (counts)	I_{max} (counts/sec)	Integral line breadth (radians) before $\alpha_1\alpha_2$ correction	Integral line breadth (radians) after $\alpha_1\alpha_2$ correction	Mean integral line breadth (radians)	P.E.(%)†
2	MgO	42·9	73441	563	474×10^{-5}	382×10^{-5}	375×10^{-5}	2
			72317	563	467	374		
			72395	568	464	370		
			73178	559	476	384		
			73869	577	465	372		
			73674	578	463	369		
3	MgO	42·9	77350	596	472	379	381×10^{-5}	2
			77154	577	486	395		
			76946	585	478	387		
			75631	592	465	372		
			76155	585	473	380		
			77158	599	468	374		
4	MgO	36·9	6157	53	423	351	362×10^{-5}	3
		42·9	76067	584	474	382		
		62·3	43308	309	510	362		
		74·7	5570	40	503	346		
		78·6	12416	84	538	370		
5*	MgO normal	62·3	40645	183	807	683	700×10^{-5}	2
	tight		43188	189	831	709		
	loose		40012	175	831	709		
6	LiF	45·0	52251	367	518	425	378×10^{-5}	3
	SiO_2	42·4	4860	37	472	387		
	MgO	42·9	76067	584	474	382		
	NaCl	45·4	29332	214	498	401		
	CaF_2	47·0	33547	253	482	376		
	KI	44·4	6261	49	468	368		
	Ag	44·3	21075	165	464	364		
	W	40·3	102460	828	450	368		
7	MgO 100%	42·9	75631	592	465	372	365×10^{-5}	2
	75%		39218	308	462	368		
	50%		22098	124	450	355		
	25%		8641	68	459	365		
	CaF_2 100%	47·0	33547	253	482	376	390×10^{-5}	3
	75%		32259	244	480	374		
	50%		22595	160	512	411		
	25%		15279	111	501	398		

* Sample shows broadening due to crystallite size. † P.E. = probable error of single determination.

The substance chosen as standard can either be mixed with the one under investigation or it can be used as an external standard. That the influence on line breadth of mixing two samples is only very slight, is shown by the results in table 7 obtained for a mixture of MgO and CaF_2. When making measurements with a Geiger counter spectrometer the external standard technique, which has obvious advantages, may be preferred. The experiments described under this section fully justify the use of an external standard.

ACKNOWLEDGMENTS

The authors wish to thank Dr. J. H. van der Merwe for helpful discussions concerning the mathematical treatment and also Mr. G. Heymann for assistance in accumulating experimental data.

This paper is published by permission of the South African Council for Scientific and Industrial Research.

REFERENCES

Alexander, L., 1950, *J. Appl. Phys.*, **21**, 126.
Alexander, L., and Klug, H. P., 1950, *J. Appl. Phys.*, **21**, 137.
Alexander, L., Kummer, E., and Klug, H. P., 1949, *J. Appl. Phys.*, **20**, 8.
Berry, O. R., 1947, *Phys. Rev.*, **72**, 942.
Brill, R., 1928, *Z. Kristallogr.*, **68**, 387.
Brill, R., and Pelzer, H., 1929, *Z. Kristallogr.*, **72**, 398; 1930, *Ibid.*, **74**, 147.
Cochrane, W., 1950, *Acta Crystallogr.*, **3**, 268.
Fricke, R., and Heinle, K., 1951, *Z. Elektrochem.*, **55**, 261.
Jones, F. W., 1938, *Proc. Roy. Soc.* A, **166**, 161.
Kochendörfer, A., 1944, *Z. Kristallogr.*, **105**, 393.
Laue, M. v., 1926, *Z. Kristallogr.*, **64**, 115.
Patterson, M. S., 1950, *Proc. Phys. Soc.*, **63**, 477.
Scherrer, P., 1920, *Zsigmondy, Kolloidchemie* (Leipzig: Springer).
Shull, C. G., 1946, *Phys. Rev.*, **70**, 679.
Stokes, A. R., 1948, *Proc. Phys. Soc.*, **61**, 382.
Taylor, A., 1941, *Phil. Mag.*, **31**, 339.
Warren, B. E., and Biscoe, J., 1938, *J. Amer. Ceram. Soc.*, **21**, 49.
Wilson, A. J. C., 1950, *J. Sci. Instrum.*, **27**, 321.
Wood, W. A., and Rachinger, W. A., 1949, *J. Inst. Met.*, **75**, 571.

The Spectral Emissivities of Iron, Nickel and Cobalt

By the late H. LUND and L. WARD*
South West Essex Technical College

Communicated by H. Lowery; MS. received 14th December 1951, and in amended form 19th March 1952

ABSTRACT. The spectral emissivities of iron, nickel and cobalt have been measured by the direct comparison of surface and black body radiation at temperatures between 1000° c and 1 300° c, over the wavelength range $1{\cdot}0\,\mu$ to $2{\cdot}6\,\mu$, using a lead sulphide cell and amplifier as the detecting unit. Values of the temperature coefficients of emissivity referred to 1000° c indicate an X point for iron at $1{\cdot}6\,\mu$, but none for nickel in this spectral range. The results for cobalt show an anomaly at a temperature close to the Curie point.

§ 1. INTRODUCTION

This work was undertaken to study two effects, (*a*) the variation of spectral emissivity with temperature for iron, nickel and cobalt, and (*b*) the variation in emissivity with composition for a series of alloys of iron and nickel.

A comprehensive review of the literature on emissivity measurements has been given by Price and Lowery (1944). As a result of his own investigations Price postulated the existence of an X point, that is, a particular wavelength characteristic of any metal at which the temperature coefficient of emissivity is zero. In giving values of the X point for a number of metals, Price used his own results at high temperatures and the mean values of other published data at low temperatures. This method is open to inaccuracy because of the surface effects.

---

* Now at University College of the Gold Coast.

The effect of the condition of the specimen surface on the value of the emissivity is very marked. Slight films of oxide cause an increase in emissivity and if insufficient care is taken in preparing and storing the specimens, contamination from the atmosphere may result. To obtain consistent results the specimens must be heated in either a reducing or a neutral atmosphere. Another surface effect is due to the recrystallization of the metal, causing a rearrangement of the crystal boundaries, which behave as partial black bodies. Schubert (1937) has observed this with platinum. Cold working or polishing invariably leaves an amorphous surface layer having different mechanical and electrical properties from the bulk material underneath. The effects on emissivity values of different surface states have not been fully investigated, but Wheeler (1913) has compared the sets of results from different workers and has shown that, although they may give different absolute values, a series of roughly parallel curves is obtained, and this he attributes to differences in surface conditions. In the present work an attempt was made to measure emissivities over a sufficiently wide range of temperatures using one specimen so that values of the temperature coefficient of emissivity could be measured without involving errors due to different surfaces.

§ 2. APPARATUS

The experimental technique was similar to that used by Price (1947) with an improved black-body source and a more sensitive radiation detector. Radiation from the hot specimen was focused on the spectrometer slit by a front silvered concave mirror, the beam being interrupted at about 750 c/s by a rotating toothed wheel. The measuring apparatus comprised a lead sulphide cell followed by an audio-frequency amplifier.

The specimen consisted of a sheet of metal 6 in. long, between 0·010 in. and 0·020 in. thick, bent to form a cylinder about $\frac{3}{8}$ in. in diameter with a longitudinal slit about $\frac{1}{32}$ in. wide (Drecq 1914). Radiation from the slit will be black-body radiation, provided there is a region of uniform temperature of length equal to about four times the diameter.

The specimens used in the present work (5 in. long) were approximately twice as long as those used by Price and, combined with an improved method of clamping, gave a zone of uniform temperature about 1 in. long. No correction was made for black-body deficiency.

The method of mounting the specimen is illustrated in fig. 1. Each end of the cylinder was cut into six longitudinal tags about $\frac{1}{2}$ in. long, which were then bent outwards at right angles and clamped between two brass rings. By means of a spigot attached to the outer of each pair of rings, the specimen was bolted to two water-cooled supports and held in a vertical position. One advantage of this method of clamping was that the bent-over tags acted as relatively weak springs and prevented serious buckling at the high temperatures due to expansion. Another was that the tags were clamped between two flat surfaces which could be easily cleaned and levelled, ensuring better electrical contact and temperature stability. The specimen was heated by connecting it via the supports to the secondary of a current transformer, the temperature being regulated by a Variac.

It was found necessary to heat all the specimens in a reducing atmosphere to prevent the formation of oxides. The specimen supports were carried through a rectangular water-cooled plate using a Wilson-type seal, which in this case also provided electrical insulation. A hollow rectangular metal box, whose upper side contained a quartz window, fitted on the base plate and was held in position by four springs. A vacuum seal between the plate and the box was made by a strip of hard rubber. The chamber could be evacuated by a rotary pump and filled with hydrogen through a needle valve.

The temperatures of the specimens were measured by a Pt–Pt–13% Rh thermocouple pushed through a small hole drilled in the specimen wall, the leads being brought out through metallized ceramic bushes—not shown on the diagram. A Hilger Barfit spectrometer employing a Wadsworth constant deviation mounting and a quartz prism was used as a means of obtaining monochromatic radiation.

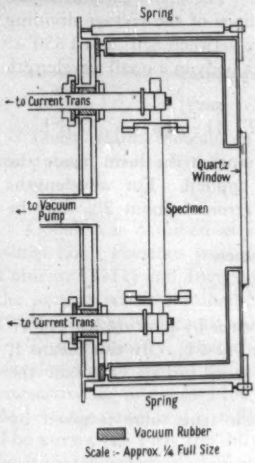

Fig. 1. Specimen box.

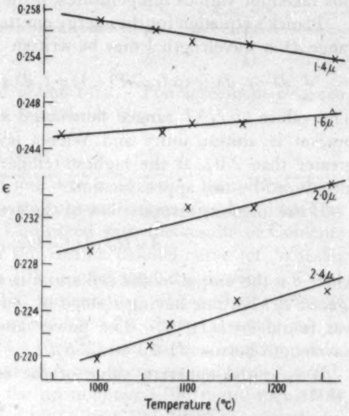

Fig. 2. Variation of emissivity of iron with temperature.

The radiation detector was a lead sulphide photo-conducting cell having a useful sensitivity in the wavelength range 1·0 to 2·6μ. The output from the cell was fed, via a cathode follower head amplifier to a voltage dividing box which was used to provide a constant input to the main audio-frequency amplifier. The latter was a straight three valve resistance capacity coupled amplifier feeding into a Cambridge vacuo junction. The thermocouple e.m.f. output from this instrument was measured on a potentiometer. As the e.m.f. was approximately proportional to the square of the output current, it was found most accurate to vary the input by the voltage dividing box so that a constant output was obtained.

The method of taking readings was first to focus the surface of the specimen on the spectrometer, set the voltage dividing box at about 0·950 and measure the output on the potentiometer. The black body was then brought into focus and the input readjusted until the same output was obtained. The ratio of these two readings gave the apparent emissivity of the surface.

The final preparation of the specimens consisted of polishing them with fine grade emery paper (grade 00) until all the scratches were removed. After mounting a further light polishing with grade 000 emery paper was given and finally the specimen was washed with ether to remove the abraded particles and grease.

It was not possible to examine the surfaces microscopically and consequently there is no evidence that this treatment gives the most characteristic value of the emissivity. In all cases the results on several specimens were in agreement to within 5%.

§ 3. CALIBRATION OF LEAD SULPHIDE CELL

It was necessary to calibrate the lead sulphide cell and head amplifier in terms of output voltage produced against incident radiation intensity. This was done by the method described by Hall (1944). The cell was illuminated with monochromatic black-body radiation, and readings of the voltage dividing box taken for various temperatures of the black body between 850° and 1 350° c.

Planck's equation for the energy emitted by a black body in a small wavelength range $d\lambda$ at wavelength λ may be written

$$J_\lambda d\lambda = c_1\, d\lambda/\{\exp(c_2/\lambda T)-1\} = c_1\, d\lambda \exp(-c_2/\lambda T)\,.\,[1-\exp(-c_2/\lambda T)]^{-1}.$$

The values of $c_2/\lambda T$ ranged between 3·5 and 13·0 so that the term inside the bracket is almost unity and Wien's law may be applied. For wavelengths greater than $2{\cdot}0\,\mu$ at the highest temperatures an error of about 2% may be introduced by this approximation.

If the intensity response law of the detector is written

$$\theta = k(J_\lambda)^{1+x} = k\{c_1 \exp(-c_2/\lambda T)\}^{1+x},$$

where θ is the output of the cell and k is a constant, then by plotting $\ln\theta + c_2/\lambda T$ against $c_2/\lambda T$ a line having a slope of $-x$ is obtained ($x \ll 1$). By this means it was found $\theta = k(J_\lambda)^{0{\cdot}95}$. The power law was the same for all values of the wavelength between $1{\cdot}0\,\mu$ and $2{\cdot}6\,\mu$.

If ϵ_1 is the apparent value of the emissivity, the true value is given by $\epsilon_1^{1/0{\cdot}95} = \epsilon_1^{1{\cdot}05}$.

§ 4. RESULTS

(i) *Nickel*

The mean results for nickel at 1 000° c are similar to those obtained by Price but are about 20% lower, most probably due to a more efficient black body. Compared with Hurst (1933) who was working at about the same temperature, the present results are higher by 5%. The results of Hagen and Rubens (1903), which were for low temperatures, agree well up to $1{\cdot}5\,\mu$ but are 12% lower at $2{\cdot}5\,\mu$.

The emissivity of nickel was found to vary markedly with temperature and the temperature coefficients for different wavelengths are given in table 1.

As it was not possible to measure the emissivity at 0° c by the present apparatus, the temperature coefficients in all cases are referred to 1 000° c, i.e. $\alpha_\lambda = (e_t - e_{1000})/e_{1000}(t-1\,000)$. The error introduced is about 10%.

Table 1

$\lambda\,(\mu)$	1·0	1·2	1·4	1·6	1·8	2·0	2·2	2·4	2·6
$\alpha\times10^{5}/^{\circ}\mathrm{c}$	10	11	12·5	13·5	14	15	16	17	17·5

The above values of the temperature coefficients were obtained from the best straight line through the points of an emissivity–temperature graph. No significant change in α with temperature could be detected.

There was no indication of an X point in the wavelength range investigated and this is in agreement with Price's conclusions. Using Hurst's values an X point is indicated at 1·5 μ.

(ii) *Iron*

The mean values at 1 000° c are again about 20% lower than those of Price. The curve due to Coblentz (1911) crosses the present one at 1·8 μ, and that due to Hagen and Rubens (1903) crosses at 2·4 μ.

The emissivity plotted against the temperature for different values of the wavelength is shown in fig. 2. The values of the temperature coefficient are given in table 2.

Table 2

	$\lambda\,(\mu)$	1·2	1·4	1·6	1·8	2·0	2·2	2·4
$\alpha\times10^{5}/^{\circ}\mathrm{c}$	Authors	−10	−5	3	9	8	10	13
	Price	−6		0		6		11

These results indicate an X point at about 1·6 μ. The agreement between the present results and those of Price is remarkably good.

(iii) *Cobalt*

Cobalt was obtained as a thin sheet and was bent into a cylindrical shape whilst hot. Previous work on cobalt in this spectral region has been done by Coblentz (1911) and Ingersoll (1910). Compared with the results of Coblentz the present values are about 20% lower but form a parallel curve (cf. Wheeler 1913). Ingersoll's results are from 5 to 10% higher than the present.

The emissivity plotted against the temperature for several different wavelengths is shown in fig. 3. The curve for 1·2 μ shows a steady fall in emissivity up to about 1 150° c ($\alpha = -24\times10^{-5}/^{\circ}\mathrm{c}$) and then a constant value. At 1·4 μ the curve is almost flat throughout: this would correspond to an X point. The curves for 1·6 μ and 2·0 μ are both flat up to about 1 100° c and then show positive temperature coefficients of $18\times10^{-5}/^{\circ}\mathrm{c}$ and $19\times10^{-5}/^{\circ}\mathrm{c}$ respectively.

The Curie point of cobalt is about 1 150° c and these changes in emissivity may be connected with changes in the structure of the cobalt. Wahlin and Knop (1948) working at 0·66 μ found a sudden discontinuity in the emissivity at the Curie point of cobalt. Ornstein and Van der Veen (1939) for iron found a discontinuity at the Curie point at 0·65 μ which disappeared at 0·45 μ. It is possible that these effects may be much smaller at the higher wavelengths.

It is proposed to extend the present work to include measurements near the Curie point of iron.

(iv) *Iron–Nickel Alloys*

A series of iron–nickel alloys at 10% intervals of composition were available in strip form. The values of emissivity plotted against the composition for various wavelengths at 1 000° c are shown in fig. 4. All the curves are of the same form showing a maximum at about 60% Ni. Ribbeck (1926) measured the resistivity of iron–nickel alloys at 1000° c and using the Hagen–Rubens formula it is possible to calculate the corresponding values of emissivity. These are plotted for 2·0 μ and are about 5% lower than the present experimental values. Values of the temperature coefficient of emissivity were scattered and no significant conclusion could be drawn from them.

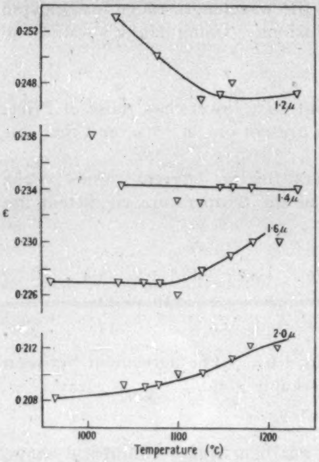

Fig. 3. Variation of emissivity of cobalt with temperature.

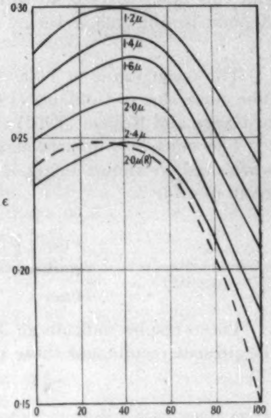

Fig. 4. Variation in emissivity at 1000° c with composition for iron–nickel alloys. Broken curve (R) Ribbeck's results.

ACKNOWLEDGMENTS

This work was undertaken for the Pyrometry Sub-Committee of the British Iron and Steel Research Association.

The authors wish to thank Dr. H. Lowery and the staff of the Physics Department of the South West Essex Technical College for their interest and help in this work.

REFERENCES

Coblentz, W. W., 1911, *Bull. Bur. Stand., Wash.*, **7,** 197.
Drecq, M., 1914, *C. R. Acad. Sci., Paris*, **158,** 1019.
Hagen, E., and Rubens, H., 1903, *Preuss. Akad. Wiss.*, **13,** 269, *Ibid.*, **19,** 410.
Hall, J. A., 1944, *J. Iron Steel Inst.*, **1,** 547.
Hurst, C., 1933, *Proc. Roy. Soc.*, A, **142,** 446.
Ingersoll, L. R., 1910, *Astrophys. J.*, **32,** 265.
Ornstein, L. S., and Van der Veen, J. H., 1936, *Physica*, **6,** 439.
Price, D. J., 1947, *Proc. Phys. Soc.*, **59,** 118, 131.
Price, D. J., and Lowery, H., 1944, *J. Iron Steel Inst.*, **1,** 523.
Ribbeck, F., 1926, *Phys. Z.*, **38,** 772; 1926, *Ibid.*, **38,** 887; 1926, *Ibid.*, **39,** 787.
Schubert, F., 1937, *Ann. Phys., Lpz.*, **29,** 473.
Wahlin, H. B., and Knop, H. W., 1948, *Phys. Rev.*, **74,** 687.
Wheeler, L. P., 1913, *Amer. J. Sci.*, **35,** 491.

A Study of Circulation Patterns within Liquid Drops moving through a Liquid

By K. E. SPELLS

Imperial Chemical Industries Limited, General Chemicals Division, Widnes, Lancs.

MS. received 4*th March* 1952

ABSTRACT. The technique used to reveal the circulation patterns was developed by Hagerty, and depends on the striae which appear in glycerine and glycerine–water mixtures when sheared.

Instantaneous flash photographs were taken of circulation patterns in drops of glycerine falling slowly (about 1 cm/sec) in castor oil, and in drops of various glycerine–water mixtures falling at about 10 cm/sec in heavy white oil (viscosity 0·37 poise at 15° c). In the former case the drops were spherical and the circulation pattern agreed reasonably well with that predicted theoretically by Hadamard; in the latter case the drops were no longer spherical and the centre of circulation was displaced below the equatorial plane.

§1. INTRODUCTION

Detailed investigation of certain industrial processes has shown the necessity for further study of the circulation which can be set up within liquid drops by their motion through a liquid medium. Among other things, knowledge is required of the circulation pattern and its dependence upon factors such as liquid properties, drop size and velocity of motion. Present information concerning circulation in moving drops may be summarized briefly as follows.

On the theoretical side Hadamard (1911) and Rybczynski (1911), independently, extended Stokes' calculation of the resistance opposing the motion of a solid sphere through a viscous medium of infinite extent to the case when the sphere is composed of fluid immiscible with the medium. Motion can then occur within the sphere, due to the action of forces of viscous origin across its surface, and Stokes' law is modified to

$$F = 6\pi k \eta a v, \qquad \ldots\ldots(1)$$

where F is the force opposing the motion of the sphere, radius a, composed of fluid, viscosity η', moving with velocity v through a medium of viscosity η, and $k=(2\eta+3\eta')/(3\eta+3\eta')$. Thus when $\eta'\to\infty$, $k\to 1$ and eqn. (1) reverts to the normal form of Stokes' law for a solid sphere. The other limiting case is when $\eta'\to 0$ (e.g. for a gas bubble in a liquid) and $k\to\frac{2}{3}$.

The Hadamard–Rybczynski calculation is subject to limitations similar to those restricting the validity of Stokes' law (i.e. effects due to inertia must be negligible compared with those due to viscosity); it therefore applies only to slowly moving spherical liquid drops or gas bubbles.

Bond (1927) and Bond and Newton (1928), in an attempt to verify eqn. (1), measured the terminal velocities of gas bubbles and liquid drops in media of high viscosity, such as golden syrup and castor oil. Very small drops and bubbles were found to obey the 'solid' form of Stokes' law, but above a certain size there was a slow transition, with increasing radius, until the velocity became consistent with that deduced from eqn. (1). It was inferred that circulation could occur within the bubble or drop, but that this circulation was restricted by the action of the surface, or interfacial, tension when the radius was appreciably smaller than a certain critical value, r_c. For the cases they investigated Bond and Newton concluded that r_c was given approximately by the value of the radius a required to make the dimensionless group $\gamma/a^2g\,|\,\sigma-\rho)\,|$ equal to unity, where σ is the density of the fluid in the drop (or bubble), ρ the density of the medium, and γ the surface, or interfacial, tension.

Direct evidence of the existence of internal circulation in moving drops was very meagre until recently, when Garner (1950) demonstrated it under certain conditions. Prior to this Barr (1931) had mentioned that circulation can be observed in large drops of, for example, alcohol rising in olive oil when they contain small particles of impurity to act as indicators.

For the slowly moving spherical drops or bubbles postulated by Hadamard and Rybczynski the theory gives the stream function representing the internal circulation pattern. No experimental work appears to have been carried out to reveal the circulation pattern in detail under these or any other circumstances. A brief account of the present experiments to determine the circulation patterns in drops of glycerine or glycerine–water mixtures falling in castor oil and heavy white oil (a thick paraffin oil) respectively may therefore be of some interest, notwithstanding the small range of conditions studied.

§ 2. EXPERIMENTAL WORK

A well-known method of determining flow or circulation patterns in fluids is to take photographs with an exposure of duration sufficient to reveal the direction of motion of small suspended particles. If applied to the study of the circulation patterns in drops, however, this would necessitate the elimination of appreciable relative motion between drop and camera, either by moving the camera at a steady rate or by causing the medium to flow. A technique suitable for use with instantaneous flash photography was therefore preferred on the grounds of simplicity.

(i) *Method for Revealing Circulation*

The technique finally adopted was developed by Hagerty (1950), and depends on the striae which appear in glycerine and in glycerine–water mixtures subjected to shear. These striae bear some resemblance to those visible in an imperfect mixture of two liquids of different refractive index. Possible causes of the phenomenon were discussed by Hagerty, who used it to reveal the vortices which occur in the liquid enclosed between two concentric cylinders when the inner one is rotated at more than a certain critical speed and the outer one is held stationary. His photographs suggest that the striae originate in a fairly restricted region during the setting up of each vortex, and are then dispersed more widely by the circulation, until a series of spirals is produced which reveals the vortex system satisfactorily. As will be shown later, much the same course of events was observed in the present experiments.

Hagerty's method would appear best fitted for the study of cases, such as the present, in which the final circulation pattern is steady and the liquid concerned in the circulation is unchanged; he states, however, that his method may be used in other cases when conditions are steady, such as for the study of flow past fixed objects.

(ii) *Scope of Investigation and Practical Details*

One series of experiments was performed with drops of glycerine (1·5% by weight of water) falling in castor oil. Further experiments were done with drops composed of 90%, 80%, 75% and 60% by weight of glycerine in water falling in heavy white oil, it being necessary to reduce the viscosity of the drop as well as that of the medium in order to obtain appreciable circulation. Finally, for reasons to be explained, drops composed of 60% glycerine, 36% water and 4% sucrose, by weight, were used in heavy white oil.

It was not considered necessary at this stage to use thermostatic control, and the experiments were performed at room temperature. As a rough guide the following data are given for the viscosities and densities, all at 15° C, of the liquids used. For glycerine (1·5% water), the viscosity is 17·5 poises and the density 1·259 g/cm^3; for the glycerine–water mixtures, the viscosities range from 3·3 poises (90%) to 0·13 poise (60%), and the densities from 1·238 g/cm^3 (90%) to 1·156 g/cm^3 (60%). Values for the media are 14·1 poises and 0·969 g/cm^3 for castor oil, and 0·37 poise and 0·866 g/cm^3 for heavy white oil.

The glass 'drop tube', at the tip of which the drops were formed, was of 10·5 mm external and 6·9 mm internal diameter. After formation, the drops fell down the axis of a vertical glass 'fall tube', 5 cm in diameter and 26 cm long, filled with the medium, to a glass observation vessel where they were photographed. The observation vessel was a Tintometer optical glass cell, 9·5 cm high × 11 cm × 6·7 cm.

The instantaneous photographs were taken by means of the flash from the discharge of a 4 μF condenser, charged at 2 500 volts, through a linear flash tube made to order by Messrs. Mullard Wireless Service Co. Ltd. Direct rear illumination of the drops was best, the flash tube being set up vertically behind a 3 in. focal length cylindrical lens to give a slightly divergent beam. Kodak Ortho-X films were used with an 8½ in. focal length Ross Xpress f/4·5 lens stopped down to f/11.

Satisfactory photographs of the circulation pattern in glycerine drops falling in castor oil were obtained with the drops in the bright centre of the beam, i.e. covering the virtual image of the flash tube. The most sensitive arrangement, however, was with the line of fall just to one side of the bright centre, and this was employed to reveal the circulation when the drops were composed of glycerine diluted with water. Only one half of the pattern was then revealed at all clearly, but as the pattern was symmetrical the resulting disadvantage was trivial.

§ 3. THE CIRCULATION PATTERNS

The plates show typical photographs taken during these experiments, all the drops except that in fig. 2 being approximately three-quarters actual size.* All but one of these photographs are of drops which had fallen about 28 cm. The exception, fig. 1 (*a*), shows a glycerine drop in the early stages of its fall in castor oil while still connected to the tip of the drop tube; to avoid distortion by the fall tube, this drop was formed in the observation vessel.

Figure 1 (*a*) is selected from photographs taken in order that the development of the circulation patterns shown in the other pictures could be visualized more readily. Two fairly broad striated regions will be seen on either side of the drop and seem to have been caused by the internal shearing forces operating during its formation. These regions evidently become extended and attenuated by the circulation taking place during fall, so that after a drop has traversed the length of the fall tube its circulation pattern is revealed.

---

* To improve clarity of reproduction, fig. 1 (*d*) has been enlarged to twice actual size.

The length of the neck, and the protuberance at the bottom of the drop in fig. 1 (*a*) were unusual, but this particular photograph was selected on account of the clarity with which the striae are shown.

Glycerine drops falling in castor oil are shown in fig. 1 (*b*) and (*c*). Owing to the high viscosity of the castor oil and the wall effect of the fall tube the rate of fall of these drops was only about 1 cm/sec.

The drops composed of various mixtures of glycerine and water falling in heavy white oil all had about the same velocity, 10 cm/sec; also, notwithstanding the range of viscosity used in the drops, they all had circulation patterns similar to those shown in fig. 1 (*d*) and fig. 2.

Figure 1 (*d*) shows a drop of 75% glycerine and water, and fig. 2 a drop composed of the 60% glycerine, 36% water and 4% sucrose mixture. In the latter case the sucrose was added in order to reduce the difference in refractive index between drop and medium (heavy white oil); either for this reason, or because the presence of the sucrose improved the clarity of the striae themselves, the best photograph of the series taken of the more rapidly falling drops resulted. This photograph has been enlarged in the form shown in fig. 2, the linear dimensions of the drop being roughly 12 times actual size.

On careful examination of fig. 2, faint horizontal lines extending between corresponding loops of the pattern on either side of the drop may be observed. According to Hagerty, for striae to be observed there should be variations in optical properties between planes to which the line of view is tangential. This condition is satisfied mainly by effects in or near the central vertical section perpendicular to that line; but it is also true for those regions of limited extent anywhere else in the drop where the direction of circulation is horizontal. The faint horizontal lines are probably due to effects in these latter places. Similar horizontal lines are also just discernible in the originals of fig. 1 (*b*) and (*c*).

§4. DISCUSSION AND CONCLUSIONS

Hadamard gave the equation

$$r^2(a^2-r^2)\sin^2\theta=\text{const.} \qquad \ldots\ldots(2)$$

as representing the circulation pattern in his assumed slowly moving spherical drops, r and θ being polar coordinates with respect to the drop centre and an axis along the direction of motion. He pointed out that, in three dimensions, the circulation should envelop a circle of radius $a/\sqrt{2}$ situated in the equatorial plane.

A two-dimensional representation of the theoretical circulation pattern is shown on the left of fig. 3. The system of curves, in this case enveloping a stagnation point distant $a/\sqrt{2}$ from the centre, was plotted after assigning values 0·1675, 0·0625, 0·125, 0·2332 and 0·25 (stagnation point) to the constant in eqn. (2). It may be mentioned that this circulation pattern is similar to the one deduced for Hill's spherical vortex (see, for example, Lamb 1932).

On the right of fig. 3 is drawn for comparison the circulation pattern determined experimentally for a glycerine drop falling in castor oil. This pattern was traced over the enlarged image of fig. 1 (*b*), projected from a lantern slide. The curves could not be completed near the drop boundary, where the striae were too close together to be clearly distinguished.

There is reasonably close correspondence between the theoretical and experimental circulation patterns in fig. 3, notwithstanding any small modification which may have been produced in the latter case by the wall effect of the fall tube. The slight upward displacement of the experimentally determined pattern near the stagnation point may be due to difficulties experienced in drawing the streamlines in that region, where the striae are in the form of a rather open spiral.

Further confirmation of the theory was provided by measuring the distance from the centre to the stagnation point on the enlarged images of three different glycerine drops, giving 0·69 *a*, 0·65 *a*, and 0·72 *a*. The measurements were inevitably rather rough, but in the circumstances they compare reasonably well* with the theoretical value, 0·71 *a* (i.e. $a/\sqrt{2}$).

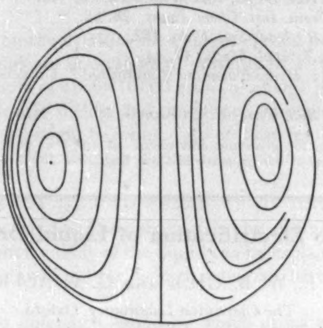

Fig. 3. Comparison of theoretical and experimental circulation patterns: slowly moving spherical drop.

One conclusion from these experiments, therefore, is that under suitable conditions the circulation pattern bears a reasonably close resemblance to the form given by the Hadamard–Rybczynski theory. Actual velocities of circulation in different parts of the drop are also calculable from the theory, but values with which these can be compared are not obtainable from the present experiments.

From a measurement of the interfacial tension between glycerine and castor oil, the critical radius at which the circulation in the glycerine drops should begin to be restricted is about 0·2 cm, according to the work of Bond and Newton. Some small drops shown in fig. 1 (*b*) and (*c*), which were formed during separation of the main drops from the drop tube, are near this size, but unfortunately there is not sufficient detail visible to provide still further evidence for the existence of a critical radius.

Figure 1 (*d*) and fig. 2 are typical examples of the circulation pattern in the more rapidly falling drops. The rate of fall was sufficient for the drops to be distorted from the spherical, but the circulation pattern is essentially the same as for the slowly falling drops; the stagnation point, however, is appreciably below the equatorial plane.

.B
5
2

The scope of the experiments which have been described was limited by the method of investigation employed, and it would obviously be of interest to develop other methods with a view to covering a wider range of conditions.

ACKNOWLEDGMENTS

I wish to express my thanks to Mr. J. McMillan for drawing my attention to Hagerty's paper, and to Mr. D. J. Roach to whose skill in photography these results are due.

REFERENCES

Barr, G., 1931, *A Monograph of Viscometry* (Oxford : University Press), p. 190.
Bond, W. N., 1927, *Phil. Mag.*, **4**, 889.
Bond, W. N., and Newton, D. A., 1928, *Phil. Mag.*, **5**, 794.
Garner, F. H., 1950, *Trans. Inst. Chem. Engrs.*, **28**, 88.
Hadamard, J., 1911, *C.R. Acad. Sci., Paris*, **152**, 1735.
Hagerty, W. W., 1950, *J. Appl. Mech.*, **17**, 54.
Lamb, Sir Horace, 1932, *Hydrodynamics*, (Cambridge : University Press, 6th edition), p. 246.
Rybczynski, W., 1911, *Bull. Acad. Sci., Cracovie*, **1**, 40.

---

* Refractive indices n_D for glycerine and castor oil are 1·47 and 1·48 respectively, so that distortion due to refraction at the drop surface was negligible.

The Electrification of Liquid Drops

By E. W. B. GILL and G. F. ALFREY
The Clarendon Laboratory, Oxford

Communicated by Lord Cherwell; MS. received 9th October 1950 *and in final form 28th February* 1952

ABSTRACT. Charges on drops breaking up in electric fields were investigated and it was found they could all be explained by the ordinary laws of electrostatic induction, with allowance for contact potential differences. Electrification due to splashing was also studied and again the effects could be explained by contact potentials alone so that theories put forward of double layers to explain previous experiments were unnecessary. A warning is given of the necessity of making due allowance for possible electrification by splashing in interpreting experimental results and a critical examination of an experiment of Zeleny is reported.

A few experiments of splashing water drops off ice gave results which may have a bearing on the production of electricity in thunderstorms.

§1. INTRODUCTION

There are various methods by which water drops can acquire charges: the simplest is when they break away in an electric field and acquire charge by ordinary induction; for instance, water falling through a narrow vertical tube and breaking into drops a few centimetres below the exit will acquire a charge if the falling column is surrounded by a metal cylinder kept at a potential different from that of the tube. The metal cylinder and the falling column are equivalent to a charged condenser so that the water surface is charged and this charge is continually carried away by the drops. A measurement of this charge gives a measure of the drop diameter at the moment of break off and proves it is about the same as the diameter of the tube. The charge carried away per cm^3

of water increases as the tube diameter decreases and it seems an almost invariable rule that however water drops are electrified the charge per cm^3 can be increased very considerably by reducing the drop size.

Even if the cylinder is at the same potential as the tube the drops still acquire a small charge because their contact potential with the tube puts the water at a potential slightly different from that of the cylinder.

The same experiment can be carried out with a spray if a charged cylinder is put round the orifice but in this case the charge carried away is much more than it would be if the drops were the same diameter as the orifice. In practice, the drops are very much smaller, and if the drop diameter is calculated from the charge carried, it may be proved that the drops get smaller and smaller as the air pressure increases.

With large voltages on the cylinder the charges carried away on such sprays are surprisingly large and are equivalent to currents of a few microamperes ; sprayed into air at this rate of about 10 000 e.s.u. of charge per second they can produce very large electric fields and it is not impossible that practical meteorological applications might be found. All of these results are in agreement with the theory that the electrification is due solely to induction.

§ 2. CHARGE DUE TO BREAK-UP OF DROPS

The experiments so far described show that any charges found on liquid drops breaking away from the body of the liquid can be explained by the ordinary laws of induction with allowances for contact potentials between the water and the containing vessel.

There is, however, a different method by which drops can acquire charges which appear when liquids are broken up by impact on solids (electrification by splashing) or, as some believe, are shattered by an air blast. Lenard (1892, 1915) was among the first to notice electrification by splashing near waterfalls, and Zeleny (1933) described a typical experiment with air shattering. The explanation usually put forward is that the effect is due to an electrical double layer within the surface (Chapman 1938) and that when a drop breaks up the outer layer is in some way scraped off, taking its charge and leaving the residue with an equal and opposite charge. Zeleny in fact refers to the production of negative ions.

It seemed worth while to see if this somewhat complicated explanation is essential or whether something based on a simpler principle would cover the facts.

The following experiment was therefore carried out with the apparatus shown in fig. 1. Water from a reservoir A passed down a copper tube of internal diameter 6 mm and drops fell from B at the rate of 1 or 2 a second.

After falling 1 cm the drops encountered an air blast from the tube C which shattered them, the spray being blown in the direction of the blast, most of it hitting the target T, 9 cm square placed 9 cm from the point of disruption. Most of the spray rebounded from the target but a little collected on the target in drops. The apparatus was contained in a metal cubical box of side 20 cm with some holes to let the air and spray out easily, and one to admit the rod holding T. T was insulated and joined to an electrometer valve. Everything else was at earth potential.

It was found when spray was blown on to the target in this way that a considerable positive charge appeared on the target. This was measured by a nul method. a condenser and a potentiometer being used to balance the collected charge, and its magnitude was found to depend on the nature of the liquid, the material of the target and the pressure of the air blast.

The variations with air pressure for a brass target are shown in fig. 2 for a few different liquids; the charges are those received for each drop that fell; the drops being approximately spheres of diameter 6 mm.

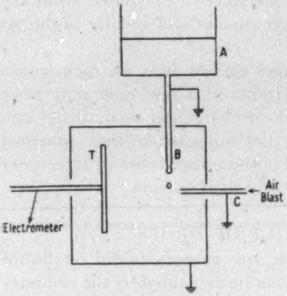

Fig. 1. Experimental arrangement.

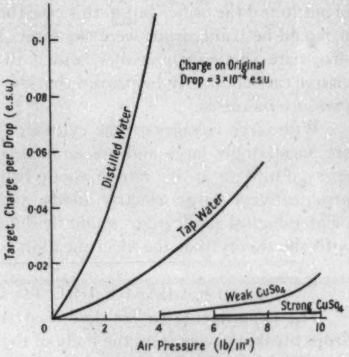

Fig. 2. Variations in air pressure with target charge per drop for distilled water, tap water and two concentrations of $CuSO_4$.

It will be seen that in all cases the charge acquired by the target increases rapidly with increase of air pressure and there is no doubt that this is because the droplets from the shattered drops become smaller as the blast pressure is increased; also the higher the conductivity of the liquid, the smaller is the charge. The effect, as might be expected, depends very much on the surface conditions; the experiments were therefore made with single drops and the target dried each time. Targets of different metals were next tried; only small variation in results were found for brass, copper or tin, but lead was some 20% more effective. If, however, the target was a dielectric, very interesting results occurred. The target was coated first with sealing wax and then with paraffin wax. In both cases the charge was not only of opposite polarity to the metal targets, that is negative, but also much larger. Sealing wax gave three times as much charge as a copper target and paraffin wax no less than nine times.

The obvious question of the origin of this charge appears to have three possible answers: either (i) it was on the original drops before they were shattered by the air blast, or (ii) it was produced as Zeleny and others suggest at the moment of shattering, or (iii) it was produced as a result of the droplets rebounding from the target. The first is easily ruled out. The charge originally on each drop by virtue of its contact potential with B was found by turning off the air, insulating the large box and measuring the charge it acquired as the drops fell into it. This was found to be negative and of the order of 3×10^{-4} e.s.u. per drop, varying slightly for the different liquids. Not only was this of opposite polarity to the target charge, but the target charge was thousands of times bigger.

As for the second alternative, if the break up of the drops really produces a number of negative ions the residue droplets must carry an equal and opposite positive charge. All these negative and positive charges are blown on to the target, and it is impossible to believe that a metal target collects only the positive charge rejecting in some way the negative ions. It is equally impossible to believe that a wax target does exactly the opposite, or that different metals or waxes collect different amounts. It seems clear therefore that the third explanation is correct and that the target charge is in some way connected with the rebounding of drops from the target. An explanation for this is possible based on the simplest principles. A liquid drop touching a metal at earth potential acquires by virtue of the contact potential v (usually negative) a charge Q. Q is, of course, v multiplied by the capacity of the drop. It is easy to see that, if the drop is subdivided into a large number of little drops before touching, the aggregate charge collected by the little drops will be far larger than Q because the capacity depends on the linear dimensions and the volume on the cube of these dimensions. For example, if divided into 1 000 parts each part has one-tenth of capacity of the original but as there are 1 000 parts the total charge taken is 100 times as great.

In the experiment the original drop has a charge of the order of magnitude of, say, $-Q$. When broken up the fragments which hit the target and rebound from it carry away a negative charge many times greater than Q, leaving a corresponding positive charge on the target. The greater the number of fragments the greater the charge transfer, which agrees with the curves of fig. 2, for increasing the air pressure increases the number of fragments. Also since the contact potential depends on the material of the target one would expect, as was found, different results with different targets, and presumably the 'contact potentials' for paraffin and sealing wax must be opposite in sign to those for metals.

.B
5
2

One fact however remains to be explained, viz. the remarkable difference between distilled water, tap water and copper sulphate solutions under like conditions, the distilled water being five times as effective as the tap water and nearly 100 times as effective as the solution. There is no reason to suppose any particular variation in the size of the fragments and the contact potentials can only differ slightly so that a much more potent reason must be found. There is an attractive hypothesis which is consistent with these results. A drop of liquid placed on a metal assumes a potential v with respect to it, and if its capacity with respect to the metal is C the charge it acquires is Cv. But one encounters here the mathematical difficulty that the capacity of two conductors approximates to infinity as they are brought closer and closer together, the infinity being due to the small elements in contact and the rest of the drop having in comparison a negligible effect.

But in practice the whole drop is not at potential v, there is not an abrupt change from 0 to v at the point of contact; instead the potential rises continuously from 0 to v as one proceeds a very small distance into the drop. Therefore at the elements near the point of contact which tend to make the capacity infinite, the potential tends to zero and the effective capacity of the whole drop is not infinite but depends on the proximity of the equipotentials in the liquid; if they are closely packed then elements of the drop very close to the metal will have an appreciable potential and the effective capacity and charge will be high. If they are more widely spaced the potentials of these near elements will be less and the effective capacity and charge less.

The earliest ideas on the origin of contact potentials throw light on the spacing of these equipotentials. The diffusion of ions out of the metal is balanced by a return current through the liquid, which in turn depends on the conductivity and the potential gradient. Hence the spacing of the equipotentials is determined by the conductivity. For poor conductors they are close together, getting further and further apart as the conductivity is increased; or in other words the equivalent capacity is high for poor conductivity and decreases as the conductivity increases.

Thus distilled water should have the highest capacity and charge, tap water lower values, weak solutions of copper sulphate lower still and strong solutions of copper sulphate should have the lowest values of all for capacity and charge; this is of the same order as the experimental results. The same variation with conductivity was found many years ago by Sir J. J. Thomson (1894) for a variety of liquids.

§3. COMPARISON WITH ZELENY'S EXPERIMENT

It may be worth while looking rather more critically at Zeleny's experiment (1933) which is usually one of those quoted as proof that if an isolated water drop is broken up by an air current ionization occurs. The arrangement he used is almost identical with fig. 1 except that the box was about half the size we used and there was no target T. His box was completely closed except for an exit hole. Most of the water droplets finally settled on the inside of the box but a fair proportion must have been carried out by the escaping air. The emerging stream was passed down an insulated cylinder with a central wire electrode and by putting an electric field across this condenser he collected and measured the charges coming out with the air stream. He found that when the air blast reached a velocity sufficient to break up the drops a negative charge was collected on the cylinder and this charge increased as the air velocity increased. He says in his introduction that "the total charge carried by negative ions which are produced in air when a water drop is disrupted was measured" and he thus claims that not only are ions produced but they are produced in the air at the moment of drop disruption.

It is suggested that the true explanation of Zeleny's results is that the disrupted drops were blown against the opposite side of the box which was, so to speak, the target of fig. 1, and, as in our experiment, rebounded with a considerable negative charge into the box in the form of smaller drops, but not ions. A proportion of these were carried out with the escaping air and their charge was the one measured.

In order to see if the magnitude of charge was correct the target used in our experiments was about the size of the side of Zeleny's box and was placed at the same distance from the drops. The diameters of the water and air tubes B and C were the same, so the drops were the same size and broken up in exactly the same way.

The current of fig. 2 should therefore give an indication of the amount of negative charge sprayed back into the box from the side opposite to the blast entry.

The biggest charge shown in Zeleny's results was 0·005 e.s.u. per drop of distilled water using an air velocity of 20 metres per second. This velocity in our experiments was produced by an air pressure of about 1·5 lb/in^2 and the resulting charge per drop from the curve is 0·025 e.s.u. It requires, therefore, only 20% of this to be blown out of the box to give the current Zeleny measured, so that the magnitudes involved are of the right order.

§4. CONCLUSION

In nature the simplest explanation is usually the correct one, and the experiments described show that Zeleny's results can be explained on the most elementary principles. Much more evidence is therefore necessary before a more complicated theory could be justified.

Many other experiments have of course been carried out by other workers on this subject, but every experiment in breaking up water drops by moving streams of air has the risk that the drops carried with the emergent air will impinge on some part of the apparatus and, because of the remarkable efficiency of this electrification by splashing, will produce charges which may be mistakenly attributed to other causes.

These splashing effects are so varied that considerable care is essential in explaining phenomena where splashing can occur. For example, when liquid drops are shattered by a metal target the spray consists of many droplets of widely varying sizes and under certain conditions many may be so small as to be confused with ions loaded with water molecules.

Another most deceptive fact is that if a stream of initially uncharged drops impinges on several metal targets in succession the first will acquire a positive charge but the remainder may acquire either a positive or a negative. The reasoning of §2 indicates that if the negatively charged droplets hitting the second target all bounce off unaltered in size they then retain their charge unaltered and the target is unaffected. If they bounce off as smaller droplets they take extra negative charge, leaving this target also positive, but if sufficient remain on this second target these may transfer to it more negative charge than that removed by those passing on, and the target becomes negative. (Pomeroy (1908), who noticed that the first target became positive and succeeding ones negative, thought this proved that in a spray the larger drops had a positive charge and the smaller ones a negative.)

Probably the most interesting application of 'electrification by splashing' is in connection with meteorology. A few experiments were carried out by coating the target of fig. 1 with ice and blowing the disrupted water drops on to this ice. Just as with the metal target, the ice acquired a very considerable positive charge and the rebounding water droplets a negative, suggesting a possible mechanism for the production of thunderstorms. This work is being continued.

ACKNOWLEDGMENTS

We should like to express our thanks to the Department of Scientific and Industrial Research who gave financial assistance to the work, and to Professor Lord Cherwell for his help with this paper.

REFERENCES

Chapman, S., 1938, *Phys. Rev.*, **54**, 520.
Lenard, P., 1892, *Ann. Phys., Lpz.*, **46**, 584; 1915, *Ibid.*, **47**, 463.
Pomeroy, J. C., 1908, *Phys. Rev.*, **27**, 492.
Thomson, J. J., 1894, *Phil. Mag.*, **37**, 341.
Zeleny, J., 1933, *Phys. Rev.*, **44**, 837.

LETTERS TO THE EDITOR

The Influence of Mercury Vapour on Selenium Rectifiers and Selenium Photoelements

Selenium rectifiers, if used or stored in a room in which the atmosphere is contaminated with mercury vapour, lose their high resistance in the blocking direction and become useless, as previously stated by the author (1943 a, b).* A similar destructive effect has been observed on selenium photoelements. This effect can be accelerated by circulating a stream of air, saturated with mercury vapour at room temperature, through the closed box which contains the element. The results of the experiments performed by the above method may be summed up in the following statements :

(i) In the circumstances mentioned above, mercury vapour diffuses through the counter-electrode of the rectifier disc (possibly through its pores) and the selenium layer in immediate contact with it is gradually converted into mercuric selenide. This is an excess semi-conductor of high conductivity (Henisch and Saker 1952).

(ii) During this process, the form of the function f in the blocking voltage–current characteristic $I_r = af(U_r)$ remains unaltered, and it is only the factor a which gradually increases. In other words, the back current will be increased at every voltage in the same proportion. This has been found to be true, with some precautions, from 0·1 volt to 15 volts.

(iii) The forward current remains unaltered, except in the neighbourhood of the origin, where the current must also increase in order to preserve the continuity of the characteristic.

(iv) The open-circuit e.m.f. of photoelements decreases rapidly under the influence of mercury vapour, while the primary (short circuit) photocurrent was found to remain unaltered.

Theoretical consequences. The statements under (i), (ii) and (iii) are in good accordance with Schottky's barrier layer theory (1942). Assuming that in consequence of the conversion of the boundary layer of selenium into mercuric selenide only the conductivity κ_R on the boundary is increased, it follows from Schottky's equation (13) that the back current will also be increased in the same proportion; while in accordance with equation (23) the capacity and its variation with the reverse voltage remains unaltered. Similarly, statement (iv) is in good agreement with the fundamental conception (Schottky 1930) that the e.m.f. of the photoelement is identical with the potential drop of the photo-current flowing back through the blocking resistance; therefore it will vanish if the blocking resistance disappears. Furthermore, it follows from these observations that the mechanisms which control the photo-sensitivity, the rectification properties and the self-capacitance, and which together form the true physical model of the photoelement (Kőrösy and Selényi 1931, 1932), are, so to speak, independent of one another: within certain limits one can damage the crystal detector without influencing the photo-response and the capacitance.

Physical Institute,
Roland Eötvös University,
Budapest, VIII.
12th May 1952.

P. Selényi.

Henisch, H. K., and Saker, E. W., 1952, *Proc. Phys. Soc.* B, **65**, 149.
Kőrösy, F., and Selényi, P., 1931, *Phys. Z.*, **32**, 848 ; 1932, *Ann. Phys., Lpz.*, (5), **13**, 703.
Selényi, P., 1943 a, *Elektrotechnika*, **36**, 107, 210 (in Hungarian) ; 1943 b, *Electrotech. Maschinenb.*, **61**, 633.
Schottky, W., 1930, *Phys. Z.*, **31**, 913; 1942, *Z. Phys.*, **118**, 539.

* I learned later, from oral communications and from the B.I.O.S. Final Report No. 725, " German Research on Rectifiers and Semi-Conductors ", that this effect has been still earlier recognized. The explanation, however, given in this Report on pages 31 and 33 (formation of a film of mercury by passing the selenium layer at its edges) is entirely insufficient.

The Dielectric Constant and Loss of Amorphous Selenium at a Wavelength of 3 cm

The dielectric constant of amorphous selenium for infra-red wavelengths has been measured. Gebbie and Saker (1951) found a value of 6·00 for wavelengths greater than 3×10^{-4} cm and Dowd (1951) a value of 6·05. For low radio frequencies the value is significantly higher; Tammann and Boehme (1931) give a value of 6·3 and D. H. Clark of Reading University (in unpublished work) also finds $6{\cdot}3\pm0{\cdot}1$ in the frequency range from 50 kc/s to 40 Mc/s. It is therefore of interest to measure the dielectric constant at some frequency between, if this can be done with sufficient accuracy for comparison with these values. Such measurements can be made at centimetre wavelengths using waveguide techniques.

Rectangular samples of amorphous selenium having thicknesses of 2 to 5 mm were made to fit closely into a 3 cm waveguide. The method of measurement was that described by Montgomery (1947) and due originally to von Hippel. In this method the dielectric constant and loss tangent are deduced from measurements made on the standing wave pattern from a shorted termination of a waveguide with and without the sample interposed. Results from a number of observations on four specimens of different thicknesses are as follows : for a frequency of $1{\cdot}024\times10^{10}$ c/s and temperature of 18°c the dielectric constant (real part) was 5·97 with standard deviation 0·04 ; the loss tangent (ratio of imaginary to real part of dielectric constant) varied from 3·2 to $5{\cdot}8\times10^{-3}$.

That the infra-red and centimetre wavelength values for the real part of the dielectric constant agree to within experimental error gives support to the suggestion (Gebbie and Cannon 1952) that there is little absorption to be expected in the far infra-red and millimetre wavelength region and that this material may have useful transmitting properties for such radiation. It also appears that there should be a region of absorption at some frequency less than 10^{10} c/s.

Acknowledgment is made to the Admiralty for permission to publish this note.

Services Electronics Research Laboratory,
Baldock, Herts.
H. A. Gebbie.
D. G. Kiely.

19th May 1952.

Dowd, J., 1951, *Proc. Phys. Soc.* B, **64**, 783.
Gebbie, H. A., and Cannon, C. G., 1952, *J. Opt. Soc. Amer.*, **42**, 277.
Gebbie, H. A., and Saker, E. W., 1951, *Proc. Phys. Soc.* B, **64**, 360.
Montgomery, C. G., 1947, *Technique of Microwave Measurements* (London : McGraw-Hill), Section 10.17.
Tammann G., and Boehme, W., 1931, *Z. anorg. Chem.*, **197**, 1.

Extinction Effects in Powders*

Recent x-ray diffraction studies on metal powders (Averbach and Warren 1949, Hall and Williamson 1951) have reported differences in the integrated intensities of the Debye–Scherrer rings for cold-worked and annealed samples. These differences have been attributed by Hall and Williamson to secondary extinction effects, whereas Averbach and Warren have suggested primary extinction. It is the purpose of this note to attempt to clarify the effects of extinction in powders.

Darwin (1922) has considered the effects of primary extinction and obtained for the ratio of the intensity with and without extinction

$$I_{\mathrm{ext}}/I=(\tanh nq)/nq \qquad \ldots\ldots(1)$$

where n is the number of diffracting planes,

$$q=Ne^2|F|\lambda a/mc^2\sin\theta_{\mathrm{B}}. \qquad \ldots\ldots(2)$$

N is the number of unit cells per cm^3, a is the unit cell size, F is the structure factor and θ_{B} is the Bragg angle. The expression was derived for a plate infinite in extent and with the diffracting planes parallel to the surface. Neither of these two conditions is approached in metal powders, the configuration of the coherently diffracting regions being more nearly equal in extent in all dimensions and the diffracting planes making somewhat arbitrary angles with the surface of the coherent region. Both these effects tend to make the average path length of the x-ray in the coherent regions the same for all diffracting planes rather than inversely proportional to $\sin\theta$, as in the Darwin expression. A 'three-dimensional' treatment for small but not negligible primary extinction has been given by Ekstein (1951) for the case of neutron scattering by a perfect crystalline sphere. The ratio of the intensity with and without extinction, modified for electromagnetic radiation, is

---

* Work carried out at Brookhaven National Laboratory under contract with A.E.C.

$$\frac{I_{\text{ext}}}{I}=1-\frac{7}{16}\left(\frac{e^2}{mc^2}|F|\,KD'N\lambda\right)^2 \qquad \ldots\ldots(3)$$

where D' is the diameter of the sphere and K is the polarization factor. An analogous expression can be obtained from Zachariasen (1945), who has considered the non-symmetrical reflection from a plate (eqns. 3.167 and 3.169). If, as suggested by Zachariasen, we equate $t_0/(|\gamma_0\gamma_H|)^{1/2}$ to the effective linear dimension of the block, D', we have

$$\frac{I_{\text{ext}}}{I}=\frac{\tanh A}{A}\simeq 1-\frac{1}{2}\left(\frac{e^2}{mc^2}|F|\,KD'N\lambda\right)^2. \qquad \ldots\ldots(4)$$

t_0 is the plate thickness, γ_0 and γ_H are the direction cosines to the normal of the plate for the incident and diffracted beams respectively, and A is given by the expression in parentheses in (4).

In the case of secondary extinction Hall and Wilkinson have used an expression of the type

$$I_{\text{ext}}/I=(1+gQ/\mu)^{-1} \quad \text{(Zachariasen 1945, eqns. 4.40 and 4.42 b)} \qquad \ldots\ldots(5)$$

where $g=(2\sqrt{\pi}\eta)^{-1}$, μ is the absorption coefficient, and

$$Q=\left(\frac{e^2}{mc^2}N|F|\right)^2\frac{\lambda^3K}{4\sin\theta_B} \quad \text{(Zachariasen 1945, eqn. 3.85).} \qquad \ldots\ldots(6)$$

η is the standard deviation of the misalignment in the coherent domains. Equation (5), however, is only valid for the symmetrical reflection of an infinitely thick imperfect crystal plate or a plate sufficiently thick such that the depth of penetration is essentially determined by the absorption coefficient. Neither the condition of symmetry nor of thickness was satisfied for the small grains used by Hall and Williamson's experiment. An expression more nearly correct can be obtained by considering the transmission expressions given by Zachariasen's equations 4.43 *b* and 4.41, for small and for neglible secondary extinction respectively. We obtain

$$\frac{I_{\text{ext}}}{I}=\exp(-gQD'')\simeq 1-\frac{gD''K\lambda}{4\sin\theta_B}\left(\frac{e^2}{mc^2}|F|N\lambda\right)^2 \qquad \ldots\ldots(7)$$

where D'' is the size of the imperfect single crystal.

The figure shows the experimental points of Hall and Williamson for aluminium, and the single solid curve is calculated from the primary extinction expression (3) for $D'=1\cdot7\times10^{-4}$ cm and from the secondary extinction expression (7) for $gD''=3\cdot8$ cm. Both values appear reasonable.

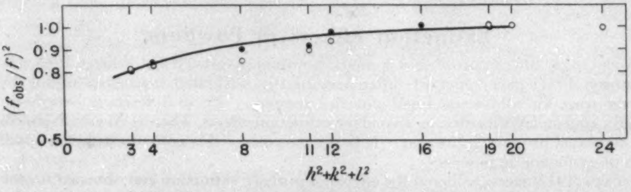

Ratio of observed to calculated intensities of powder diffraction peaks in annealed pure aluminium taken from Hall and Williamson (1951) (p. 942 open circles, p. 949 heavy circles).

Our conclusion is that on the basis of the available data one cannot distinguish between primary and secondary extinction. It is felt, however, that one could distinguish between the two types of extinction by varying D''. The angular dependences of (3) and (7), unfortunately, are quite similar, the extra polarization factor in (3) being approximately compensated by the $\sin\theta_B$ factor in (7).

Since cold-worked metals exhibit a marked decrease in extinction, it appears that the mosaic block size D' decreases if the extinction is primary, or the reciprocal of the mosaic block misalignment g and/or the imperfect crystal size D'' decreases if the extinction is secondary. These questions should be decided to better understand the dynamics of plastic deformation.

Watertown Arsenal,
Watertown, Mass.
10th April 1952.

R. J. Weiss.

Averbach, B. L., and Warren, B. E., 1949, *J. Appl. Phys.*, **20**, 1066.
Darwin, C. G., 1922, *Phil. Mag.*, **1**, 800.
Ekstein, H., 1951, *Phys. Rev.*, **83**, 721.
Hall, W. H., and Williamson, C. K., 1951, *Proc. Phys. Soc.* B, **64**, 937.
Zachariasen, W. H., 1945, *Theory of X-ray Diffraction in Crystals* (New York: Wiley).

CORRIGENDA

An Improved Frequency Equation for Contour Modes of Square Plates of Anisotropic Material, by R. Bechmann (*Proc. Phys. Soc.* B, 1952, **65**, 368).

P. 369. Equation (2), line 2: $(s_{16}-s_{26})$ *should read* $(s_{16}+s_{26})$.
P. 371. Equation (9): a in expressions for A and C *should read* a_0.
P. 371. Condition 2: $\gamma_{16}=\gamma_{26}\neq 0$ *should read* $\gamma_{16}=\gamma_{26}=0$.
P. 372. Condition 4: $\gamma_{16}=\gamma_{26}=0$ *should read* $\gamma_{16}=\gamma_{26}\neq 0$.

The Absorption Spectra of Single Crystals of Lead Sulphide, Selenide and Telluride, by A. F. Gibson (*Proc. Phys. Soc.* B, 1952, **65**, 378).

In the derivation of the theoretical equations on pages 381 and 384 of the above paper a factor $4\pi^2$ has been omitted from the denominator. The theoretical absorption coefficient is therefore considerably less than that quoted and much less than the experimentally obtained values. The discrepancy between theory and experiment is therefore of the same order of magnitude as that found in germanium. I am indebted to Dr. W. Paul of Aberdeen University for pointing out this error.

REVIEWS OF BOOKS

The Science of Flames and Furnaces, by M. W. Thring. Pp. xiv+416. (London: Chapman and Hall, 1952.) 42*s*.

A considerable fraction of the nation's fuel (coal, gas and oil) is used in furnaces, and yet the scientific design and control of furnaces has received much less attention than have other forms of combustion such as internal combustion engines and gas turbines. This welcome and valuable book aims at making such knowledge as is available more readily accessible, and also at stimulating further research into furnace problems.

The first section reviews briefly, but with many diagrams, the various types of furnace in use in the iron, steel, glass, chemical, non-ferrous metals, cement and coal-carbonizing industries. The next section deals with the laws of thermodynamics and their application to the achievement of maximum efficiency. The meaning of efficiency is discussed, and it is pointed out that in some cases it may be expressed simply in terms of fuel required to reach the desired end, and in other cases may include the heat removed in the final products and the possibility of re-using this heat with pre-heaters; the formation of steel from pig-iron is, for example, an exothermic process and would not require any fuel if the heat from the cooling steel ingots could be utilized! The third section reviews briefly, but clearly, the nature of combustion processes in gas mixtures and solid fuel beds. The fourth section, on heat transfer, deals with conduction, natural convection and forced convection, and is especially good on heat transfer by radiation from luminous flame gases. The long section on the aerodynamics of hot systems is about gas flows and the effects of buoyancy and turbulence and describes the measurement of gas flows and velocities under furnace conditions. The last two sections deal with the practical design of furnaces—types of refractory, roof supports, etc.—and the application of scientific methods in the design of new furnaces.

Mr. Thring has himself done much valuable work on furnace design, especially of open hearth furnaces, and on flame radiation and the use of scale models. For this book he has also had the help of several colleagues at B.I.S.R.A. and B.C.U.R.A. Diagrams are used freely to explain various concepts; in some cases it is unfortunate that the diagrams are not on the same page. There is a rather brief subject index, but no author index. The style is reasonably clear and the book is well produced. It is an authoritative treatment of the subject and may be warmly recommended. A. G. G.

Advances in Physics : A Quarterly Supplement of the 'Philosophical Magazine', Vol. 1, *No.* 1, *January* 1952. Editor : Professor N. F. MOTT, F.R.S. Pp. 109. (London : Taylor and Francis.) 15*s*.

Advances in Physics is a supplement to the *Philosophical Magazine* which will appear quarterly, from January of this year. The Editor, in his introductory remarks about the new journal, describes its purpose as follows : " The aim of the journal is to publish specialist articles, of admittedly ephemeral value, in rather narrow fields, and to publish them quickly ".

It is natural to compare the journal with the Physical Society's annual *Reports on Progress in Physics*. Some differences are already clear. The intended practice of publishing small quarterly numbers, each containing about three articles linked to some extent in their subject matter, rather than large annual volumes covering diverse branches of physics, will open the way towards giving each number a specialist appeal rather than a wide interest. The effect of this, together with the policy of inviting 'stop press' accounts of subjects at present in a state of flux, should be that the new journal will complement the *Reports*. One imagines that people will turn to the *Reports* to see how the frontiers of physics are advancing as a whole, and to the *Advances* to join in forays and thrusts that are now being made in particular fields.

The three articles in this opening number deal with problems of crystals. Dr. Sondheimer writes on the mean free paths of electrons in metals, Professor Seitz on the generation of vacancies by moving dislocations, and Dr. Frank on crystal growth and dislocations.

Dr. Sondheimer gives a most interesting account of recent work on methods of finding the mean free path of electrons in metals. The idea in all cases is to measure electrical resistance under such circumstances that this path is about equal to some other characteristic length in a metal. The simplest case occurs with thin films at low temperatures, where the mean free path may equal the thickness of the metal. Another case is a magneto-resistance effect, where the important length is the radius of a free electron orbit in a magnetic field. Lastly, there is the anomalous skin effect, which involves the depth to which a high frequency electric field penetrates a metal.

Professor Seitz accepts the Editor's hint by concentrating intentionally on ideas that are still mainly speculative. His main point is that vacant lattice sites can be generated from moving dislocations. The consideration of special processes, such as intersecting screw dislocations cutting through one another, shows that this idea is very reasonable, and several experiments exist which go some way towards confirming it. In his final pages Professor Seitz speculates in a most interesting and provocative way about the origins of work hardening.

Dr. Frank in his article describes a delightful chapter of post-war physics, his own dislocation theory of crystal growth and its dramatic confirmation by the work of Griffin, Dawson and others. It seems hardly necessary even to read Dr. Frank's closely reasoned argument, for the beautiful photographs speak so eloquently in support of the main idea of his theory, which is that growth is catalysed at the points where dislocation lines emerge on the surface of the crystal.

The Editor is to be congratulated on having made such a good start to his new journal; it will whet the reader's appetite for future numbers.

A. H. COTTRELL.

An Introduction to Acoustics, by R. H. RANDALL. Pp. xii + 340. (Cambridge, Mass.: Addison-Wesley, 1951.) $6.00

This is frankly a student's text, making no pretence to be a reference book. All unnecessary descriptive material and many matters only distantly connected with acoustics to be found in other works have evidently been deliberately omitted. For example there is no mention of such fascinating but antique devices and techniques as the hot wire microphone, the phonodeik, sound ranging or sound location. There is not even a passing reference to the cathode-ray oscillograph. The author's main object is clearly to give a simple introduction to the fundamentals of acoustic theory without any advanced mathematics, and with a few practical examples by way of illustration.

The earlier chapters are devoted to a clear elementary exposition on familiar lines of the theory of vibrations of particles, waves in free space, interference and diffraction, acoustic impedance, the behaviour of vibrating strings and air columns, and reflection and absorption by boundaries. Refraction effects are treated descriptively and rather briefly. The later chapters are on speech and hearing, experimental acoustics, sound reproduction, and miscellaneous applications. Ultrasonic phenomena are included among the latter, but the important relaxation phenomena giving rise to dispersion and anomalous absorption in liquids and gases are not discussed.

The author's style is easy but lapses occasionally into the colloquial. There do not appear to be many misprints but the last equation on p. 128 is incorrect. Each chapter ends with a set of questions to which the answers are printed at the end of the book, and there is an index. The book is very clearly printed on good paper and is well bound.

J. M. M. P.

Bibliography on the Measurement of Gas Temperature, by PAUL D. FREEZE, National Bureau of Standards Circular 513. Pp. iv+14. (Washington, D.C.: U.S. Department of Commerce, 1952.) 15*c*.

Calibration of Commercial Radio Field-Strength Meters at the National Bureau of Standards, by FRANK M. GREENE, National Bureau of Standards Circular 517. Pp. ii+5. (Washington, D.C.: U.S. Department of Commerce, 1952.) 10*c*.

Printed Circuit Techniques: An Adhesive Tape-Resistor System, by B. L. DAVIS, National Bureau of Standards Circular 530. Pp. iv+83. (Washington, D.C.: U.S. Department of Commerce, 1952.) 30*c*.

Directory for the British Glass Industry, compiled by D. W. ROLLIN and E. ROLLIN. Pp. 415. 5th Edition. (Sheffield: The Society of Glass Technology, 1951.) 12*s*. 6*d*.

Table of Dielectric Constants of Pure Liquids, by A. A. Maryott and E. R. Smith. United States Department of Commerce, National Bureau of Standards. Pp. iv + 44. (Washington: U.S. Government Printing Office, 1951.) 30*c*.

Exercices de radioéléctricité, by S. Albagli. Pp. 76. (Paris: Gauthier-Villars, 1952.) 80 fr.

Étude des perturbations cristallines produites dans les métaux par des efforts alternés, by Paul Laurent. Pp. 116. (Paris: Publications Scientifiques et Techniques du Ministère de l'Air, 1952.) 1000 fr.

Étude d'équations aux dérivées partielles rencontrées dans la théorie des phénomènes de torsion, by Pierre Brousse. Pp. 76. (Paris: Publications Scientifiques et Techniques du Ministère de l'Air, 1952.) 600 fr.

Radiological Monitoring Methods and Instruments, National Bureau of Standards, Handbook 51. Pp. iv + 33. (Washington, D.C.: U.S. Department of Commerce, 1952.) 15*c*.

CONTENTS FOR SECTION A

Dr. H. Messel. The Solution of the Fluctuation Problem in Nucleon Cascade Theory: Homogeneous Nuclear Matter 465
Dr. H. Messel and Dr. R. B. Potts. The Solution of the Fluctuation Problem in a Finite Absorber for Nucleon Cascades 473
Dr. L. R. B. Elton. On the Scattering of Fast Electrons by Nuclei 481
Mr. R. Richmond, Dr. P. J. Grant and Mr. H. Rose. The Decay of ^{188}Re . . 484
Mr. H. N. V. Temperley. On the Relationships between the Landau and London–Tisza Models of Liquid Helium II 490
Dr. R. Bowers. The Thermal Conductivity of Liquid Helium I 511
Dr. J. L. Olsen. Heat Transport in Lead–Bismuth Alloys 518
Dr. K. G. Ramanathan. Infra-Red Absorption by Metals at Low Temperatures . 532
Mr. J. M. Ziman. Antiferromagnetism by the Spin Wave Method: I—The Energy Levels 540
Mr. J. M. Ziman. Antiferromagnetism by the Spin Wave Method: II—Magnetic Properties 548

Letters to the Editor:

Prof. E. Amaldi, Mr C. Castagnoli, Mr. S. Sciuti and Mr. A. Gigli. An Anticoincidence Experiment on Cosmic Rays at a Depth of 50 Metres Water Equivalent 556
Dr. Carl M. York. Note on the Differential Momentum Spectrum of Cosmic-Ray Protons at Sea Level. 558
Dr. B. Bleaney and Mr. R. S. Trenam. Paramagnetic Resonance in Ferric Rubidium Sulphate Alum 560
Dr. E. H. Sondheimer. A Note on the Theory of Conduction in Metals . 561
Dr. E. H. Sondheimer. The Thermal Conductivity of Metals at Low Temperatures 562
Mr. G. Harries and Dr. W. T. Davies. The 7 mev Level of ^{12}C . . . 564
Mr. R. C. Bannerman. An Investigation of the Decay Scheme of ^{153}Sm . 565
Reviews of Books 566
Contents for Section B 573
Abstracts for Section B 574

ABSTRACTS FOR SECTION A

The Solution of the Fluctuation Problem in Nucleon Cascade Theory: Homogeneous Nuclear Matter, by H. MESSEL.

ABSTRACT. Solutions are presented for the general number distribution function in cascade theory and for the kth moments of the distribution. The Jánossy G-equation is solved. The methods of solution developed are applicable to the similar problem in the electron–photon case.

The Solution of the Fluctuation Problem in a Finite Absorber for Nucleon Cascades, by H. MESSEL and R. B. POTTS.

ABSTRACT. The complete analytical solution of the fluctuation problem for nucleon cascades developing in a finite absorber is given. Expressions are obtained for the general number distribution function and for the nth moments.

On the Scattering of Fast Electrons by Nuclei, by L. R. B. ELTON.

ABSTRACT. It is shown that, contrary to expectations from the non-relativistic case, the phase-shift ζ_n between the partial waves of electrons scattered by a point nucleus and by an extended nucleus respectively is positive for sufficiently large n, and that this is a spin effect and not merely a relativistic one. An approximate formula for ζ_n is evolved and its usefulness is discussed.

The Decay of ^{188}Re, by R. RICHMOND, P. J. GRANT and H. ROSE.

ABSTRACT. The gamma-rays emitted in the decay of ^{188}Re have been investigated by means of absorption and coincidence techniques and by the use of a thin lens beta-ray spectrometer. The gamma-ray intensities (expressed as a percentage of the total number of beta-disintegrations) have been measured and a probable decay scheme is proposed.

On the Relationships Between the Landau and London–Tisza Models of Liquid Helium II, by H. N. V. TEMPERLEY.

ABSTRACT. The Landau (1941) picture of liquid helium II as a modified Debye model is critically compared with the London–Tisza picture of liquid helium II as a condensed Bose–Einstein assembly in an attempt to find some common features. Two such common features are found, first that the criterion for Bose–Einstein condensation in a one-particle model is $(\partial S/\partial N)_{E,V} \leqslant 0$ or $g=(\partial F/\partial N)_{V,T} \geqslant 0$, a condition that can also be satisfied by the Debye model below a certain temperature. Secondly, an assembly satisfying such a condition, is in principle, capable of being in thermodynamic equilibrium with a weakly adsorbed film or with free atoms of small energy. It is also suggested that such atoms may make possible the observed phenomena of superfluid flow because their wave-functions are abnormally sensitive to small applied external fields of force, and some evidence in support of this is presented.

A numerical study of the Landau–Debye model shows that, in accordance with observed facts on helium II, its energy spectrum is probably modified considerably in channels of less than 10^{-4} cm width. It is also concluded that the Debye model is probably not a workable approximation near the λ-point, but that it is correct at sufficiently low temperatures.

The Thermal Conductivity of Liquid Helium I, by R. BOWERS.

ABSTRACT. The thermal conductivity of liquid helium has been measured between 2·2 and 4° K. It is found to increase with temperature over the whole range and shows no sign of anomalous behaviour just above the λ-point.

This variation is compared with that of the viscosity and entropy in the same temperature range.

Heat Transport in Lead–Bismuth Alloys, by J. L. OLSEN.

ABSTRACT. The variation with temperature and with magnetic field of the heat conductivity of a series of lead–bismuth alloys has been measured. As the concentration of bismuth is increased the heat conductivity in the normal state falls below that in the superconducting state, contrary to the case in pure superconductors. Estimates have been made from the experimental data of the processes contributing to the heat conductivity, and of the resistances due to the various scattering mechanisms limiting these conductivities.

Infra-Red Absorption by Metals at Low Temperatures, by K. G. RAMANATHAN.

ABSTRACT. The infra-red absorptivities of several electropolished metal surfaces have been measured at liquid helium temperatures with a specially designed radiation cryostat with a black body at room temperature as the source and a differential helium gas thermometer as the detector. It is found that the absorptivity of tin at 1·95° K for the mean estimated wavelength $14\,\mu$ remains the same in the normal and superconducting states to within a probable error of 0·3%. The absorptivities of the normal metals, which include a number of alloys, are compared with the values calculated by various theories of metallic reflection. The classical Hagen–Rubens formula is found to be valid for the alloys except where there are complications such as the internal photoelectric effect. The absorptivities of the pure metals are in fair agreement with the values calculated by the anomalous skin effect theory neglecting relaxation effects.

Antiferromagnetism by the Spin Wave Method: I—The Energy Levels, by J. M. ZIMAN.

ABSTRACT. The Hamiltonian operator for an exchange antiferromagnet is expressed in terms of the deviations of the spins from the basic ordered antiparallel arrangement. By a Fourier transformation the Hamiltonian may be approximately represented as a sum of harmonic oscillator terms, corresponding to spin waves. The role of anisotropy energy in fixing the domain axis is discussed, and the energy levels are calculated for the case of an external field parallel to this axis. The ground-state energy includes the zero-point energy of the spin waves and is in good agreement with other theories. Formulae are quoted for a Hamiltonian including dipole–dipole interaction between non-isotropic spins.

Antiferromagnetism by the Spin Wave Method: II—Magnetic Properties, by J. M. ZIMAN.

ABSTRACT. From the energy levels obtained in a previous paper by the author the partition function and magnetic susceptibilities are calculated. $\chi_{\parallel}$ behaves like aT^2 at low temperatures, whilst $\chi_{\perp}$ is constant. The magnetic resonance absorption frequencies are also calculated and shown to depend strongly on the anisotropy field. By representing the true Hamiltonian in terms of the operators of the approximate Hamiltonian, correction is made for the disordering of the system by the spin waves, and susceptibility curves agreeing well with experiment can be calculated. The method is applicable to different types of lattice and of interaction, is not confined to zero fields, and is valid up to near the critical temperature.

. B
5
2

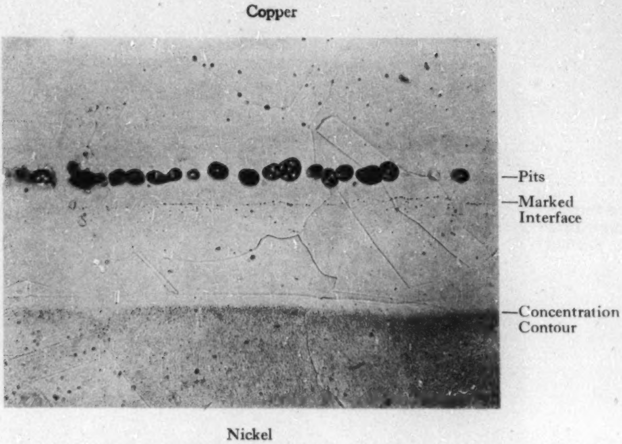
Copper
—Pits
—Marked Interface
—Concentration Contour
Nickel

Fig. 5. Photomicrograph of electropolished copper–nickel couple diffused for 68 h at 1010° c in argon. ×150.

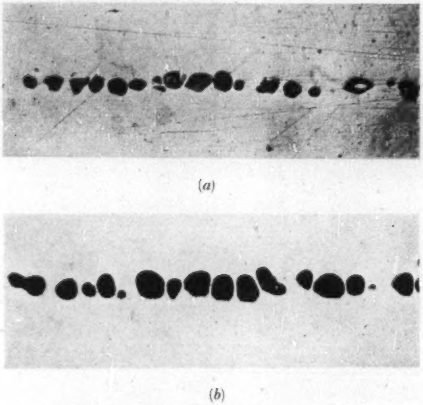
(a)

(b)

Fig. 6. Photomicrographs of mechanically polished copper–nickel couples diffused for 68 h in hydrogen at (a) 1010° c and (b) 1080° c. ×150.

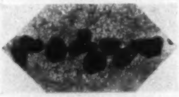

Fig. 7. Microradiograph using cobalt radiation of a section 0·002 in. thick of a copper–nickel sandwich diffused for 68 h at 1047° c in an argon atmosphere. ×150.

Plate I.

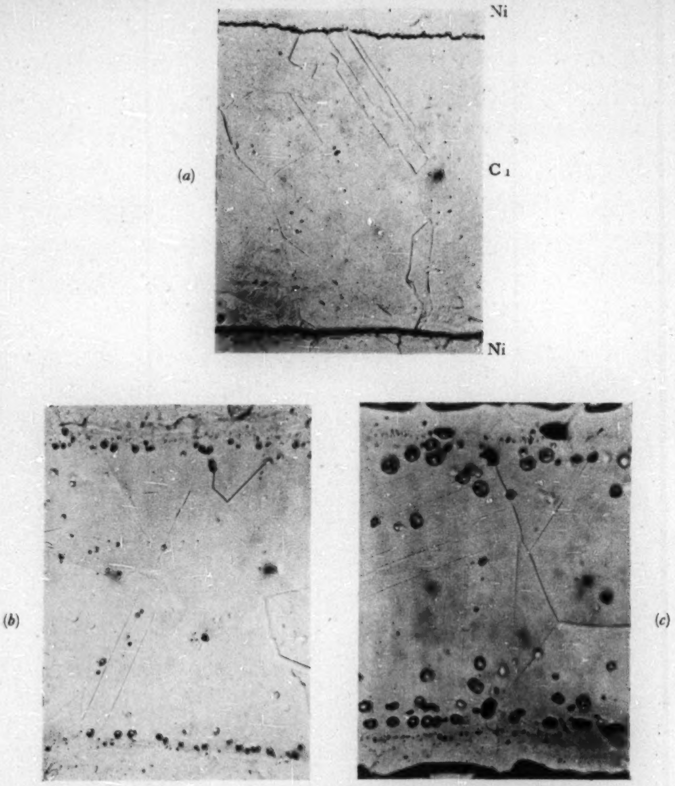

Fig. 8. Photomicrographs of the electropolished copper-rich region of a copper–nickel sandwich annealed in purified argon at 1000° C (*a*) immediately after preparation, (*b*) after a 15 min anneal, (*c*) after a 2 h 15 min anneal. ×360.

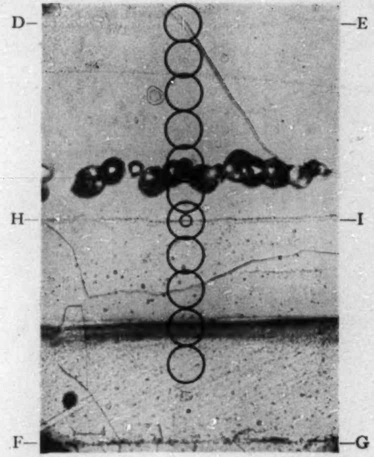

Fig. 9. The region investigated by X-rays, the small circles indicating the areas for which back-reflection photographs were taken. ×125.

PLATE II.

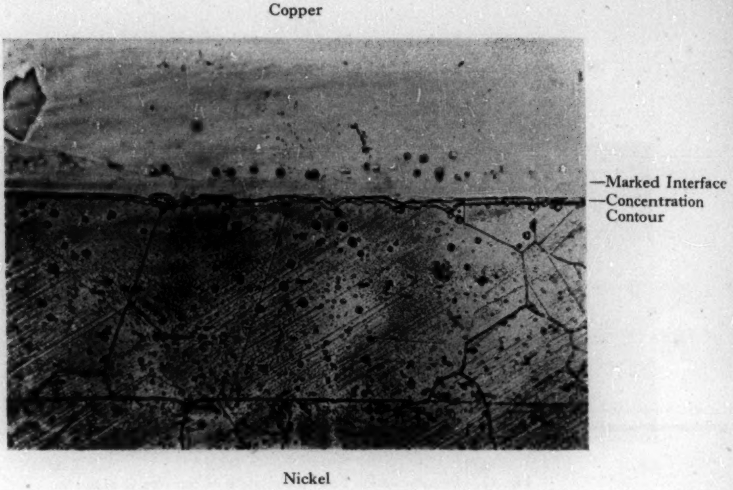
Copper
—Marked Interface
—Concentration Contour
Nickel

Fig. 10. Photomicrograph of an electropolished copper–nickel couple diffused for 1 h at 1070° c *in vacuo*. ×170.

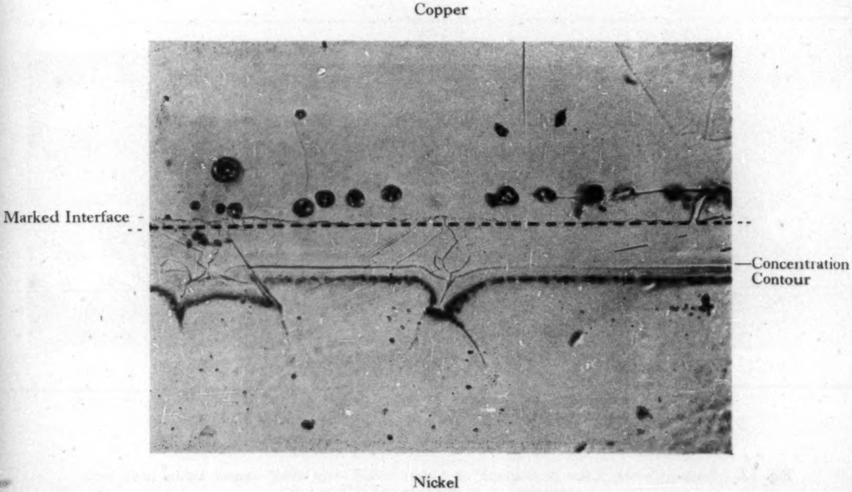
Copper
Marked Interface
—Concentration Contour
Nickel

Fig. 11. Photomicrograph of an electropolished copper–nickel couple diffused for 66 h at 940° c in argon. ×170.

PLATE III.

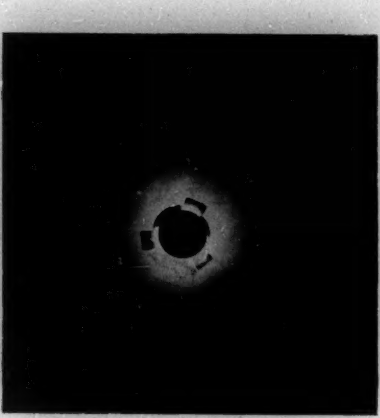

Fig. 12. Back-reflection Laue photograph of the area O in fig. 9.

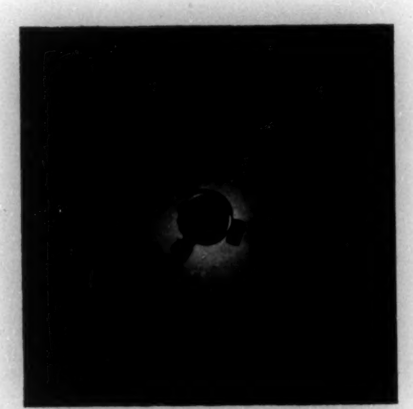

Fig. 13. Back-reflection Laue photograph of a thin nickel strip after copper atoms have been evaporated on to one side and diffused in.

Plate IV.

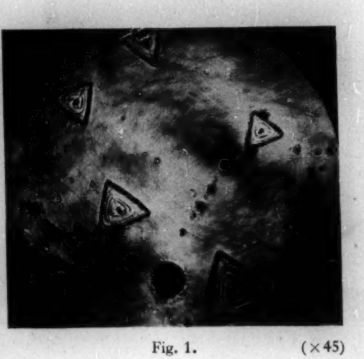

Fig. 1. (×45)

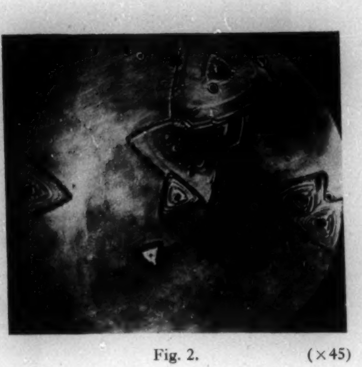

Fig. 2. (×45)

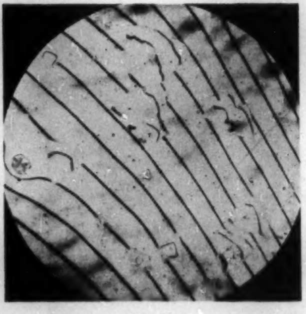

Fig. 3. (×25)

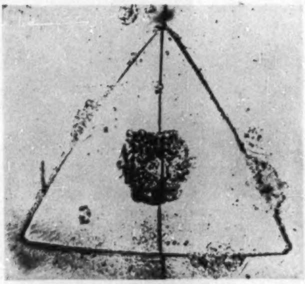

Fig. 5. (×600)

Plate I.

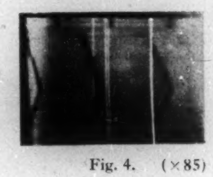

Fig. 4. (×85)

Fig. 6. (×45)

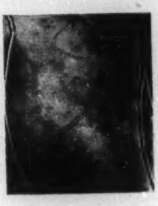

Fig. 7. (×45)

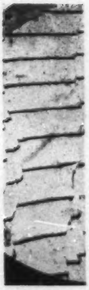

Fig. 8. (×15)

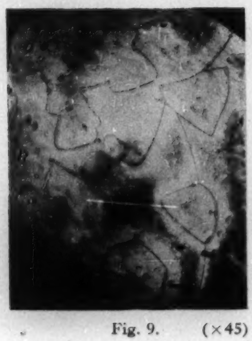

Fig. 9. (×45)

PLATE II.

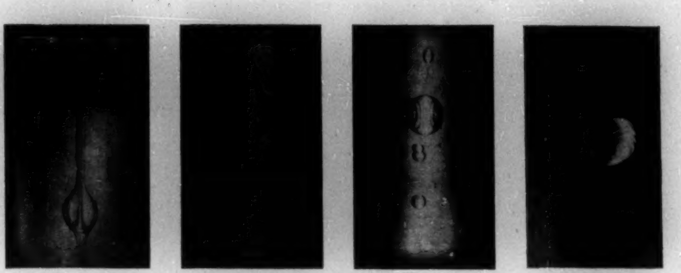

Fig. 1. Circulation patterns in falling drops. *a* to *c*, glycerine in castor oil (approximately ¾ actual size). *d*, 75% glycerine-water in heavy white oil (approximately twice actual size).

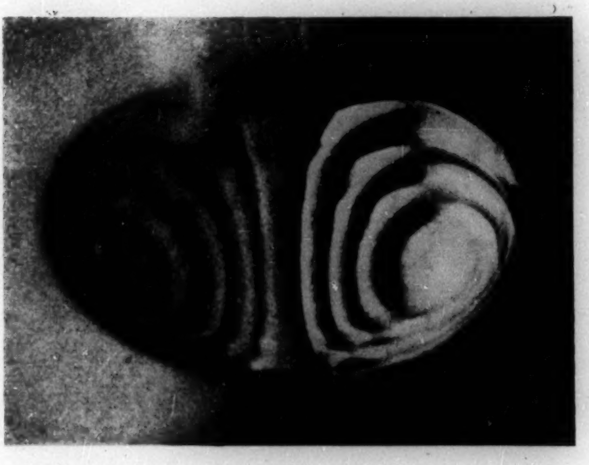

Fig 2. 60% glycerine-water drop (4% sucrose) falling in heavy white oil. Linear magnification ×12.

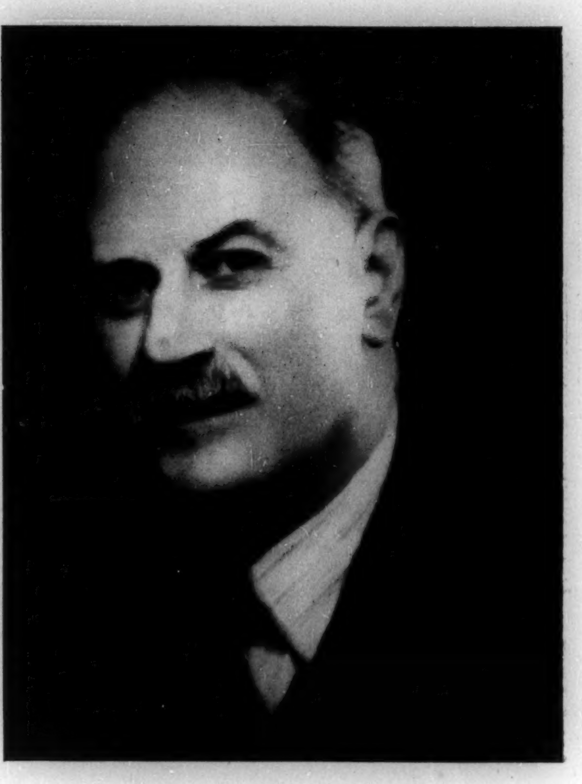

PROFESSOR L. F. BATES, D.Sc., Ph.D., F.R.S.
President of the Physical Society 1950–52.

(The Presidential Address is published in the August issue of the *Proceedings*, A, page 577.)